



# Short Haul Civil Tiltrotor Contingency Power System Preliminary Design

David J.H. Eames  
Rolls-Royce Corporation, Indianapolis, Indiana

## The NASA STI Program Office . . . in Profile

Since its founding, NASA has been dedicated to the advancement of aeronautics and space science. The NASA Scientific and Technical Information (STI) Program Office plays a key part in helping NASA maintain this important role.

The NASA STI Program Office is operated by Langley Research Center, the Lead Center for NASA's scientific and technical information. The NASA STI Program Office provides access to the NASA STI Database, the largest collection of aeronautical and space science STI in the world. The Program Office is also NASA's institutional mechanism for disseminating the results of its research and development activities. These results are published by NASA in the NASA STI Report Series, which includes the following report types:

- **TECHNICAL PUBLICATION.** Reports of completed research or a major significant phase of research that present the results of NASA programs and include extensive data or theoretical analysis. Includes compilations of significant scientific and technical data and information deemed to be of continuing reference value. NASA's counterpart of peer-reviewed formal professional papers but has less stringent limitations on manuscript length and extent of graphic presentations.
- **TECHNICAL MEMORANDUM.** Scientific and technical findings that are preliminary or of specialized interest, e.g., quick release reports, working papers, and bibliographies that contain minimal annotation. Does not contain extensive analysis.
- **CONTRACTOR REPORT.** Scientific and technical findings by NASA-sponsored contractors and grantees.

- **CONFERENCE PUBLICATION.** Collected papers from scientific and technical conferences, symposia, seminars, or other meetings sponsored or cosponsored by NASA.
- **SPECIAL PUBLICATION.** Scientific, technical, or historical information from NASA programs, projects, and missions, often concerned with subjects having substantial public interest.
- **TECHNICAL TRANSLATION.** English-language translations of foreign scientific and technical material pertinent to NASA's mission.

Specialized services that complement the STI Program Office's diverse offerings include creating custom thesauri, building customized databases, organizing and publishing research results . . . even providing videos.

For more information about the NASA STI Program Office, see the following:

- Access the NASA STI Program Home Page at <http://www.sti.nasa.gov>
- E-mail your question via the Internet to [help@sti.nasa.gov](mailto:help@sti.nasa.gov)
- Fax your question to the NASA Access Help Desk at 301-621-0134
- Telephone the NASA Access Help Desk at 301-621-0390
- Write to:  
NASA Access Help Desk  
NASA Center for AeroSpace Information  
7121 Standard Drive  
Hanover, MD 21076



# Short Haul Civil Tiltrotor Contingency Power System Preliminary Design

David J.H. Eames  
Rolls-Royce Corporation, Indianapolis, Indiana

Prepared under Contract NAS3-97029

National Aeronautics and  
Space Administration

Glenn Research Center

## Acknowledgments

The author would like to acknowledge the assistance of those individuals from Rolls-Royce Corporation (formerly Rolls-Royce Allison) who aided in the preparation of this document. Rob Hanesworth and his staff, in particular Tera Miles and Craig McCall, for technical editing of the final report. Also, thank you to Bob Burgun for his assistance in preparing the graphic content for the report.

This report contains preliminary findings, subject to revision as analysis proceeds.

Available from

NASA Center for Aerospace Information  
7121 Standard Drive  
Hanover, MD 21076

National Technical Information Service  
5285 Port Royal Road  
Springfield, VA 22100

Available electronically at <http://gltrs.grc.nasa.gov>

## Executive Summary

The NASA Short Haul Civil Tiltrotor (SHCT) Contingency Power System Preliminary Design contract represents the second phase of an ongoing effort to study low cost and safe one-engine inoperative (OEI) contingency power propulsion system concepts. Phase I of this study developed several candidate contingency power system concepts with the potential for significantly increasing the OEI power available from the powerplant. The objective of the current Phase II study was to select two different high ranking concepts from the Phase I study and develop these to a point where more refined vehicle direct operating cost (DOC) computations could be performed. Figure 1 shows a NASA concept of the SHCT.

Of the multiple novel propulsion system concepts studied during the Phase I program, two were carried forward to Phase II. They were water/methanol injection into the engine inlet and a variable geometry boost compressor. These systems show a high payoff and illustrate a total system approach to reducing tiltrotor DOC by means of boosting the engine OEI power. In carrying these two concepts into Phase II, the advanced water/methanol injection system showed the highest potential DOC improvement and was the subject of a preliminary design study.

In parallel with these studies, experiments on a modern water/methanol injection system were conducted with Purdue University. Bell Helicopter Textron, Inc., provided information to Rolls-Royce Allison on tank location, sizing, and mounting for a conceptual SHCT aircraft. The work was concluded by performing a direct operating cost analysis for an aircraft powered by a baseline unaugmented engine compared with a resized SHCT aircraft powered by a smaller water/methanol injection engine.



*Figure 1. Artist concept of the NASA Short Haul Civil Tiltrotor.*

The tasks performed in this program were:

- Task 1—Define Propulsion System Requirements:  
Task 1 included publishing the engine cycles (which involved conducting the mission analyses, publishing the baseline engine cycle, and publishing the injected engine cycle) and publishing the aerodynamic flow path.
- Task 2—Identify Propulsion System Concepts:  
Task 2 included documenting the downselected and alternate concepts, defining the water/methanol injection system requirements, conducting the water/methanol injection system analysis, and defining and documenting the water/methanol injection system design requirements.
- Task 3—Preliminary Design:  
The majority of the effort was expended in Task 3 and included defining the preliminary design of the compressor, combustor, turbine, mechanical systems, water/methanol injection system, and the whole engine. The whole engine preliminary design effort also included the economic analysis, which demonstrated the significant DOC advantage of an SHCT powered by the water/methanol injected engine compared with the baseline engine.
- Task 4—Meetings and Reporting:  
This final task included all of the NASA required reporting activities.

This program has defined an affordable SHCT baseline engine suitable for 2005 entry into service (EIS) and identified a simple, low cost SHCT OEI concept. This was achieved by applying improved analytical techniques for predicting water droplet trajectories and evaporation throughout the compression process. To support the analysis, an improved water/methanol injector was demonstrated on a rig. These improved injection techniques yield a 35% power boost and the resulting resized SHCT yields a 6.5 to 7.3% DOC improvement compared with the unaugmented baseline. The baseline and injected engines are shown in Figures 2 and 3 respectively. These figures indicate the size reduction made possible with the addition of water/methanol injection. Engine length reduces by 12 in. and height reduces by 5.5 in. Meanwhile, the total propulsion system weight is reduced from 1209 lb to 952 lb. As a result of the reduced core size of the injected engine, fuel burn is lowered by 15% for the 200 nautical mile mission.

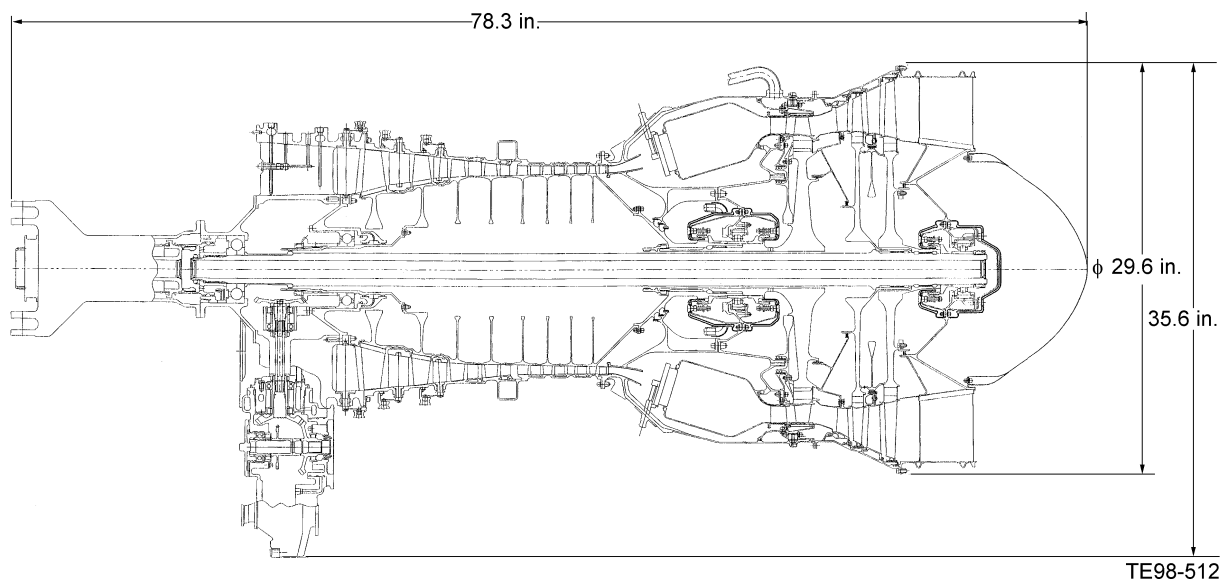


*Figure 2. Baseline unaugmented engine.*

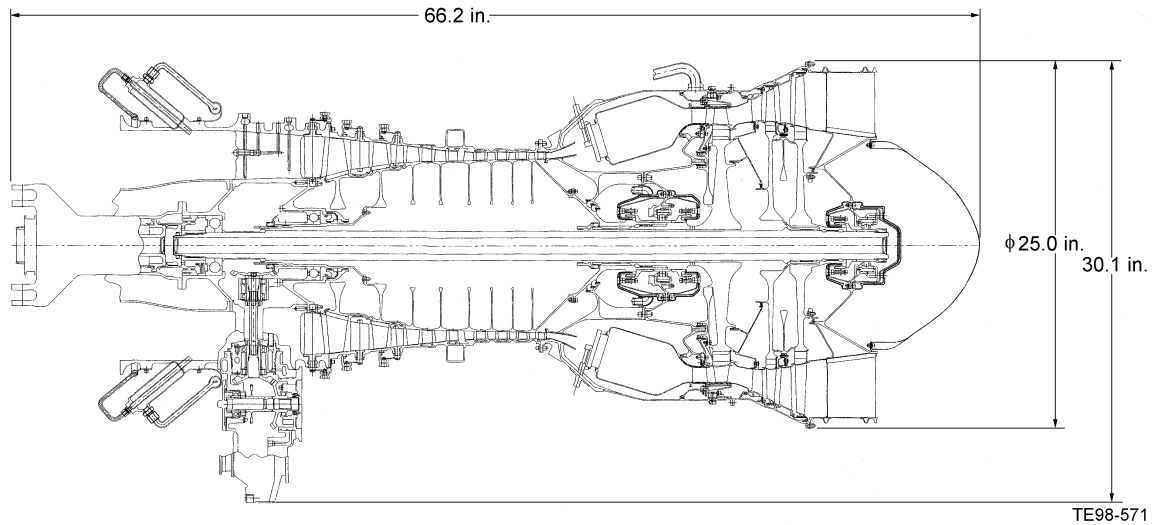


*Figure 3. Water/methanol injected engine.*

It is recommended that the next step should be to plan for an engine demonstration that would include optimization of the chosen injection system concept; rig testing of injection system hardware; manufacture of engine components for rematching; engine build; and engine test. It is also recommended that, in parallel with the engine demonstration, several component programs that would contribute significantly to the development of an affordable SHCT powerplant be started. These component programs include a low part count compressor program; an affordable low emissions combustor program; a reduced part count high pressure and low pressure turbine program; and a mechanical design program.



# Table of Contents

<b>Executive Summary .....</b>	<b>iii</b>
<b>1.0 Introduction.....</b>	<b>1</b>
1.1 Phase I Background.....	1
1.1.1 Initial Phase I Concepts .....	1
1.1.2 Phase I Detailed Analysis .....	2
1.1.3 Phase I Concept Ranking.....	2
1.1.4 Concepts Recommended for Phase II Study.....	2
1.2 Scope .....	8
1.3 Objectives.....	9
<b>2.0 Approach .....</b>	<b>11</b>
2.1 Work Performed Prior to Reprogramming.....	11
2.1.1 Variable Geometry Boost Compressor .....	11
2.1.2 Pump and Line Sizing.....	12
2.1.3 Bell Helicopter Studies .....	12
2.1.4 Concept Down-Select for Reprogrammed Effort .....	13
2.2 Reprogrammed Tasks.....	14
2.2.1 Task 1—Define Propulsion System Requirements.....	14
2.2.2 Task 2—Identify Propulsion System Concepts .....	14
2.2.3 Task 3—Preliminary Design .....	14
2.2.4 Task 4—Meetings and Reporting.....	14
<b>3.0 Task 1—Define Propulsion System Requirements .....</b>	<b>15</b>
3.1 Reprogramming Tasks .....	15
3.2 Mission Analysis.....	15
3.3 Baseline Engine Cycle .....	15
3.4 Injected Engine Cycle .....	15
3.5 Aerodynamic Flow Path.....	16
<b>4.0 Task 2—Identify Propulsion System Concepts.....</b>	<b>17</b>
4.1 Down-Selected and Alternate Concepts.....	17
4.2 Water/Methanol Injection Studies.....	17
4.2.1 Three-Dimensional Aerothermal Analysis Code.....	17
4.2.2 Design and Rig Testing of Atomizers.....	24
4.3 Turbine Bypass System Requirements.....	33
<b>5.0 Task 3—Preliminary Design .....</b>	<b>35</b>
5.1 Compressor Preliminary Design .....	35
5.1.1 Baseline Aerodynamic Design.....	35
5.1.2 Effect of Water/Methanol Injection on Compressor Performance .....	36
5.1.3 Trade Study Options.....	37
5.1.4 Mechanical Design Considerations .....	39
5.1.5 Manufacturing and Cost Analysis .....	41
5.1.6 Materials Considerations .....	41
5.1.7 Recommendations for Further Work .....	42

## Table of Contents (cont)

5.2 Combustor Preliminary Design .....	42
5.2.1 Injection Fluid Selection .....	43
5.2.2 Airflow Analysis .....	43
5.2.3 Heat Transfer .....	46
5.2.4 Emissions .....	47
5.2.5 Recommendations for Further Work .....	47
5.3 Turbine Preliminary Design .....	48
5.3.1 Aerodynamic Design .....	48
5.3.2 Heat Transfer .....	55
5.3.3 Mechanical Design .....	61
5.3.4 Stress Analysis .....	62
5.3.5 Component Cost Estimates .....	63
5.3.6 Recommendations for Further Work .....	63
5.4 Mechanical Systems Preliminary Design .....	65
5.4.1 Sumps .....	65
5.4.2 Lubrication System .....	67
5.4.3 Define Scaled AE 1107C Accessory Drives (Accessory Gearbox and Power Takeoff Gearbox) .....	67
5.4.4 Rotor Dynamics/LP and HP Shafting .....	68
5.4.5 Recommendations for Future Work .....	71
5.5 Water/Methanol Injection System Preliminary Design .....	72
5.5.1 Water/Methanol Injection System Description .....	72
5.5.2 Front Frame Design .....	73
5.5.3 Water/Methanol Injection Preliminary Design Scheme .....	73
5.5.4 Recommendations for Further Effort .....	73
5.6 Whole Engine Preliminary Design .....	74
5.6.1 Engine Life Requirements .....	74
5.6.2 Baseline Engine Preliminary Design .....	75
5.6.3 Injected Engine Preliminary Design .....	80
5.6.4 Economic Analysis .....	85
5.6.5 Future Work .....	88
<b>6.0 Task 4—Meetings and Reporting .....</b>	<b>89</b>
6.1 Weekly Progress Meetings .....	89
6.2 Monthly Written Reports .....	89
6.3 Prepare Final Report Outline .....	89
6.4 Document Completed Work .....	89
6.5 Prepare Final Report .....	89
<b>7.0 Conclusions .....</b>	<b>91</b>
<b>8.0 Recommendations .....</b>	<b>93</b>
8.1 Engine Demonstration Program .....	93
8.2 Component Programs .....	93
8.2.1 Low Part Count Compressor Program .....	93
8.2.2 Affordable Low Emissions Combustor Program .....	94
8.2.3 Reduced Part Count HP and LP Turbine Program .....	94
8.2.4 Mechanical Design Programs .....	94

## Table of Contents (cont)

9.0 References .....	95
Appendix A .....	97

## List of Illustrations

Figure 1. Artist concept of the NASA short haul civil tiltrotor.....	iii
Figure 2. Baseline unaugmented engine.....	iv
Figure 3. Water/methanol injected engine.....	v
Figure 4. Water/methanol system schematic.....	5
Figure 5. Engine mounted components.....	6
Figure 6. The additional compressor stage, shaft and clutching, and inlet housing for the variable geometry boost compressor.....	7
Figure 7. Compressor flow path.....	8
Figure 8. Compressor system maps for takeoff and cruise conditions.....	8
Figure 9. Compressor section size comparison.....	12
Figure 10. Bell conceptual design.....	13
Figure 11. Engine flow path.....	16
Figure 12. T56 engine test demonstrates the increase in shaft horsepower with water/methanol injection.....	20
Figure 13. Measured temperature difference between compressor discharge and casing temperature resulting from water/methanol injection.....	21
Figure 14. Computed droplet trajectories in the T56 compressor for various droplet sizes.....	21
Figure 15. Computed droplet evaporation as a function of compressor axial length for various droplet sizes.....	22
Figure 16. Computed gas temperature as a function of axial length for a T56 engine.....	23
Figure 17. Typical computed droplet trajectories (civil tiltrotor engine).....	23
Figure 18. Computed droplet evaporation as a function of axial length for an average droplet diameter of 8 microns (NASA civil tiltrotor engine).....	24
Figure 19. Computed gas temperature as a function of axial length for an average droplet diameter of 8 microns (NASA civil tiltrotor engine).....	25
Figure 20. Plain jet atomizer setup.....	25
Figure 21. Plain jet atomizer flow characteristics, hole diameter 0.025 in., L/d = 2, water.....	26
Figure 22. Plain jet atomizer flow characteristics, hole diameter 0.025 in., L/d = 2, water.....	26
Figure 23. Rosin-rammler droplet size distribution for a plain jet atomizer (n = 1.74, x bar = 84, sauter mean diameter = 40 μm, orifice diameter = 0.025, injection pressure = 667 psig).....	27
Figure 24. Experimental arrangement used to evaluate the effervescent atomizer.....	28
Figure 25. Drop characteristics for the 1 mm nozzle at an axial location of 50 mm.....	29
Figure 26. Drop characteristics of the 1 mm nozzle at an axial location of 100 mm.....	30
Figure 27. Drop characteristics of the 3 mm nozzle at an axial location of 50 mm.....	30
Figure 28. Drop characteristics of the 3 mm nozzle at an axial location of 100 mm.....	31
Figure 29. PDFs of the droplets obtained using a 1 mm diameter effervescent spray.....	31
Figure 30. PDFs of the droplets obtained using a 3 mm diameter effervescent spray.....	32
Figure 31. Change in the spray characteristics with the addition of methanol.....	33
Figure 32. PDFs of the droplets obtained using methanol/water mixture.....	34
Figure 33. Compressor efficiency is aggressive compared with state of the art.....	35
Figure 34. Compressor flow-path cross section.....	36
Figure 35. Overall compressor map.....	38
Figure 36. Schematic of lean direct injection fuel module AST6-b.....	44
Figure 37. Schematic of baseline cycle combustion system.....	45
Figure 38. Circumferential fuel staging scheme for shct combustor.....	45
Figure 39. Predicted inner and outer liner wall temperatures at maximum power condition for baseline cycle SHCT combustor.....	46
Figure 40. Gas generator turbine and power turbine flow path schematic at design point.....	49
Figure 41. Gas generator turbine inlet temperature profile at design point conditions.....	50
Figure 42. Gas generator turbine and power turbine design point controlled-vortex velocity diagrams.....	51
Figure 43. Gas generator turbine airfoils and surface velocities.....	52
Figure 44. Power turbine airfoils and surface velocities.....	53
Figure 45. Gas generator turbine overall map.....	56
Figure 46. Power turbine overall map.....	57

## List of Illustrations (cont)

Figure 47. GGT vane cooling scheme.....	58
Figure 48. GGT blade cooling scheme.....	59
Figure 49. Gas generator turbine and power turbine secondary flows.....	60
Figure 50. Conservative axial vane-blade spacings result in low predicted dynamic stresses.....	64
Figure 51. Sump pressurization.....	66
Figure 52. LP shaft and turbine modal deflections.....	69
Figure 53. HP rotor modal deflections.....	71
Figure 54. Schematic of nozzle spacing.....	73
Figure 55. Baseline engine generator arrangement.....	75
Figure 56. Baseline engine size.....	77
Figure 57. Injected engine general arrangement.....	81
Figure 58. Injection system schematic.....	81
Figure 59. Line locations in wing.....	82
Figure 60. Injected engine size.....	83
Figure 61. Water/methanol tank location.....	84

## List of Tables

Table I. Initial Phase I concepts for achieving OEI power.....	1
Table II. Concepts carried through detailed Phase I analysis.....	2
Table III. Sizing results.....	3
Table IV. Concept ranking.....	4
Table V. Water tank design loads.....	14
Table VI. Baseline and injected engine performance.....	15
Table VII. Water-methanol injection conditions for T56 analysis.....	21
Table VIII. Water/methanol injection conditions for the tiltrotor engine.....	23
Table IX. Operating conditions used for the evaluation tests.....	28
Table X. Momentum flux of the effervescent atomizer.....	32
Table XI. Compressor design parameter comparison.....	36
Table XII. Trade study option summary.....	39
Table XIII. Compressor trade study—weight comparisons.....	41
Table XIV. Compressor trade study—relative costs.....	41
Table XV. Injection fluid characteristics.....	43
Table XVI. Combustion design parameters for baseline and methanol/water injected engine (length, aspect ratio, nozzle spacing/annulus height, and system pressure drop).....	43
Table XVII. Landing takeoff cycle emissions estimates for baseline cycle low emissions combustor and typical diffusion flame combustor.....	47
Table XVIII. Gas generator turbine and power turbine aerodynamic design point parameters.....	49
Table XIX. Turbine flow-path hot corner point dimensions at design point conditions.....	49
Table XX. Gas generator turbine and power turbine velocity diagram parameters at 25,000 ft, 350 ktas, ISA, maximum cruise design point conditions.....	51
Table XXI. Gas generator turbine and power turbine mean-line geometric blading parameters.....	55
Table XXII. Typical mission profiles.....	62
Table XXIII. Gas generator turbine and power turbine vane, blade, and wheel materials.....	62
Table XXIV. Gas generator turbine vane and blade life.....	63
Table XXV. Turbine assemblies breakdown.....	64
Table XXVI. The low pressure, small diameter shaft design allows for very low bearing and seal speeds.....	65
Table XXVII. Parameters for 200 nautical mile mission.....	75
Table XXVIII. Weight summary.....	77
Table XXIX. Cost summary.....	78
Table XXX. Main drivers on the DOC components.....	86
Table XXXI. Injected configuration DOC cost trends, injected compared to baseline.....	86
Table XXXII. Economic analysis summary.....	87
Table XXXIII. Cost benefits.....	87

## Acronyms

ALR	Air-to-liquid ratio
APU	Auxiliary power unit
AST	Advanced Subsonic Transport
Blisk	Integrally bladed disk
$B_y$	Mass transfer number
$C_d$	Droplet coefficient of drag
CL	Centerline
CO	Carbon monoxide
CVG	Compressor variable geometry
EB	Electron beam
EEE	Energy Efficient Engine
EIS	Entry into service
FADEC	Full-authority digital engine control
FOD	Foreign object damage
FPMU	Fuel pump and metering unit
ft	Feet
gal	Gallons
GG	Gas generator
GGT	Gas generator turbine
gpm	Gallons per minute
HP	High pressure
hr	Hour
ISA	International Standard Atmosphere
ktas	knots true airspeed
LCF	Low cycle fatigue
LeRC	Lewis Research Center
LDI	Lean direct injection
LP	Low pressure
LRU	Line replaceable unit
LTO	Landing takeoff
$M_{convection}$	Droplet evaporation rate with convection
min	Minute
NO <sub>x</sub>	Oxides of nitrogen
nm	Nautical miles
OD	Outer diameter
OEI	One-engine inoperative
PDF	Probability density function
PRD	Product requirements document
PT	Power turbine
$Re_d$	Reynolds number past a spherical droplet
RIT	Rotor inlet temperature
rpm	Revolutions per minute

SFC	Specific fuel consumption
SHCT	Short Haul Civil Tiltrotor
shp	Shaft horsepower
SMD	Sauter mean diameter
SOW	Statement of work
TBC	Thermal barrier coating
TIT	Turbine inlet temperature
TOGW	Takeoff gross weight
UHC	Unburned hydrocarbon
V	Velocity
VGW	Variable guide vane
V/STOL	Vertical or short takeoff or landing
VTO	Vertical takeoff
$Y_{Fs}$	Mass fraction of vapor at droplet surface
2D	Two-dimensional
3D	Three-dimensional
°F	Degrees Fahrenheit

## 1.0 Introduction

The NASA *Short Haul Civil Tiltrotor (SHCT) Contingency Power System Preliminary Design* contract represents the second phase of an ongoing effort to study low cost and safe OEI contingency power propulsion system concepts. Phase I of this study developed several candidate contingency power system concepts with the potential for significantly increasing the OEI power available from the powerplant. The original objective of the current Phase II study was to select two different high ranking concepts from the Phase I study and develop them to a point where more refined vehicle DOC computations could be performed. However, part way through the Phase II program, funding for the contract was significantly cut. NASA requested definition of a reprogrammed effort, which is outlined in the Statement of Work (SOW) shown in Appendix A.

### 1.1 Phase I Background

NASA and Rolls-Royce Allison believe there is a payoff in developing an SHCT OEI propulsion system concept that provides the necessary power boost for safe OEI flight and that does not incur the usual penalties associated with simply oversizing the engine. It is believed an affordable, low risk OEI concept could make the SHCT aircraft a truly viable proposition. The objective of the Phase I study was to evaluate the potential cost benefits.

In pursuit of this objective, Rolls-Royce Allison conceived several OEI concepts, screened the concepts for high potential, conceptualized the design of the high potential concepts, evaluated the cost impact on aircraft DOC, and ranked the concepts in terms of improved DOC. New technologies required to enable development of the candidate OEI concepts were also identified.

#### 1.1.1 Initial Phase I Concepts

A list of possible OEI concepts was developed using input from senior Rolls-Royce Allison engineers, who had experience in new concept development, high risk projects, or with vertical or short takeoff or landing (V/STOL) programs. The initial list of concepts is given in Table I.

*Table I. Initial Phase I concepts for achieving OEI power.*

Concept	Description
1	APU drive into gearbox, T800 engine to replace/in addition to auxiliary power unit (APU)
2	Variable geometry boost compressor
3	External solid fuel exhaust into low pressure turbine inlet
4	Fuel cooling air heat exchanger
5	Increased compressor overspeed
6	Inter-turbine combustor
7	Liquid nitrogen injected into compressor inlet
8	Liquid compressed nitrogen injected into compressor discharge
9	Modulated turbine cooling flow
10	Water/methanol injection into inlet
11	Water/methanol injection at compressor discharge
12	Water injection into cooling flow
13	Variable geometry turbine

### 1.1.2 Phase I Detailed Analysis

Seven concepts and variations on two of the seven concepts were carried through to detailed analysis, and are listed in Table II. It was hoped each of the seven concepts had a reasonable chance of showing a significant DOC benefit for the SHCT system. The results of the analysis are shown in Table III.

### 1.1.3 Phase I Concept Ranking

The concepts shown in Table III can be ranked based on DOC results. For convenience, these results are shown in Table IV.

### 1.1.4 Concepts Recommended for Phase II Study

The first- and third-ranked concepts, water/methanol injection into the engine inlet with turbine bypass and variable geometry boost compressor, were proposed and accepted by NASA for further study in the Phase II program. These systems show a high payoff and illustrate a total system approach to reducing tiltrotor DOC by means of boosting the engine OEI power. While the second-ranked concept, water/methanol injection into the engine inlet, provides more payoff than the variable geometry boost compressor, the concept is little different than its variation with turbine bypass. The variable geometry boost compressor concept is a completely different approach to the OEI power boost and has the potential for providing additional DOC savings, if innovative ways of reducing the cost of the system are adequately explored. The two accepted concepts are described in more detail in the following subsections.

#### 1.1.4.1 Water/Methanol Injection into the Engine Inlet

Water/methanol injection into the engine inlet is an established method of increasing engine power that is usually used to boost hot day performance in older aircraft and some helicopter systems. In the past, water/methanol injection has been implemented using only trial-and-error and empirical methods without extensive testing or analysis. The injection boosts engine shaft power by increasing engine mass flow and by decreasing compressor discharge temperature, thereby allowing a commensurate increase in fuel to restore turbine rotor inlet temperature (RIT). Turbine cooling temperature is also reduced and flow rate increased, which allows higher RIT at the same blade metal temperatures, which further increases power.

*Table II. Concepts carried through detailed Phase I analysis.*

<b>Concept</b>	<b>Description</b>
1	Water/methanol injection into the engine inlet
1x	Water/methanol injection into the engine inlet with turbine bypass (variation)
2	Water/methanol injection into turbine cooling air
3	Modulated turbine cooling
4	Water/methanol injection into compressor discharge air
5	Boost compressor
5x	Variable geometry boost compressor (variation)
6	APU drive into gearbox—extra T800 engine to cross-shaft
7	APU drive into gearbox—T800 replaces APU

Table III. Sizing results.

	Baseline	1	2	3	4	5	6	7	1X	5X
OEI power	10,426 hp	26.00%	19.20%	0.00%	18.00%	32.40%	15.30%	15.30%	37.70%	31.00%
Weight	1238 lb	17.90%	6.60%	0.80%	17.90%	17.90%	16.50%	17.90%	18.60%	5.48%
SFC	0.339 lb/hr/hp	0.30%	0.00%	-3.30%	0.00%	0.00%	0.00%	0.00%	0.30%	0.00%
Acquisition cost	\$1,161,485	1.25%	1.25%	0.16%	1.25%	11.50%	23.00%	18.40%	1.28%	10.00%
Maintenance cost	\$127.00	1.50%	1.50%	5.00%	1.50%	11.30%	32.50%	17.30%	1.53%	10.00%
Takeoff horsepower	8850	6878	7256	8791	7408	6500	7601	7601	6229	6520
Required cruise horsepower	6388	6209	6219	6354	6272	6160	6292	6292	6132	6126
Fuel flow—lb/hr	2215	2177	2163	2131	2181	2167	2186	2186	2181	2152
Takeoff gross weight—lb	45,923	44,952	44,869	45,618	45,361	44,632	45,477	45,477	44,952	44,284
Wing area—ft <sup>2</sup>	382.8	374.6	373.9	380.2	378.0	371.9	379.0	379.0	370.6	369.0
Propeller diameter—ft	41.1	40.7	40.6	41.0	40.9	40.5	40.9	40.9	40.5	40.4
Engine weight (2 eng)—lb	2001.0	1922.7	1814.0	2005.8	2040.0	1839.2	2058.0	2058.0	1789.6	1654.3
Empty weight—lb	31,325	30,569	30,490	31,225	30,927	30,305	31,019	31,019	30,148	29,989
Operating weight empty—lb	32,213	31,457	31,378	32,113	31,815	31,193	31,907	31,907	31,036	30,877
Payload—lb	8000	8000	8000	8000	8000	8000	8000	8000	8000	8000
Fuel—lb	5719.1	5494.9	5491.9	5504.9	5546.3	5439.1	5570.3	5570.3	5438.0	5406.8
Total flatplate area—ft <sup>2</sup>	17.496	16.897	16.955	17.470	17.091	16.753	17.154	17.154	16.664	16.683
Fuel required (200 nm)—lb	1397.6	1334.0	1335.1	1344.0	1348.6	1318.4	1355.2	1355.2	1317.3	1310.9
Fuel required (600 nm)—lb	3882.4	3771.0	3758.7	3735.7	3793.1	3742.7	3805.2	3805.2	3752.5	3719.0
Airframe cost—\$	13,554,090	13,262,258	13,301,444	13,531,445	13,352,195	13,196,158	13,382,208	13,382,212	13,152,280	13,174,936
Cruise engine cost—\$	1,943,908	1,637,441	1,702,581	1,965,425	1,728,640	1,730,436	2,139,704	2,059,675	1,528,052	1,710,942
Dynamic system cost—\$	1,773,370	1,742,622	1,740,049	1,763,542	1,755,485	1,732,570	1,759,114	1,759,114	1,727,618	1,721,628
Spares cost—\$	1,270,112	1,176,271	1,196,128	1,282,874	1,206,424	1,246,404	1,447,896	1,395,342	1,141,379	1,232,058
Total cost—\$	18,541,480	17,818,592	17,940,202	18,543,286	18,042,744	17,905,568	18,728,922	18,596,343	17,549,329	17,839,564
Block time	0.826	0.827	0.827	0.826	0.826	0.828	0.826	0.826	0.830	0.828
Crew—\$	165.00	165.17	165.04	164.99	165.01	165.39	165.01	165.01	165.64	165.30
Fuel and oil—\$	140.39	134.00	134.11	135.01	135.47	132.44	136.14	136.14	132.33	131.68
Insurance—\$	285.30	275.34	276.81	285.14	278.22	276.03	285.54	284.22	272.30	275.08
Airframe maintenance—\$	212.50	208.60	209.01	212.15	209.80	207.76	210.21	210.21	207.25	207.33
Engine maintenance—\$	123.57	109.53	112.58	127.21	113.79	117.02	145.54	134.06	104.61	116.31
Dynamic system maintenance—\$	67.69	66.47	66.30	67.27	66.94	66.14	67.09	67.09	66.04	65.64
Maintenance burden—\$	381.15	368.05	370.09	386.28	372.34	376.06	410.39	392.49	363.45	374.89
Depreciation—\$	367.54	353.76	355.90	367.60	357.78	356.01	371.36	368.73	349.49	354.58
Interest—\$	296.35	285.24	286.96	296.40	288.48	287.06	299.43	297.31	281.80	285.90
Total trip DOC	\$2,039.49	\$1,966.16	\$1,976.80	\$2,042.05	\$1,987.83	\$1,983.91	\$2,090.71	\$2,055.26	\$1,942.91	\$1,976.71
Difference	N/A	-3.60%	-3.07%	0.13%	-2.53%	-2.73%	2.51%	0.77%	-4.74%	-3.08%
Prior phase configurations:	<ol style="list-style-type: none"> <li>1. Water/methanol injection into inlet</li> <li>2. Water injection into turbine cooling air</li> <li>3. Advanced turbine cooling concepts—modulated cooling flow</li> <li>4. Water/methanol injection into compressor discharge air</li> <li>5. Boost compressor fan</li> <li>6. APU drive to gearbox—extra T800 to C shaft</li> <li>7. APU drive to gearbox—T800 replaces APU</li> <li>1X Water/methanol injection into inlet with turbine bypass</li> <li>5X Variable geometry booster compressor</li> </ol>									

Table IV. Concept ranking.

Ranking	Concept	$\Delta$ DOC—%
1	Water/methanol injection into the engine inlet with turbine bypass	-4.74
2	Water/methanol injection into the engine inlet	-3.60
3	Variable geometry boost compressor	-3.08
4	Water/methanol injection into turbine cooling air	-3.07
5	Boost compressor	-2.73
6	Water/methanol injection into compressor discharge	-2.53
7	Modulated turbine cooling	+0.13
8	APU drive to gearbox—T800 replaces APU	+0.77
9	APU drive to gearbox—extra T800 to cross-shaft	+2.51

Much of the analysis of this concept was based on Rolls-Royce Allison experience with water/methanol injection on engines such as the T56-A-425 on a carrier based aircraft. This engine demonstrated that the addition of 0.625 lb/sec (1.88% by weight) of water/methanol to the engine inlet resulted in a 13.9% power boost. Other testing showed that for the T56 Series III engine a power gain of 25% could be achieved with the addition of water up to 1.146 lb/sec (3.45%) of water/methanol. However, this increase was accompanied by a permanent loss of 0.30% in specific fuel consumption (SFC) due to the compressor blade tip rubbing, which occurred during the first high volume injection. The tip rub increased the blade tip clearance, which permanently reduced compressor efficiency and increased SFC.

Cycle studies for the Phase I water/methanol injected engine indicated that a 26.3% power boost might be possible with 3.45% fluid injection. For this study, eight flat sheet spray nozzles were mounted on the compressor inlet case outer wall, the same setup as was done for the Rolls-Royce Allison 578-DX propfan. A mixture by volume of 33% methanol and 67% de-ionized water was provided to the individual engines from a common, centrally located, serviceable, aircraft-mounted tank. The system schematics are shown in Figure 4.

A bypass return line to the aircraft tank minimized the time lag for fluid injection. A solenoid valve directed the bypass flow into the engine during OEI. This procedure minimized time lag and also allowed for system checkout and monitoring up to the time of need. The engine-mounted components are shown in Figure 5.

A tank containing enough fluid for 4 minutes of OEI operation at the maximum flow rate of 1.446 lb/sec would add approximately 350 lb to the aircraft weight. The aircraft tank and plumbing would weigh 64.6 lb and the engine-mounted hardware 6.2 lb per engine. Total weight penalty per engine would be 213.5 lb or about 19.7%. The learned out cost of the system hardware is calculated to be 1.25% of the baseline engine costs. The direct maintenance cost increase for this system is estimated to be 1.5%. This concept reduces DOC by -3.60% over the baseline engine sized to perform the OEI requirement.

The aircraft resizing results (Table III) illustrate the changes to the total aircraft system with the changes in engine power, weight, and costs. The takeoff horsepower of the engine goes down by more than the amount of the OEI power boost. This is due to the combined effects of the OEI boost and an overall reduction in aircraft takeoff gross weight (TOGW), which itself is reduced by 2%. The reduction in TOGW also affects wing area and propeller diameter, with respect to aircraft design, and the airframe cost on the economic side. The reduction in wing area reduces the total flat plate area, a measure of aircraft drag, which, with the lower overall aircraft weight and, more importantly, a smaller engine

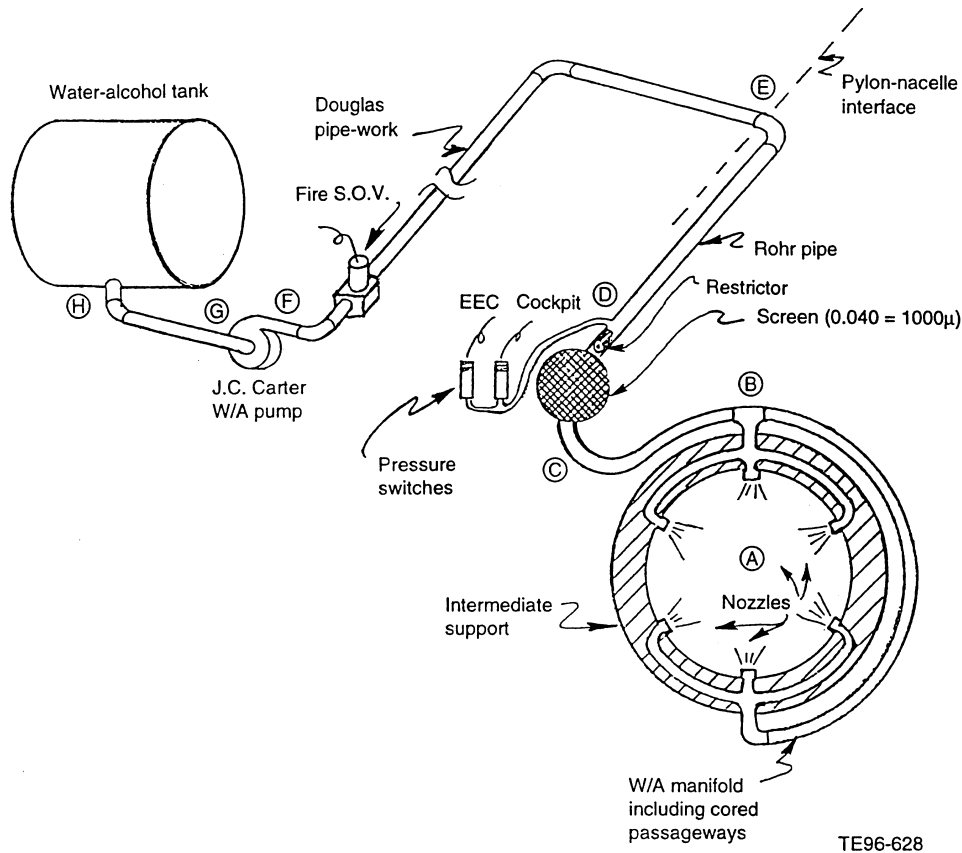
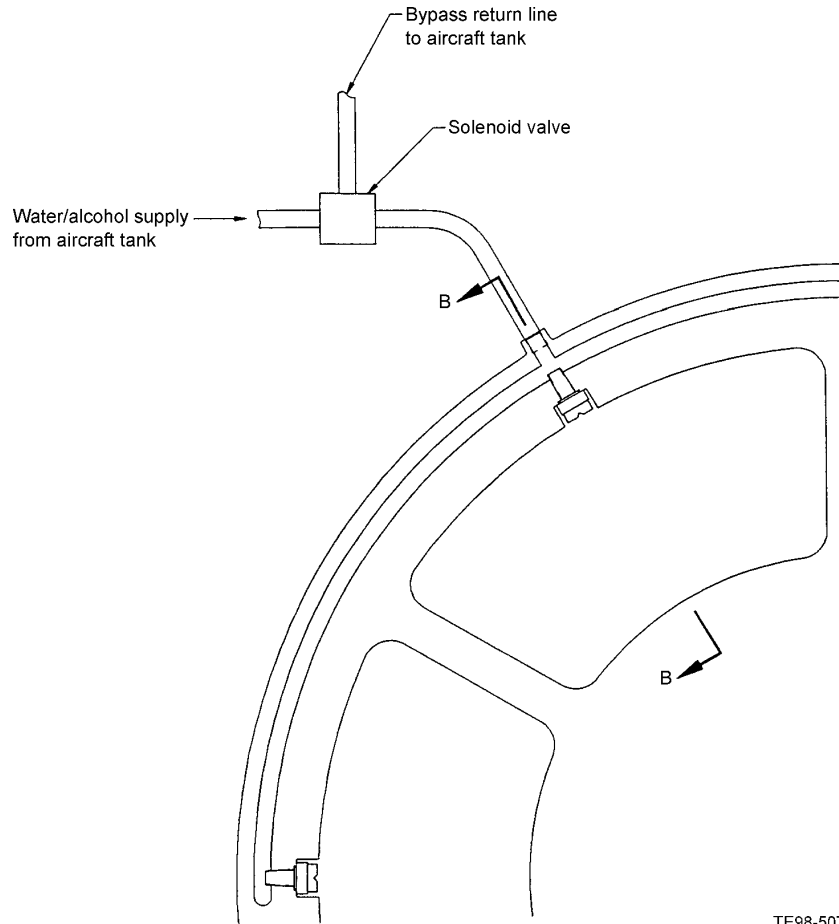


Figure 4. Water/methanol system schematic.

operating closer to the bottom of the SFC curve, results in a more efficient cruise. The fuel required for 200 nm decreases by 4.5%, even though for this concept the engine SFC is penalized by 0.30%. Regarding the economic components, in addition to the airframe cost reduction, the engine cost is reduced with the -22% engine scale down overwhelming the 1.25% increase in acquisition cost. Dynamic system cost is reduced due to lower engine horsepower requirements. Maintenance costs for both airframe and engine are reduced due to less airframe weight and lower engine horsepower; again the engine scale down is much larger than the 1.5% increase in unscaled engine maintenance cost.

Additional studies on water injection proved an additional power boost is available by a combination of additional water injection and RIT throttle push to values producing turbine blade metal temperatures matching the baseline engine. This scheme resulted in an overall increase in engine power for OEI of 37%, but created a surge margin problem. The increased engine RIT reduced the compressor surge margin to unacceptably low levels. To resolve this issue, a system was designed for use with the concept that bypassed a portion of compressor discharge air around the combustor and high pressure turbine to just in front of the power turbine. This also allowed cooling of the vanes, which might require cooling due to the higher RIT values. New weight and cost values were determined for this modified water/methanol injection design. The weight penalty for water/methanol with bypass was 18.6 lb, while the acquisition cost increase was 1.28%. SFC was not affected and maintenance costs were increased to 1.53%. The DOC impact of the modified water/methanol concept was -4.74%.



TE98-507

*Figure 5. Engine mounted components.*

In the case of the variation, the aircraft design changes were magnified by the additional OEI power boost for a small additional boost in system weight. Engine size decreased an additional 7% to a total of 29.6%. Aircraft TOGW change over the baseline matched the original water/methanol into the engine inlet concept. Acquisition and maintenance costs were boosted by fractions of a percent due to an additional valve and plumbing. The variation produced a larger DOC improvement by significantly adding to the OEI power boost without correspondingly large changes in engine weight, acquisition cost, or maintenance cost.

#### *1.1.4.2 Variable Geometry Boost Compressor*

The variable geometry boost compressor concept boosted power by adding to the engine flow capacity and overall pressure ratio by the addition of a boost compressor stage. The initial concept for a boost compressor had a clutched 1.5 pressure ratio stage with fixed inlet and exit guide vanes that was revealed to the flow by way of a translating ring and ramped flow surface. The boost compressor stage was driven by the core compressor shaft through a wet disc clutch that would be engaged as required to drive the boost compressor. To have the extra power immediately available and to reduce clutch power demands, the clutch would be engaged prior to each vertical liftoff and approach to landing and disengaged after transition from vertical to horizontal flight. Clutch plates were used to bring the boost compressor rotor and core compressor rotor to synchronous speed, then a no-slip, spline-to-spline rotor lockup would be made. A drawing of the additional compressor stage, shaft and clutching, and inlet housing is shown in Figure 6.

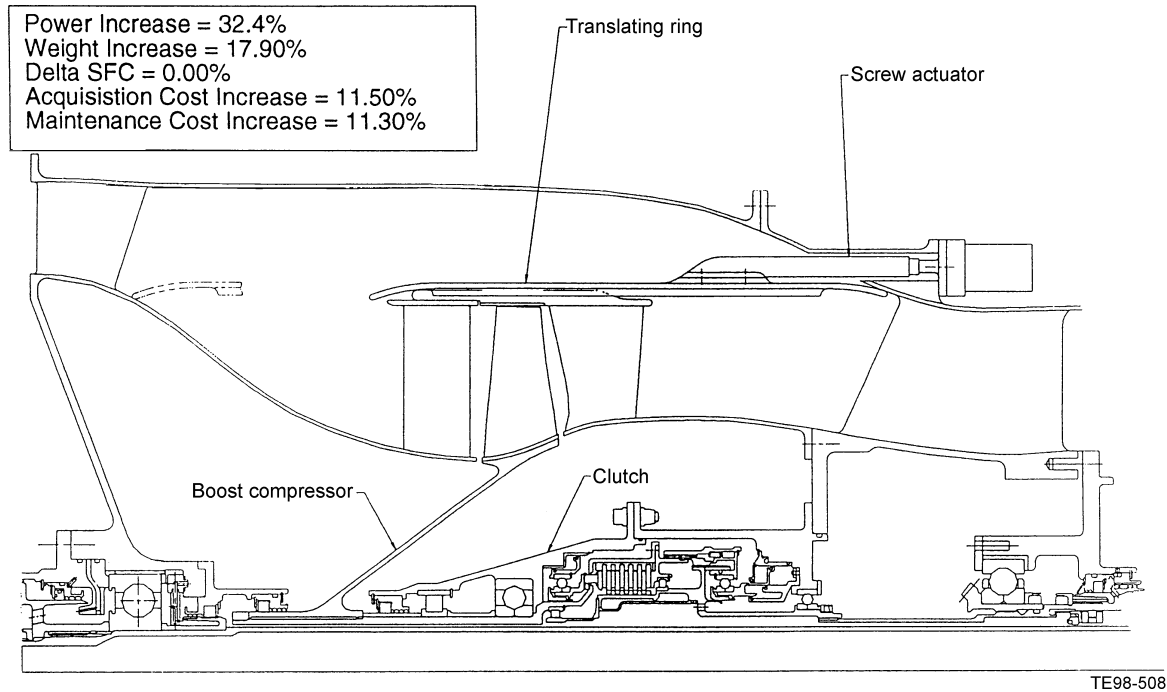


Figure 6. The additional compressor stage, shaft and clutching, and inlet housing for the variable geometry boost compressor.

The concept resulted in a power boost of 32.4% over the baseline engine. A weight rollup of the boost compressor concept showed a 17.9% increase. The acquisition cost was increased by 11.5% and the maintenance cost increase was 11.3%. Aircraft DOC went down by 2.73%.

The aircraft design changes resulting from this concept were dramatic, with an engine takeoff horsepower 26.5% less than the baseline. Aircraft TOGW was less by 2.8%. The large OEI power boost resulted in an engine that at cruise would be at the bottom of the SFC curve, and resulted in a 200 nm fuel burn that was 5.7% less than the baseline. On the cost side, however, the significant engine scale down was mostly offset by an 11.5% increase in engine acquisition cost and an 11.3% increase in engine maintenance cost. Due to the cost increases, the dramatic aircraft design changes resulted in a disappointing DOC decrease.

Additional work was performed on this concept, since it showed a good DOC benefit but not as good as was hoped for with a fully developed system. An alternative to the translating ring and clutched boost compressor design (which effectively blocks all airflow to the boost compressor at the expense of hardware complication and weight and inlet pressure losses) was a design in which air would flow through the boost compressor in all phases of operation. Cost and weight would be saved in this variation by shifting compressor stages off the high pressure compressor and onto the variable geometry low pressure booster. Where before, the boost stages were in addition to the baseline engine design, in the variation the total stage count from the baseline would not increase. This concept is shown in Figure 7.

By utilizing the low pressure shaft speed difference between takeoff and up-and-away flight and the traditional variable compressor vane geometry, the boost compressor could be made to provide a power boost for takeoff, giving sufficient power for OEI and in cruise restricting airflow so the engine looks “smaller.” Figure 8 shows the compression system maps for the takeoff condition and for the cruise condition with the variable geometry as assumed for the analysis of this concept. This smaller cruise engine operates more efficiently than an engine sized for OEI requirements.

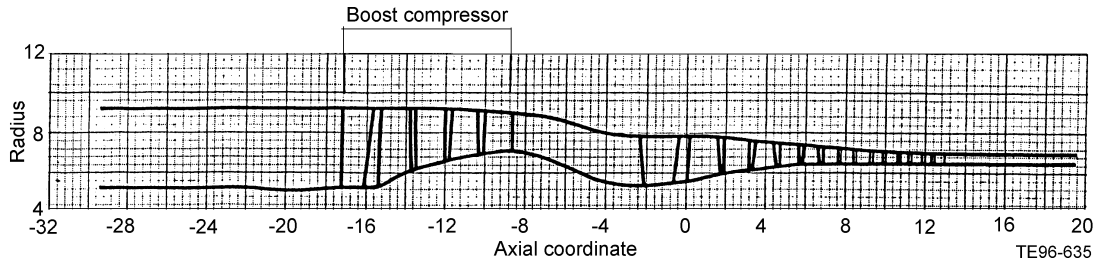


Figure 7. Compressor flow path.

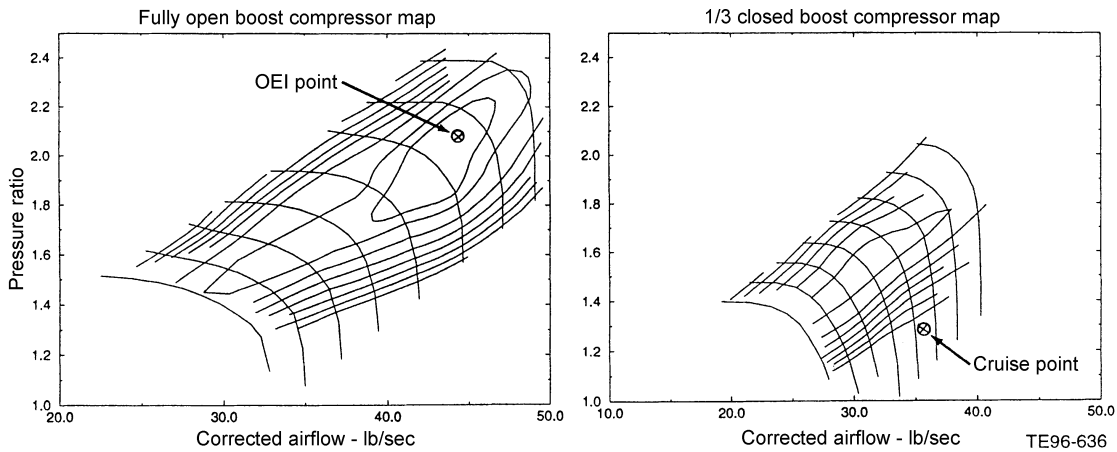


Figure 8. Compressor system maps for takeoff and cruise conditions.

The reworked variable geometry boost compressor concept produced a 31% increase in OEI power, at the decreased penalty of a 5.48% increase in system weight and a 10% increase in both acquisition cost and maintenance cost. In the economic analysis, the SFC benefit was not included, though it is believed to be about 1 to 2%. With these improvements, the DOC decrease was 3.08%.

For the boost compressor variation, some OEI power boost is given up to save a large amount of weight and some cost. The resulting scaled engine size is slightly larger than the original boost

compressor concept, but the aircraft size is decreased by an additional 0.8%, directly affecting airframe price and cruise efficiency. Along with a 1.5% and 1.3% decrease in acquisition and maintenance cost, respectively, the DOC for this variation is decreased another 0.35% when compared to the original boost compressor concept.

## 1.2 Scope

This program built upon the work performed in the Phase I study and developed two promising contingency power concepts to a point where a sensible downselect could be made. In parallel with these studies, experiments on a modern water/methanol injection system were conducted with Purdue University. Bell Helicopter Textron, Inc., provided information to Rolls-Royce Allison on tank location, sizing, and mounting for a conceptual SHCT aircraft. The work was concluded by performing a DOC analysis for an aircraft powered by a baseline unaugmented engine compared with a resized SHCT aircraft powered by a smaller water/methanol injection engine.

### **1.3 Objectives**

The original program objective prior to reprogramming was to develop the critical technologies for providing a low cost and safe OEI contingency power propulsion system for the vehicle. The goal of this contract was to refine and develop the most promising contingency power propulsion system concept(s) through analysis and preliminary design, and to then define an outline technology program. However, the reprogramming effort forced Rolls-Royce Allison to restrict the analysis and preliminary design to a single concept and to replace the outline technology plan with an outline plan for the demonstration of the preferred water/methanol injection system on an engine.



## 2.0 Approach

The engine concept used as the baseline for the Phase I studies was intended to be carried forward into the Phase II program; however, during Phase II, the opportunity was taken to make the engine compatible with the component improvement goals defined in the NASA Advanced Subsonic Transport (AST) program. The Phase II contract therefore included significant design work to more completely define the baseline engine, from which the OEI concepts could be compared.

This section describes the work performed up until the reprogramming and concludes with a description of the reprogrammed tasks. The results of the reprogrammed tasks are described in Sections 3 through 6.

### 2.1 Work Performed Prior to Reprogramming

Prior to the reprogramming, Rolls-Royce Allison had two subcontracts, one with Bell Helicopter Textron, Inc., and the other with Purdue University. Bell was asked to provide the preferred location for the water/methanol tank and to define the design requirements. The intention was also to ask Bell to examine the logistics issues associated with supporting a water/methanol equipped aircraft. However, this latter activity was dropped as a result of reprogramming due to lack of funding. Purdue University conducted an experimental program to investigate the characteristics of a new water/methanol injection system.

In parallel with these activities, Rolls-Royce Allison embarked upon refining the definition of the baseline engine, the water/methanol injection system, and the variable geometry boost compressor. Since the work on the baseline engine and the water/methanol injection system forms the basis of the reprogrammed effort, descriptions of these activities appear in Section 5. All other work performed prior to the reprogrammed effort is outlined below.

#### 2.1.1 Variable Geometry Boost Compressor

Rolls-Royce Allison has previously employed a boost compressor on the low pressure spool as a method of boosting power output of engines without changing the core engine. This is frequently done with industrial engines, such as the 501-K series. This method to boost power was also used on the Rolls-Royce Allison/Pratt & Whitney propfan demonstrator, which was driven by a Rolls-Royce Allison 578DX. This engine employed three stages of boost compressor attached to the low pressure spool. The boost stages utilized variable geometry vanes to enhance operability, but also, more importantly, to produce a variable cycle effect. This effect allowed the airflow and pressure ratio to be maximized at takeoff and then reduced at cruise to allow the core engine to operate more near its point of best efficiency. A variation on this concept was proposed for use in the SHCT. The aim was to produce an engine that could “look big” for takeoff and be optimized for best efficiency at cruise.

The Compressor group generated compressor geometries to try to meet the goal of two design points. The boost compressor design that resulted had one stage of boost and eight stages of core compressor, one fewer than the baseline shown in Figure 9. The boost compressor is driven off the low pressure spool, which also drives the power output shaft. The boost compressor has inlet and exit vanes that are variable to allow optimization of both cruise and takeoff airflow.

The results of the design were disappointing, however, since the size of the engine relative to the baseline could not be reduced. The compressor section became quite a bit longer than the nine-stage baseline, as an additional variable vane and a transition duct were added. This comparison as shown in Figure 9. The number of high pressure turbine stages could not be eliminated since the work split was not significantly changed, so we could not realize any other engine architecture benefits.

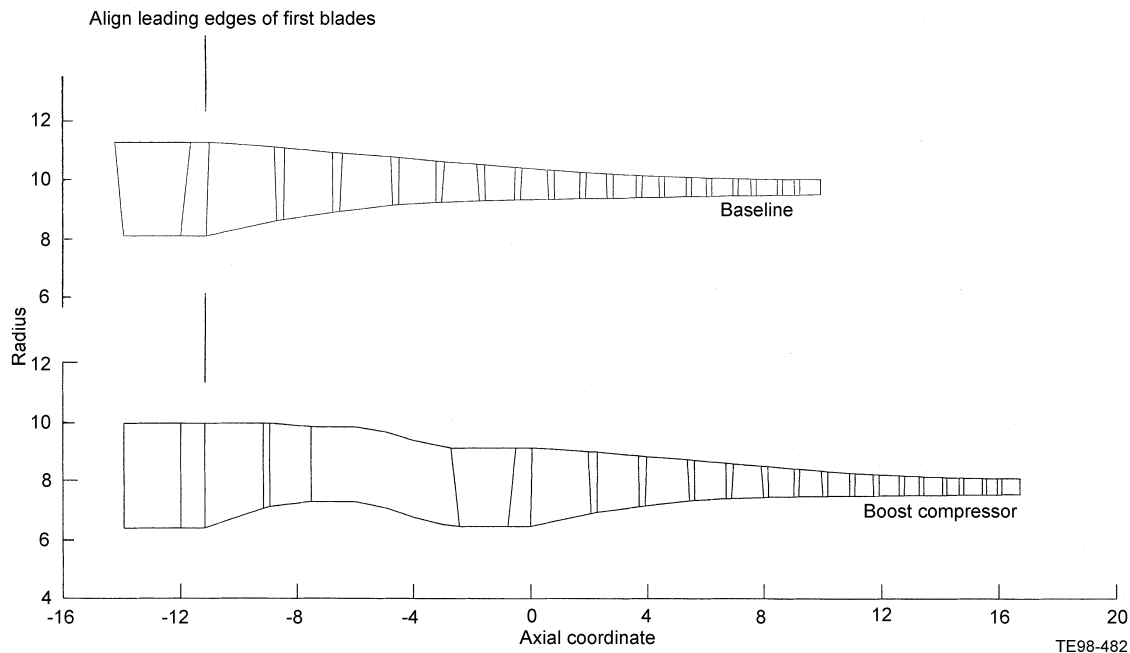


Figure 9. Compressor section size comparison.

The benefits of this concept, therefore, were limited to those seen by optimizing takeoff and cruise operating points. Though not insignificant, this kind of benefit manifesting itself as an SFC decrease at the cruise point does not produce the desired, large overall system cost decrease. The 3.3% SFC benefit with minimal engine weight increase that was seen for modulated turbine cooling in Phase I produced only a 0.13% decrease in SHCT DOC. The variable geometry boost compressor concept produces a similar SFC benefit, but with an assumed large increase in engine weight. We have to conclude that our estimates used in Phase I for the boost compressor were optimistic and further design efforts would be required to find a DOC benefit from this concept. Even the Phase I estimates ranked the variable geometry boost compressor concept as third, behind two different water/methanol injection designs, though at the time of the proposal there were strong indications the boost compressor concept had further payoffs not fully explored within the constraints of the Phase I effort.

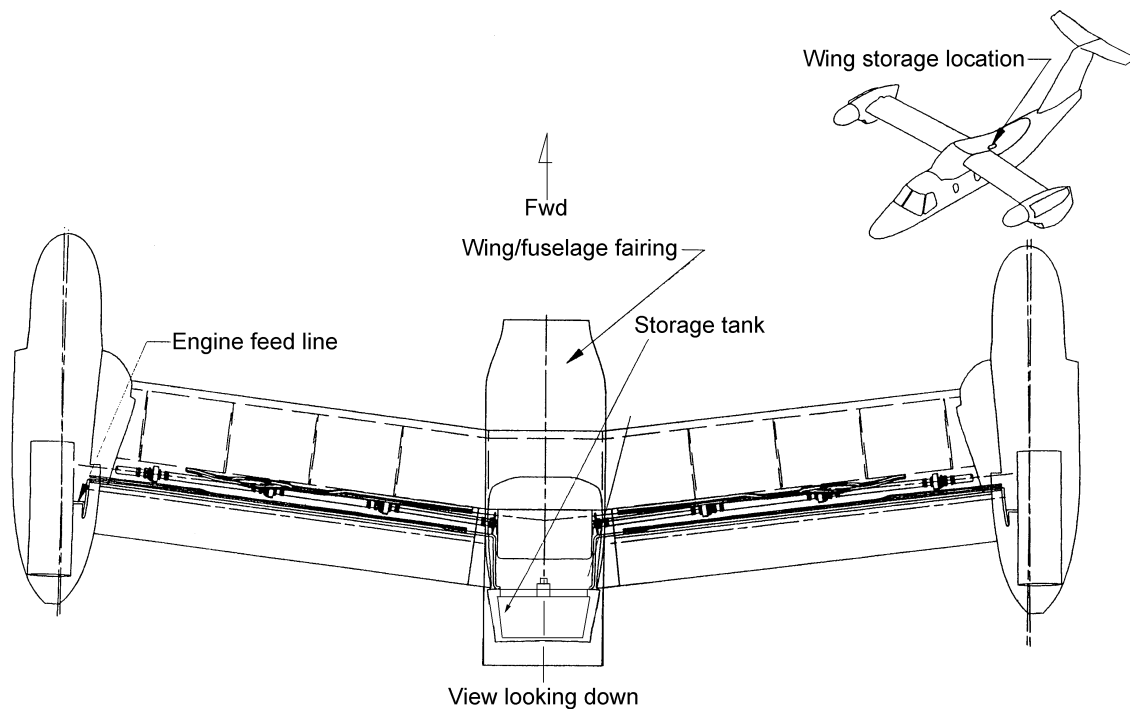
### 2.1.2 Pump and Line Sizing

Prior to the reprogramming a water injection system was designed using a 30-gallon (gal) tank located in the fuselage. The lines in the wings were pressurized by an 11.4 gal/min positive displacement pump. The pump ran continuously and maintained the pressure in the engine supply lines. To keep the pump cool, the fluid could bypass the wing lines and flow back to the tank.

The rerouted fluid passed through a filter on the way back to the tank. A check valve was mounted in parallel with the filter to permit water/methanol to bypass a clogged filter. At the exit of the wing lines a metering valve controlled the flow to the distribution manifold for the nozzles.

### 2.1.3 Bell Helicopter Studies

Bell Helicopter Textron, Inc., performed subcontract work for Rolls-Royce Allison on this contract. Bell provided guidance in integrating the water/methanol injection system into the tiltrotor aircraft design. Bell also provided drawings based on the Bell-Boeing 609 that defined water holding tank and supply line locations. This input was invaluable in providing realistic aircraft design information about the available volumes and open space within the aircraft structure. The Bell conceptual design can be seen in the drawings shown in Figure 10. The drawings show the water storage location, supply lines, and



TE98-572

Figure 10. Bell conceptual design.

the swivel attachment to accommodate the tilting nacelle. These drawings were scaled up to the NASA civil tiltrotor size by Rolls-Royce Allison to estimate system component weights and costs.

As shown in Figure 10, Bell assumed the water/methanol would be held and propelled to the engines by means of two pressurized tanks contained in the wing aft fairing area. The wing aft fairing is also where Rolls-Royce Allison assumed the water/methanol holding tank would be located. The system has been designed, however, to be unpressurized. The water/methanol would be pumped to the operating engine in the event of an OEI occurrence instead of forced from the pressurized tanks. Using an unpressurized, common storage tank and pump supplying water/methanol to either engine reduces the weight of the total system, since only the low diameter supply lines need to be strong enough to handle high pressure fluid. Also, the preflight

check of OEI availability consisting of a pressure check with the system armed can ensure water/methanol delivery pressure is available to the solenoid valve at the engine, instead of just giving a tank pressure reading.

Bell also provided water/methanol holding tank design requirements as a part of its subcontract work. These requirements are given in Table V. Since the tanks won't be pressurized, there are no additional burst containment requirements.

#### 2.1.4 Concept Down-Select for Reprogrammed Effort

The reprogramming exercise, which reduced both the time and money available for the program, forced Rolls-Royce Allison to prematurely choose a preferred concept for further refinement. The preliminary work on the boost compressor concept indicated the water/methanol injection concept should be the focus of the remainder of the program. Detailed cycle, weight, or cost analyses were not performed on the boost compressor concept, but the data acquired strongly indicated the boost compressor concept would not show as large a decrease, if any, in SHCT DOC as the water/methanol injection concept.

Table V. Water tank design loads.

Direction	g load
Lateral	6
Down	12
Forward	12

Furthermore, the nonrecurring development and certification costs of the boost compressor would be significantly higher than the water/methanol injection system. Therefore, Rolls-Royce Allison in consultation with the NASA Lewis Research Center (LeRC) program manager decided to continue work on the water/methanol injection system and not pursue the boost compressor design.

## 2.2 Reprogrammed Tasks

At NASA's request, the SHCT program was reprogrammed to accommodate a reduction in available funding. This section provides an overview of the four reprogrammed tasks. More detail can be found in the statement of work (SOW) contained in Appendix A.

### 2.2.1 Task 1—Define Propulsion System Requirements

Task 1 included the activities of defining the revised SOW and schedule; agreeing to the reprogrammed effort with the NASA LeRC program manager; defining the resource managers and control account managers; securing Rolls-Royce Allison engineering resource commitments; publishing work packages; and holding the reprogrammed effort kick-off meeting. The technical tasks in Task 1 included publishing the engine cycles (which involved conducting the mission analyses, publishing the baseline engine cycle, and publishing the injected engine cycle) and publishing the aerodynamic flow path.

### 2.2.2 Task 2—Identify Propulsion System Concepts

Task 2 included the activities of documenting the down-selected and alternate concepts; defining the water/methanol injection system requirements; conducting the water/methanol injection system analysis; defining and documenting the water/methanol injection system design requirements; and defining the turbine bypass system requirements.

### 2.2.3 Task 3—Preliminary Design

Task 3 was where the majority of the reprogrammed effort was expended. This task included defining preliminary design of the compressor, combustor, turbine, mechanical systems, water injection system, and the whole engine. The whole engine preliminary design effort also included the economic analysis that demonstrated the significant DOC advantage of an SHCT powered by the water/methanol injected engine compared with the baseline engine.

### 2.2.4 Task 4—Meetings and Reporting

This final task included all of the NASA required reporting activities. It also included the meetings required to track the reprogrammed effort using the newly acquired Rolls-Royce earned value analysis program management procedure. The earned value approach to program management has been effective at tracking customer value against expended cost.

## 3.0 Task 1—Define Propulsion System Requirements

### 3.1 Reprogramming Tasks

Task 1 included the reprogramming effort to properly capture costs to the NASA SHCT program. The specific activities included in this effort included defining the revised SOW and schedule; agreeing to the reprogrammed effort with the NASA LeRC program manager; defining the resource managers and control account managers; securing Rolls-Royce Allison engineering resource commitments; publishing work packages; and holding a kick-off meeting for the reprogrammed effort. A description of the reprogrammed tasks was presented in subsection 2.2.

### 3.2 Mission Analysis

A candidate engine cycle in the 40 lb/sec airflow class was generated and a mission analysis was conducted to determine the correct engine size. The VASCOMP computer program was used to perform the aircraft mission analysis. The results of this analysis were used to fix the baseline engine's core flow (37.9 lb/sec). Following this, the water/methanol injected baseline engine had an airflow of 27.1 lb/sec. In both cases, the OEI power requirements sized the engines.

### 3.3 Baseline Engine Cycle

The baseline engine cycle was sized by the OEI requirements. This engine is characterized by a 37.9 lb/sec mass flow. The following turbine RIT limits were set: 2650°F for takeoff, 2600°F for maximum cruise, and 2800°F for the OEI condition. The baseline engine performance at several operating points is summarized in Table VI.

### 3.4 Injected Engine Cycle

The goal of this program is to design a small engine that operates efficiently at cruise but can be operated at very high power levels consistent with a much larger engine during an OEI situation. This results in lower acquisition costs, less fuel use, and ultimately lower DOC. To achieve the necessary power increase, a water/methanol injected engine cycle was defined.

*Table VI. Baseline and injected engine performance.*

Engine	Rating	Sea level ambient temperature—°F	Altitude—ft	Velocity—ktas	Output power—shp	SFC—lb/hp-hr	RIT—°F
Baseline	OEI	88	2,000	0	8847	0.39	2800
	Idle	59	0	0	500	1.5	1394
	Takeoff	59	0	0	9295	0.39	2650
	Maximum cruise	59	25,000	350	4966	0.35	2456
	Typical cruise	59	25,000	350	3321	0.36	2067
Injected	OEI	88	2,000	0	8480	0.39	2705
	Idle	59	0	0	500	1.5	1456
	Takeoff	59	0	0	5630	0.41	2650
	Maximum cruise	59	25,000	350	3257	0.36	2493
	Typical cruise	59	25,000	350	3120	0.36	2468

The injected cycle is a modified baseline engine cycle. The amount of water/methanol injected is 5% of the core's total mass flow. The same temperature limits used in the baseline engine cycle were used here (i.e., 2650°F for takeoff, 2600°F for maximum cruise, and 2800°F for the OEI condition). To maximize the power boost at the OEI condition, the cycle was rematched at a lower corrected speed. This achieved a 34% power boost over the baseline engine cycle. The typical cruise *rated* power was maintained as a percent of the OEI power, as was done for the baseline engine. After running the VASCOMP mission analysis program, the correct flow size was determined to be 27.1 lb/sec. A summary of the injected engine's performance is detailed in Table VI.

### 3.5 Aerodynamic Flow Path

The aerodynamic flow path of the baseline engine is illustrated in Figure 11. The compressor is an eight-stage unit with a pressure ratio of 18.1:1. The polytropic efficiency is 89% and has a surge margin of 20%. This design is characterized by high stage loading with a relatively small airflow size. The inlet guide vane plus the first three stator rows have variable geometry. A compressor bleed is placed at the exit of stage 4. The combustor was sized for low emissions. The turbine configuration is a single-stage high pressure (HP) turbine and a two-stage low pressure (LP) turbine connected by a short transition duct. To reduce secondary losses in the power turbine first-stage vane, the HP and LP turbines are designed to rotate in opposite directions. This has an additional advantage of reducing the net gyroscopic moment of the engine. The turbine aerodynamic design point was selected at a 25,000 ft, 350 ktas, International Standard Atmosphere (ISA), cruise condition. The HP and LP turbines have efficiencies of 84.1% and 92.1%, respectively.

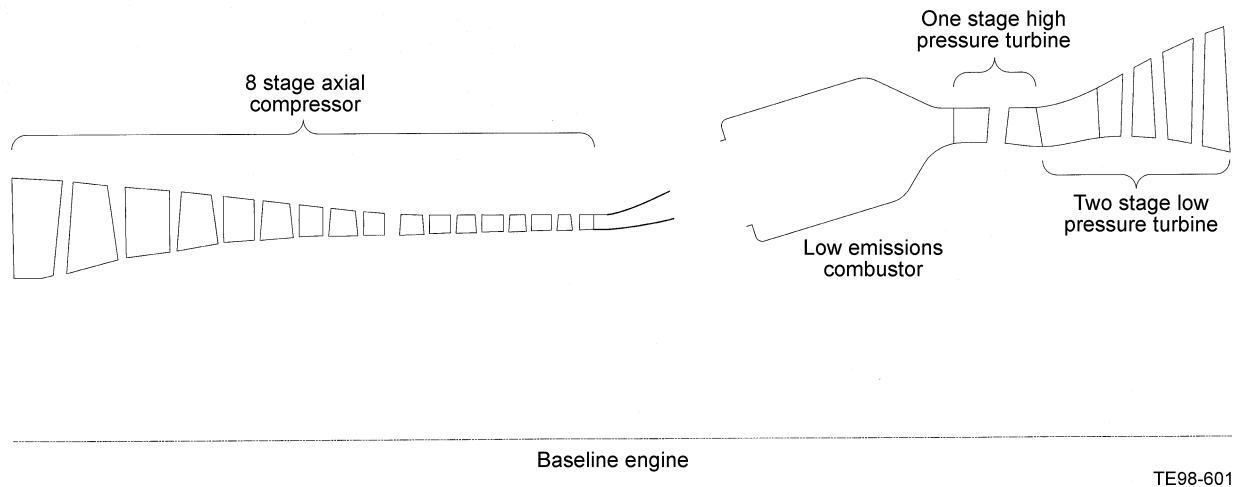


Figure 11. Engine flow path.

## **4.0 Task 2—Identify Propulsion System Concepts**

This section describes the work performed on verifying the proposed water/methanol injection concept was viable. The down-selection process and the turbine bypass system requirements were trivial exercises, but are included below to maintain consistency with the statement of work prior to reprogramming.

### **4.1 Down-Selected and Alternate Concepts**

As stated in subsection 2.1.6, the reprogramming exercise, which reduced both the time and money available for the program, forced Rolls-Royce Allison to prematurely choose a preferred concept for further refinement. The preliminary work on the boost compressor concept indicated the water/methanol injection concept should be the focus of the remainder of the program. Detailed cycle, weight, and cost analyses were not performed on the boost compressor concept, but the data acquired strongly indicate the boost compressor concept would not show as large a decrease, if any, in SHCT DOC as the water/methanol injection concept. Furthermore, the nonrecurring development and certification costs of the boost compressor would be significantly higher than the water/methanol injection system. Therefore Rolls-Royce Allison, in consultation with the NASA LeRC program manager, decided to continue work on the water/methanol injection system and not to further pursue the boost compressor design.

### **4.2 Water/Methanol Injection Studies**

Two major studies were successfully completed as part of the NASA Civil Tiltrotor Engine program. The first study was the development of a three-dimensional (3D) aerothermal analysis code to simulate the water droplet trajectories and evaporation in a multistage axial flow compressor. The second study was the design and rig testing of a plain jet atomizer and an effervescent-water/methanol atomizer for the production of very small (<10 microns) droplets.

To aid in the design of an optimum water/methanol injection system, a 3D aerothermal analysis code was developed to study the droplet trajectory and evaporation characteristics in a multistage axial flow compressor. The numerical results show that to get maximum benefit out of a water/methanol injection system in a gas turbine engine, the liquid has to be atomized to very small droplets (<10 microns). Rig test results show the plain jet atomizers are not feasible in an aircraft application such as the SHCT engine, because hundreds of injectors are needed to get the required liquid flow and droplet sizes. Rig tests show sprays with sub 10-micron droplets can be obtained at an air-to-liquid ratio (ALR) in an injector of 0.10 and an injection pressure of 250 psi using effervescent atomizers. Addition of methanol to water lowers the Sauter mean diameter (SMD) of the spray. With a water/methanol spray, consistent sub 10-micron SMDs can be obtained even with an injection pressure of 150 psi and an ALR of 0.05 using effervescent atomizers. The work described in the following subsections demonstrates the feasibility of using an efficient water/methanol injection system for aircraft gas turbine engine power enhancements.

#### **4.2.1 Three-Dimensional Aerothermal Analysis Code**

As a first step in the design of an efficient water/methanol injection system, it was decided to develop a 3D aerothermal analysis code to simulate water injection into a compressor. This code aids in the design of an optimized injection system for maximum evaporation of the droplets with minimal impingement on the casing. This section of the report presents the development of a 3D aerothermal analysis code, experimental data on an engine test carried out with water-methanol injection, and the results of the analysis and limited comparison with test data.

##### **4.2.1.1 Numerical Analysis**

The analysis combines solutions of complex equations for 3D compressor flow prediction, computation of 3D droplet trajectories, droplet evaporation characteristics, and droplet impingement locations on both the hub and casing surfaces of the compressor.

The multistage compressor flow field can be computed using any of the established solvers, such as Euler, Navier-Stokes, or streamline curvature methods. In this case, the streamline curvature code was used to establish the 3D flow pattern in the compressor.

The droplet dynamics of a gas-droplet suspension are determined by the gas-droplet interaction and droplet-solid boundary impacts. The trajectory of a droplet in a moving fluid is governed by the vector balance of its rate of change of momentum and the external force field. The streamline curve computation provides the external flow field. The motion of the droplet is described by the 3D Lagrangian equations of motion. These equations are given by:

$$\frac{d^2x}{dt^2} = G \left( v_x - \frac{dx}{dt} \right)$$

$$\frac{d^2r}{dt^2} = G \left( v_r - \frac{dr}{dt} \right) + r \left( \frac{d\Theta}{dt} \right)^2$$

$$\frac{d^2\Theta}{dt^2} = \frac{G}{r} \left( v_\Theta - \frac{d\Theta}{dt} \right) + \frac{2}{r} \frac{dr}{dt} \frac{d\Theta}{dt}$$

where

$$G = \frac{\Pi C_d}{8DZ} \frac{\rho}{\rho p} v_{rel}$$

and x, r, and q define the droplet location in axial, radial, and tangential directions. The coefficient of drag of the droplet,  $C_d$ , is calculated from empirical correlations. The correlations are a result of extensive droplet characterization studies conducted at Rolls-Royce Allison on a specially built wind tunnel that simulates altitude conditions to 20,000 ft.

The 3D flow field strongly influences the droplet evaporation characteristics. The evaporation of the droplet is due mainly to convection and is a strong function of the droplet Reynolds number. The Reynolds number past a spherical droplet is:

$$Re_d = \rho V d / \mu$$

where the velocity, V, is either the relative velocity between the droplet and the airstream or the flow turbulent velocity.

$$V = u' = \text{turbulent intensity} * V_{air}, \text{ magnitude}$$

The droplet Reynolds number is used to calculate the droplet evaporation rate with convection.

$$m_{\text{convection}} = (1+0.3 \cdot \text{Re}_d^{1/2} \text{Pr}_g^{1/3}) * 2 \Pi d (k/C_p) g \ln(1+B_y)$$

where  $B_y$ , the mass transfer number, is:

$$B_y = Y_{F_s} / (1 - Y_{F_s})$$

and  $Y_{F_s}$ , the mass fraction of vapor at the drop surface, is given by:

$$Y_{F_s} = P_{F_s} M_F / (P_{F_s} M_F + (P - P_{F_s}) M_A)$$

The rate of evaporation is used in the heat transfer equations. The convection heat transfer to the air is given by:

$$Q_{\text{convection}} = 2 \Pi d k_g (T_{\infty} - T_s) (1+0.3 \cdot \text{Re}_d^{1/2} \text{Pr}_g^{1/3}) * \ln(1+B_y) / B_y$$

and

$$Q_{\text{evaporation}} = m_{\text{convection}} L_{\text{evap}} ((T_{\text{cr}} - T_s) / (T_{\text{cr}} - T_{\text{BN}}))^{0.38}$$

The time rate of temperature change is calculated as:

$$Q_{\text{evaporation}} - Q_{\text{convection}} = \Pi/6 \rho_{\text{liquid}} d^3 C_{p, \text{liquid}} dT_s/dt$$

From these equations, the temperature change of the droplet and the surrounding air can be calculated for a given time step.

The droplets are introduced at the inlet of the compressor at various radial locations and their paths are traced through the compressor. The droplet equations of motion and evaporation are solved at small time intervals. The trajectories are computed until the droplets exit from the compressor, completely evaporate, or impinge on either the hub or shroud surface of the compressor.

#### 4.2.1.2 Comparison of Numerical Results with Limited Test Data

Rolls-Royce Allison has been very successful in using 3D trajectory codes on previous programs such as Comanche/T801 inlet particle separator and AE 1107C turbofan engine rain and hail ingestion studies. To further validate the code, it was decided to compare numerical results with previously run Rolls-Royce Allison T56 engine water ingestion test data.

##### 4.2.1.2.1 T56 Engine Test

A Rolls-Royce Allison T56 turboshaft engine was tested with water/methanol injection to measure the effects of the injection on turboshaft performance.<sup>1</sup> The engine tested was an earlier version of the T56, rated at 4500 shp with an airflow of 32.4 lb/sec. The compressor had 14 stages and was 26-in. long with a compressor pressure ratio of 9.6:1. The turbine had four stages.

The water/methanol mixture flow rates injected were 1, 2, 3, 3.5, 4, and 5.2 gallons per minute (gpm). The compressor inlet air temperature was 60°F and the water/methanol mixture temperature was 30°F. The turbine inlet temperature (TIT) was held constant at 1780°F for each injection flow rate. The increase in shaft horsepower is plotted in Figure 12 as a function of the water/methanol flow injected. The maximum increase in shaft horsepower obtained during this testing was 14.5%. After each water/methanol flow condition tested, the engine was run in the dry condition, i.e., no water/methanol injection. In the dry condition, the worst case measured shaft horsepower decreased by 2.1% relative to the performance of the engine before any water/methanol was injected. After all water/methanol testing was completed, the compressor was cleaned by injecting crushed walnut shells into the compressor. Engine testing at the dry condition after this cleaning resulted in a shaft horsepower 1.3% below the initial dry value. This is considered a permanent loss in shaft horsepower.

The loss in power after water/methanol injection was caused by the compressor blades rubbing the compressor casing during the wet condition, which resulted in increased compressor blade tip clearances during the dry condition. During the T56 test, temperatures were measured on the compressor casing. In addition, a thermocouple rake was used to measure the air liquid mixture temperature at the compressor exit. The thermocouple rake measurements were impinged on by water and air, so the measurements were representative of the compressor blade temperatures. The temperature differences between the case and the thermocouple rake closest to the case are shown in Figure 13 for various water-methanol flow rates. Clearly, the drop in case temperature relative to blade temperature is significant. This temperature difference between the rotating blades and the stationary casing drastically reduces the clearances between them.

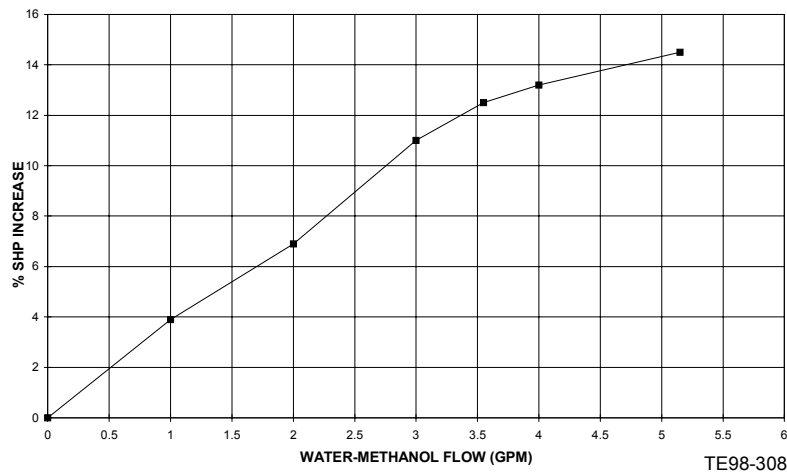


Figure 12. T56 engine test demonstrates the increase in shaft horsepower with water/methanol injection.

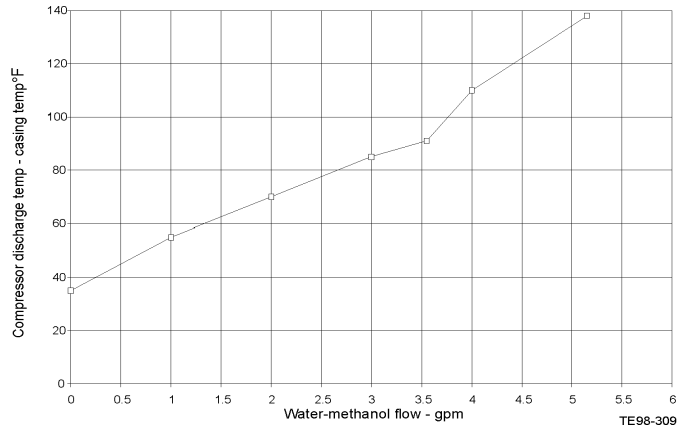


Figure 13. Measured temperature difference between compressor discharge and casing temperature resulting from water/methanol injection.

Numerical simulation of the droplet trajectories clearly shows the impingement locations on the casing for various droplet sizes in Figure 14. The droplets injected into the air stream have droplet diameters ranging from 200 to 2000 microns. The water/methanol injection conditions are the same as those used in the engine test and are described in Table VII.

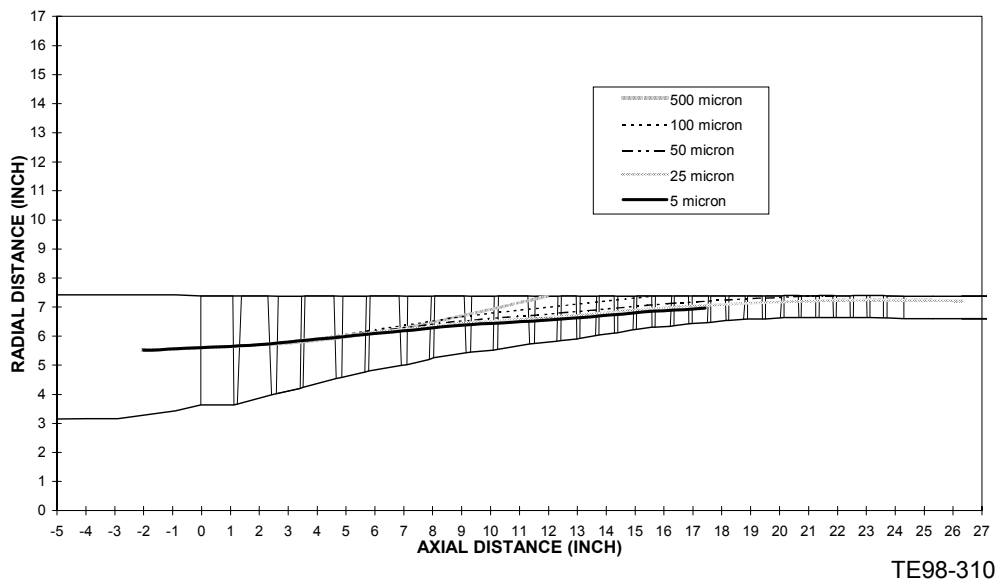


Figure 14. Computed droplet trajectories in the T56 compressor for various droplet sizes.

Table VII. Water-methanol injection conditions for T56 analysis.

Engine airflow—lbm/sec	32.4
Water/methanol flow	4.0 gpm = 0.5 lbm/sec
Liquid supply pressure—psig	72
Injection nozzle diameter—in.	0.052
Injected liquid velocity—ft/sec	77
Initial droplet temperature—°F	30.0
Water mass fraction	0.56
Turbulence—%	4

As shown in Figure 14, all droplets with initial diameters greater than 50 microns will impinge on the casing. The code does not take into account the droplet interaction with the vanes/blades, therefore all droplet trajectories shown are without vane/blade impingement. The movement of droplets to outer radii is caused by the angular rotation of the flow field. The angular rotation of the flow field gives the droplets angular rotation, which causes the large droplets to be centrifuged to the casing. As shown in Figure 14, the droplet size must be 50 to 25 microns or smaller to avoid case impingement. These smaller sized drops do not hit the casing because they are small enough to follow the flow field very closely. The analytical results show the 200- to 2000-micron droplets injected during the T56 engine test impinge on the compressor casing. This result corroborates the Figure 13 test data showing the reduction in case temperature due to water/methanol impingement.

The amount of evaporation resulting for the injected droplets is plotted in Figure 15 versus axial distance. Note that no significant evaporation occurs for the 200-micron droplets. While about 30% of the 25-micron droplets evaporate, only 20% evaporate upstream of 23 in., which is the axial location of the last row of blades. The droplet sizes need to get down into the 5 to 10-micron range before complete evaporation occurs. The static gas temperature in the compressor is plotted in Figure 16. No appreciable drop in static temperature occurs for the 200-micron droplets. Once again, the droplets need to be in the 5- to 10-micron range for the static temperature reduction to be significant.

#### 4.2.1.3 Computer Simulation of Water/Methanol Injection in the Civil Tiltrotor Compressor

The input conditions for this analysis are listed in Table VIII, and a layout of the compressor is shown in Figure 17. A Rolls-Royce Allison generated 3D compressor flow field was used.

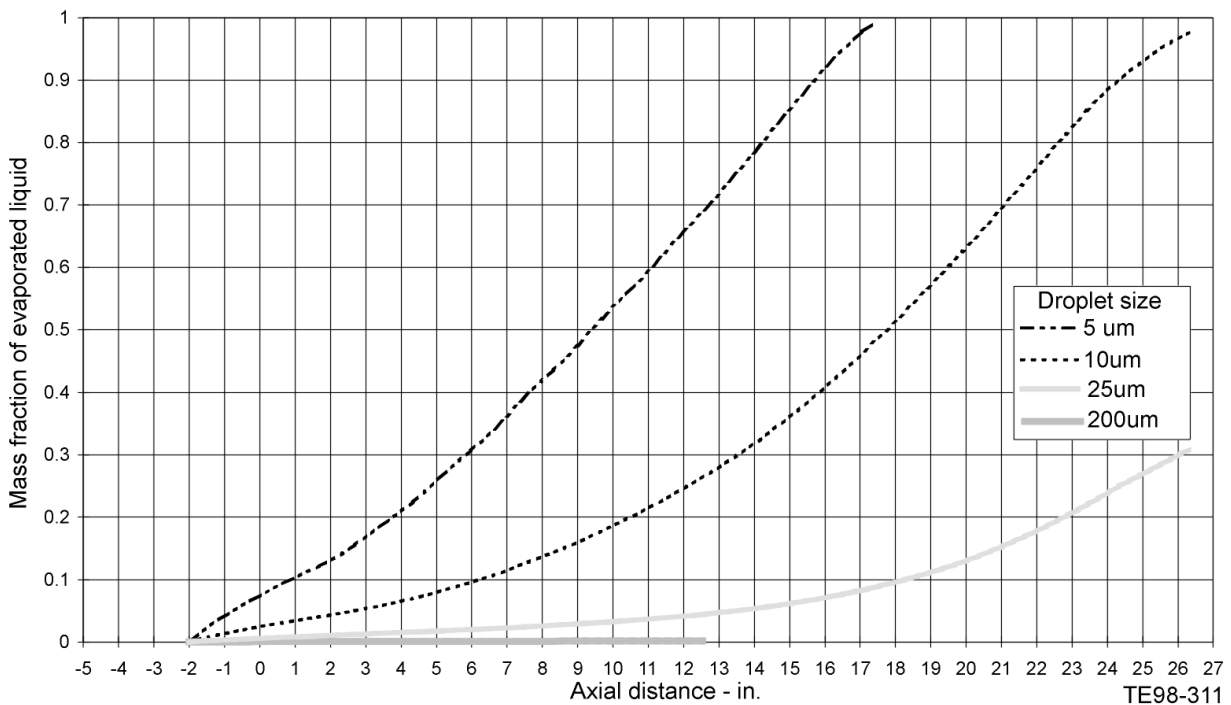


Figure 15. Computed droplet evaporation as a function of compressor axial length for various droplet sizes.

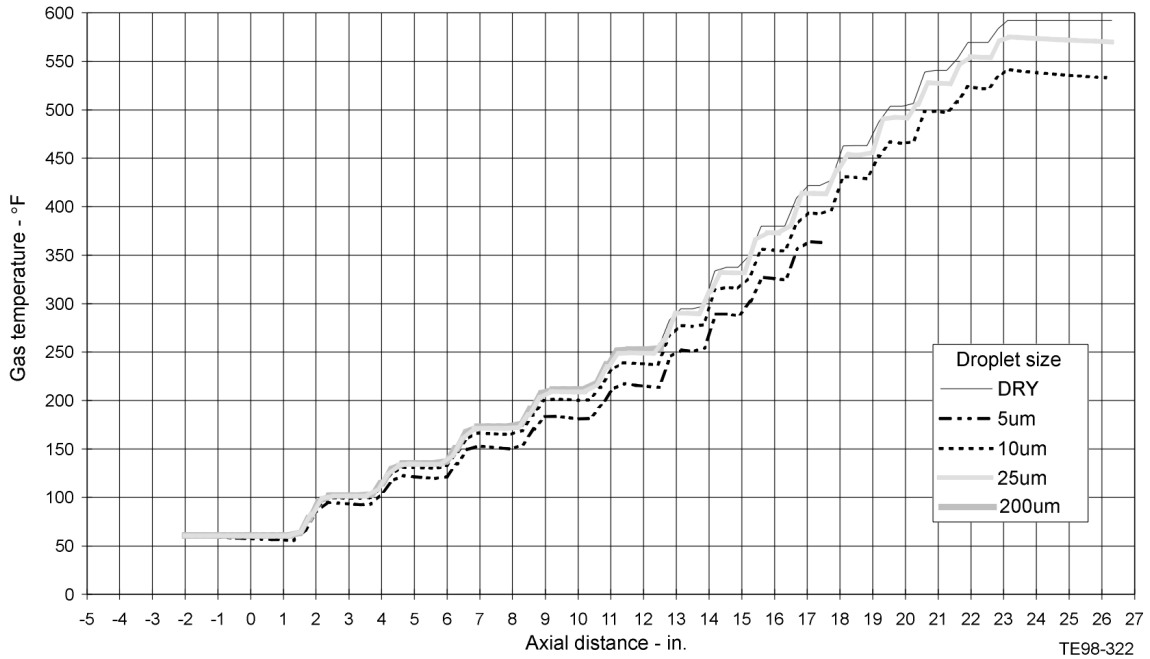


Figure 16. Computed gas temperature as a function of axial length for a T56 engine.

Table VIII. Water/methanol injection conditions for the tiltrotor engine.

Engine airflow—lbm/sec	37.6
Water/methanol flow—lbm/sec	1.326
Liquid supply pressure—psig	667
Injection nozzle diameter—in.	0.025
Injected liquid velocity—ft/sec	220
Initial droplet temperature—°F	58.7
Water mass fraction	0.7
Turbulence—%	4

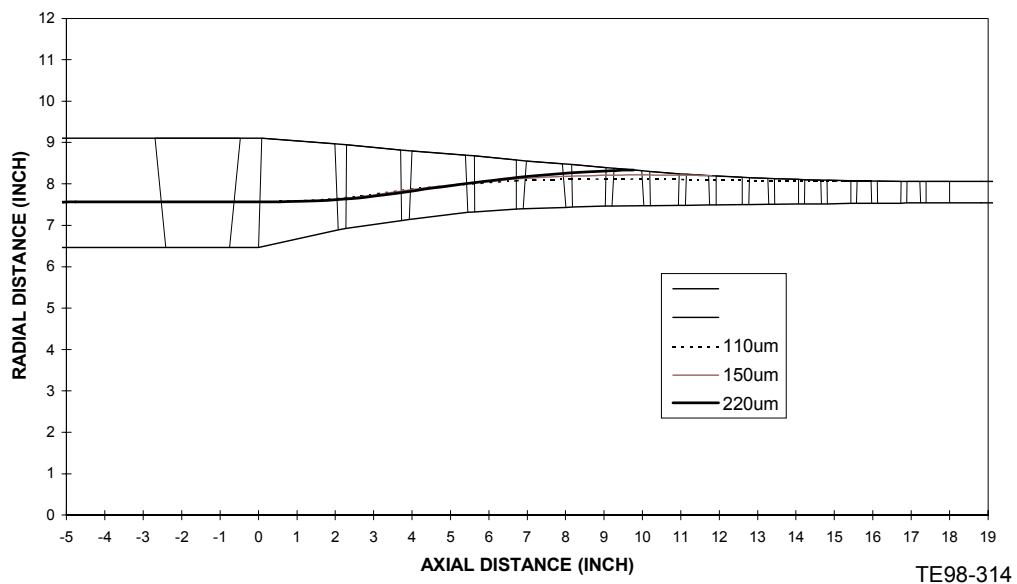


Figure 17. Typical computed droplet trajectories (civil tiltrotor engine).

As shown in Figure 17, larger droplets tend to migrate toward the casing, while smaller droplets follow the streamlines and completely evaporate. Figure 18 shows the percentage of liquid evaporated as a function of compressor axial distance, for 8-micron diameter droplets. Figure 19 shows the corresponding reduction in average gas temperature as a function of compressor axial distance for various water/methanol flow rates expressed as a percentage of compressor airflow rate ( $w_{25\%} = 42$  lb/sec for this case).

The 3D droplet simulation code is a good tool that yields the relevant parameters so a compressor analyst can revise the compressor performance map to take into account the effect of water droplets.

#### 4.2.2 Design and Rig Testing of Atomizers

The computer simulation of the droplets in an axial compressor clearly showed the importance of atomizing water/methanol into very small droplets (<10 microns). To achieve this, we looked into two types of atomizers: (a) plain jet and (b) effervescent atomizers.

##### 4.2.2.1 Plain Jet Atomizer

A plain jet atomizer (Figure 20) was designed and tested in the Rolls-Royce Allison research laboratories to evaluate droplet size distribution. The atomizer was run at different pressure and the droplet size distribution was measured using Malvern laser droplet analyzer.

Figure 21 shows the water flow rate as a function of nozzle pressure drop, while Figure 22 shows how the droplet size decreases with increase in nozzle pressure drop. Figure 23 shows the Rosin-Rammler droplet size distribution at a nozzle pressure drop of 667 psig.

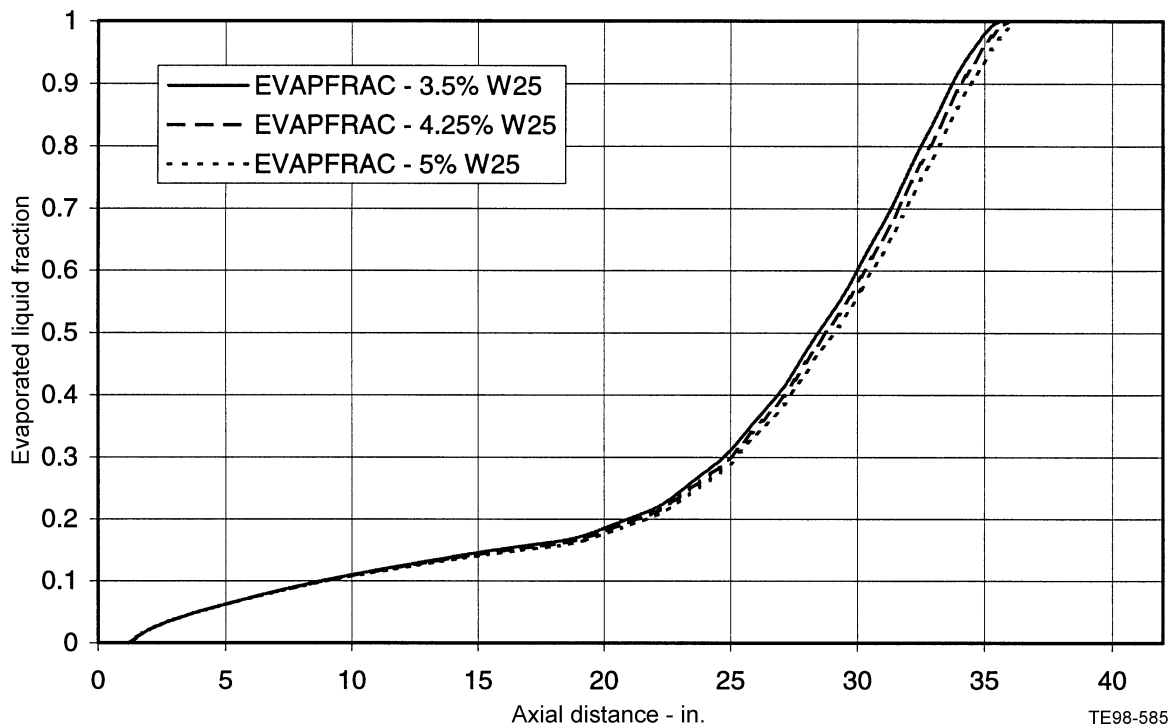


Figure 18. Computed droplet evaporation as a function of axial length for an average droplet diameter of 8 microns (NASA civil tiltrotor engine).

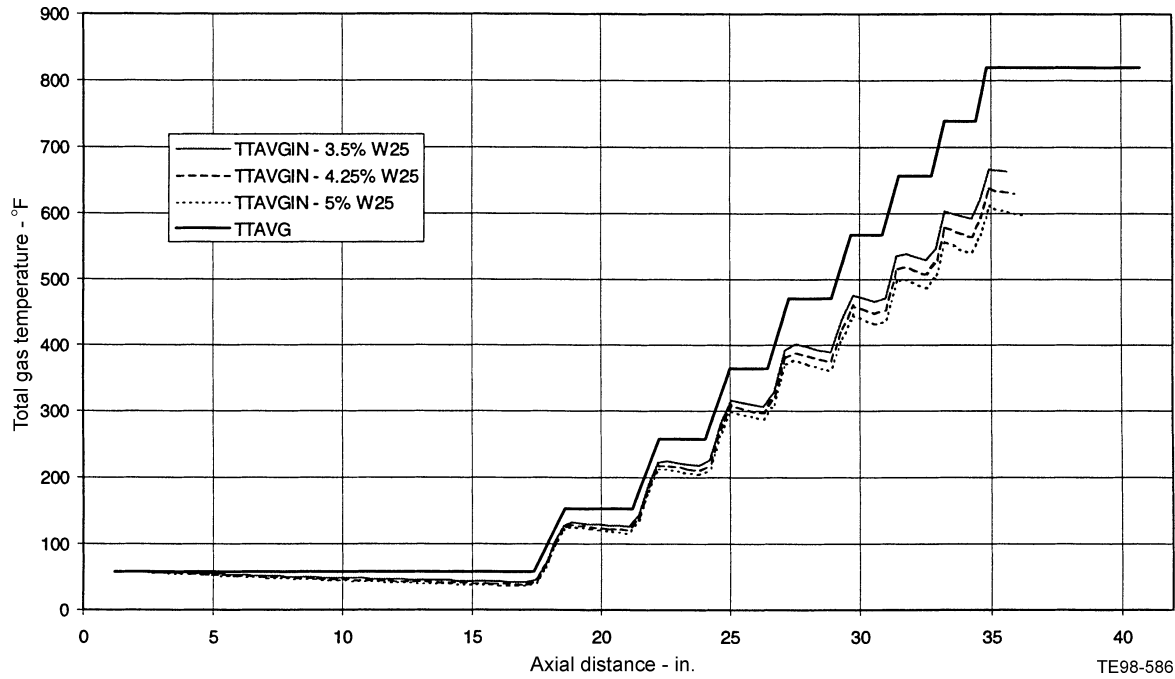


Figure 19. Computed gas temperature as a function of axial length for an average droplet diameter of 8 microns (NASA civil tiltrotor engine).

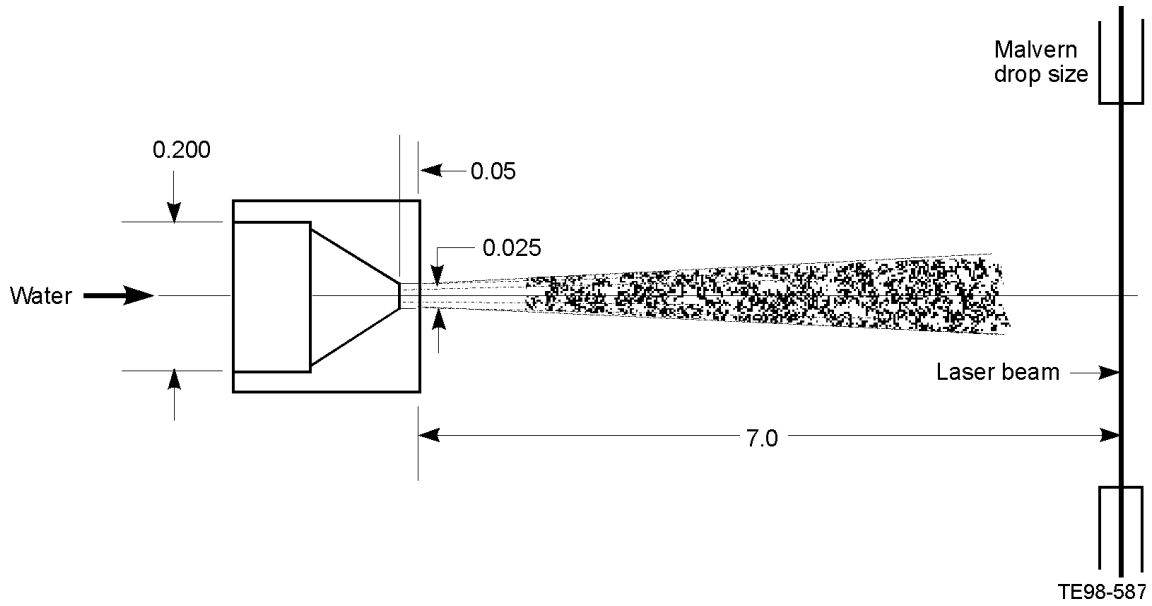
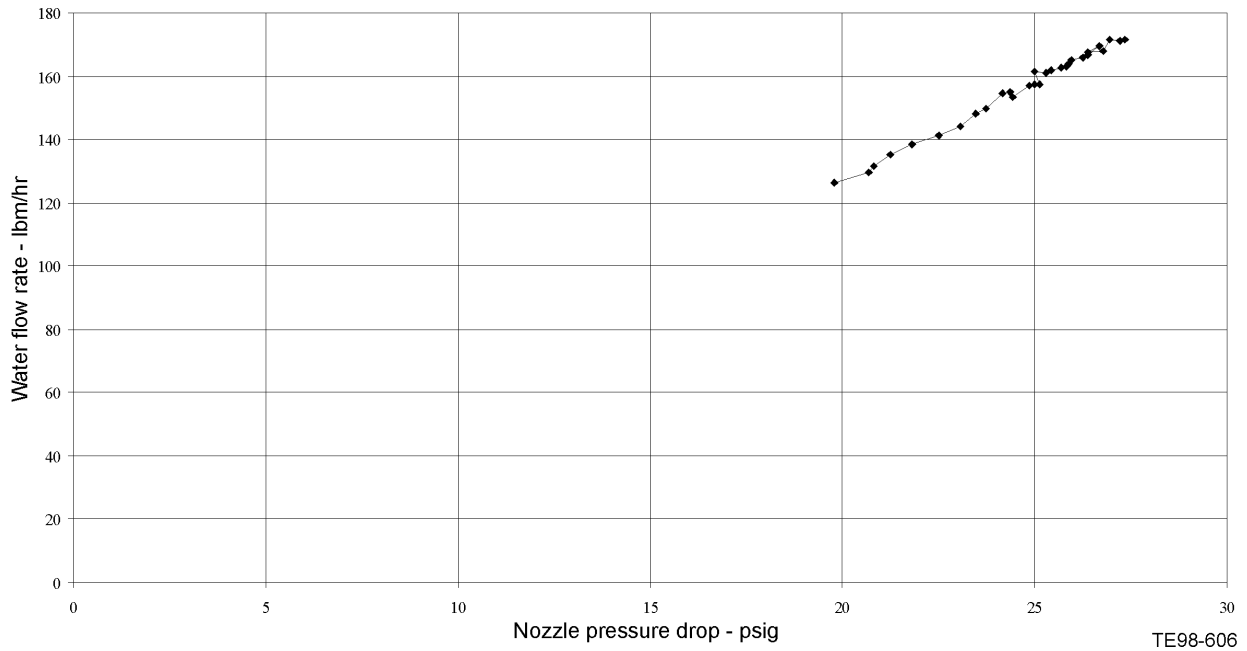
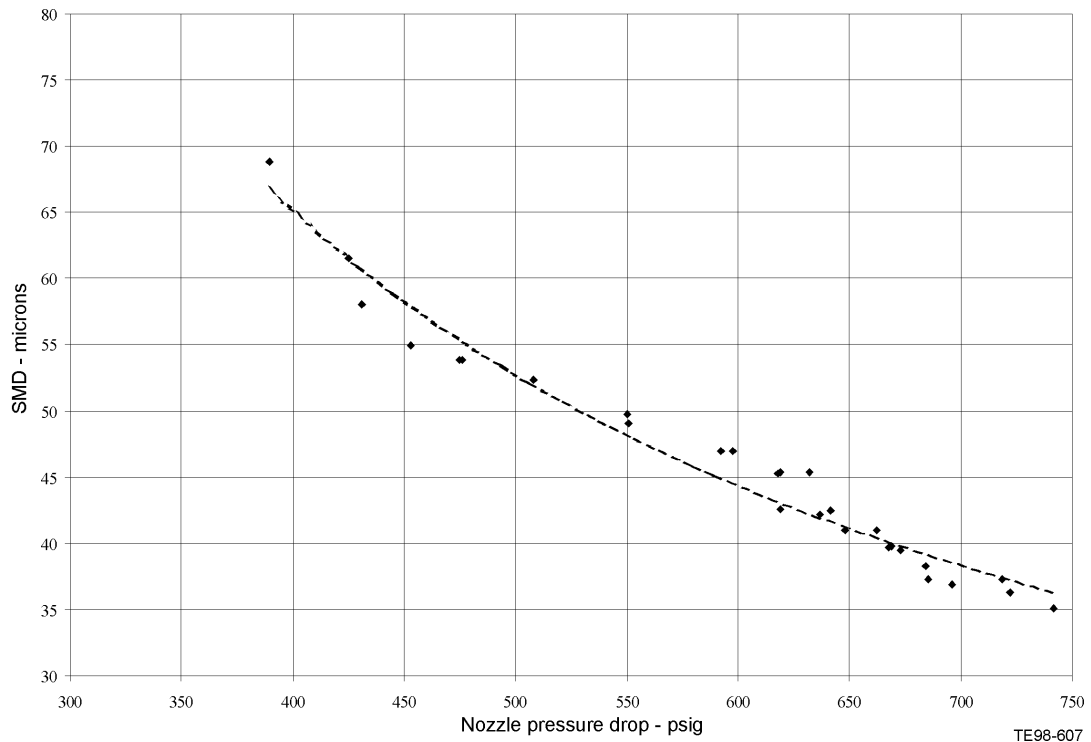


Figure 20. Plain jet atomizer setup.



TE98-606

Figure 21. Plain jet atomizer flow characteristics, hole diameter 0.025 in.,  $L/D = 2$ , water.



TE98-607

Figure 22. Plain jet atomizer flow characteristics, hole diameter 0.025 in.,  $L/D = 2$ , water.

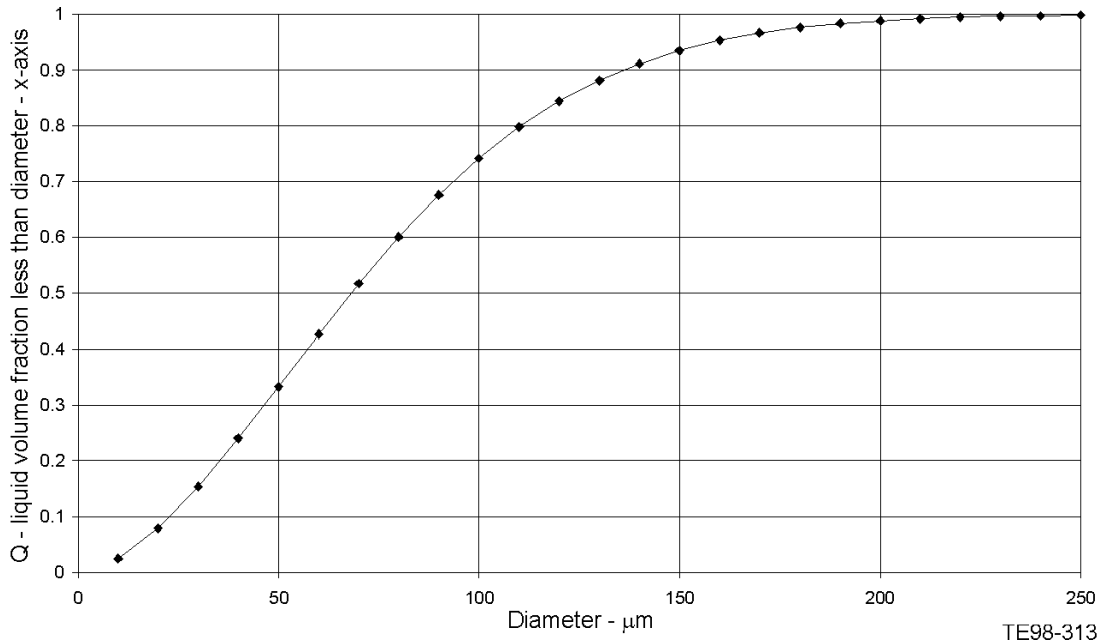


Figure 23. Rosin-Rammler droplet size distribution for a plain jet atomizer ( $n = 1.74$ ,  $x \text{ bar} = 84$ , Sauter mean diameter =  $40 \mu\text{m}$ , orifice diameter =  $0.025$ , injection pressure =  $667 \text{ psig}$ ).

The rig test data clearly showed that to get smaller than 10-micron sized droplets, very small diameter orifice ( $<0.025 \text{ in.}$ ) injectors need to be used along with very high pressure pumps ( $>3000 \text{ psi}$ ). This would entail hundreds of atomizers to be used in the civil tiltrotor engine application with heavy duty piping to withstand high liquid pressures. This is clearly not feasible for aircraft application, so it was then decided to explore effervescent atomizers.

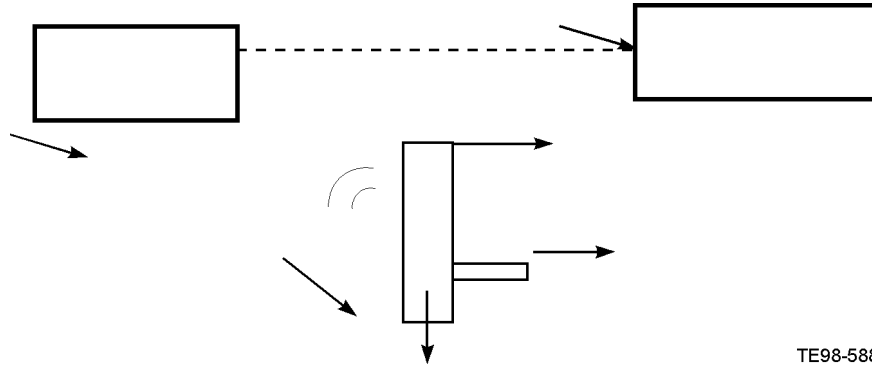
#### 4.2.2.2 Effervescent Atomizers

The overall objective was to examine the feasibility of obtaining sub 10-micron mean drop size sprays using an effervescent atomizer with low injection pressures ( $250 \text{ psi}$ ), high liquid loading ( $25 \text{ to } 100 \text{ gm/s}$ ), and with ALRs below 10%. A subcontract was awarded to En'Urga Inc, which conducted the rig tests at the Purdue University Aerothermal Laboratories.

##### 4.2.2.2.1 Experimental Arrangement

The experimental arrangement used for the feasibility study of the effervescent atomizer is shown in Figure 24. The SMD of the effervescent spray was measured using a Malvern particle analyzer. The Malvern particle analyzer was mounted horizontally and the effervescent atomizer was mounted on a vertical traversing mechanism. This allowed radial profiles of the SMD of the spray to be measured at any axial location. Two different nozzle diameters ( $1 \text{ mm}$  and  $3 \text{ mm}$ ) were used for the experiments. Figure 24 shows a typical effervescent atomizer.

Measurements were taken for eight test conditions using water and four test conditions using a mixture of 30% methanol and 70% water (by weight). The test conditions are shown in Table IX. The test conditions involved the two nozzles operating at two different ALRs each. For each injector diameter and ALR condition, two operating pressures were used. Measurement of SMD was obtained at axial distances of  $50 \text{ and } 100 \text{ mm}$ . Attempts to obtain SMD measurements at greater than  $100 \text{ mm}$  were not successful due to wetting of the Malvern lens by the spray. The momentum fluxes for the water sprays were obtained using a laboratory scale.



TE98-588

Figure 24. Experimental arrangement used to evaluate the effervescent atomizer.

Table IX. Operating conditions used for the evaluation tests.

Nozzle diameter—mm	Liquid flow rate—gm/s	Both liquids	ALR	Nominal pressure—psi
3.0	45.2	No	0.097	150 <sup>a</sup>
3.0	64.8	No	0.052	150
3.0	63.9	No	0.100	250 <sup>b</sup>
3.0	94.4	No	0.053	250
1.0	13.0	Yes	0.100	150
1.0	19.8	Yes	0.047	150
1.0	22.8	Yes	0.097	250
1.0	30.2	Yes	0.050	250

<sup>a</sup> Pressure achieved within the injector was 125 psi.  
<sup>b</sup> Pressure achieved within the injector was 225 psi.

#### 4.2.2.2.2 Results and Discussion

The results obtained from the tests are shown in three sections. The first section describes the droplet size distribution of the water spray. The second section describes the momentum flux obtained using a laboratory scale, and the last section details results obtained using a mixture of 30% methanol/70% water (by weight).

**Drop Size Characterization for the Water Spray** The spray characterizations for the 1 mm diameter nozzle at an axial location of 50 mm and for the different operating conditions are shown in Figure 25. The objective of obtaining the radial profiles is to study the variation in the SMDs as well as the 10 and 90% diameters. Diameters of 10 and 90% are sizes below which 10 and 90% of the spray mass resides, respectively. Figure 25 shows the obscuration for the 150 psi injection pressure is always less than 0.91. The profiles are smooth and the confidence level of these measurements is very high. For the 250 psi injection pressure, the results for the 5% ALR are also obtained with low centerline obscuration rates. For the 10% ALR condition, the obscuration rates are high, but the SMDs are expected to be lower than those obtained with the lower ALR of 5%. The results confirm this expectation and are reasonably accurate despite the high obscuration ratios. However, the 90% diameter result for high ALR (0.1) and high injection pressure (250 psi) is not accurate as shown by discontinuity in the radial profile. The 90% diameter could be as high as 50 microns instead of the 20 microns obtained from the Malvern measurements.

The measurements were repeated at an axial location of 100 mm. The reason for repeating the measurements at another location was to take advantage of the spread of the spray in an effort to reduce the centerline (CL) obscuration. The spray characteristics obtained for the 1 mm nozzle at an axial

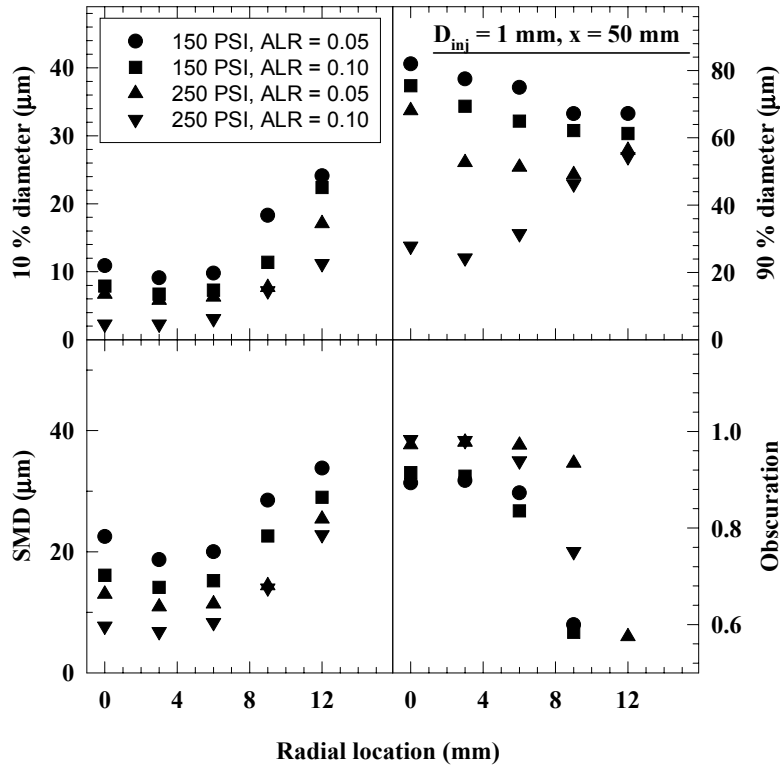


Figure 25. Drop characteristics for the 1 mm nozzle at an axial location of 50 mm.

location of 100 mm are shown in Figure 26. The results obtained show the SMDs are slightly higher than those obtained at 50 mm. This is expected since the very small droplets are expected to evaporate or coalesce, causing an upward bias in the drop diameters. From the 90% diameter plot, it can be seen that 90% of the droplets are smaller than 50 microns for an ALR of 0.10 and smaller than 60 microns for an ALR of 0.05. The important trend observed is that the higher injection pressure reduces the SMD of the spray significantly without changing the 90% diameter, while higher ALRs reduce the 90% diameter as well.

The spray characteristics obtained with the 3 mm diameter nozzle at an axial location of 50 mm are shown in Figure 27. The results show smooth radial profiles for the 150 mm psi injection pressure even though the CL obscuration ratios are higher than 0.99; therefore, the confidence level in these measurements is high. From the 90% diameter profile, some inversion can be seen for the higher ALR ratio at 150 psi; however, even close to the edge, the 90% diameter is 50 microns. It is expected that the 90% diameter of the spray is less than 60 microns. For the 250 psi injection pressure, the centerline SMDs are very low at less than 5 microns; however, the radial profiles of the 90 and 10% diameters cast doubts on the accuracy of these measurements. The very high obscuration prevents the measurements of the higher diameter droplets; therefore, the SMD is expected to be less than 10 microns (based on the results obtained at 150 psi) despite the lack of corroborating evidence.

The spray characteristics for the 3 mm diameter nozzle at an axial location of 100 mm with an injection pressure of 150 psi are shown in Figure 28. For the 250 psi injection pressure, the radial spread of the spray was too high, preventing any measurements even at distances of 75 mm. The results in general confirm the SMD of the spray is less than 10 microns and the 90% diameter for the lower ALR is approximately 60 microns. For the higher ALR, the 90% diameter value is not very reliable even though the results show a value of less than 40 microns.

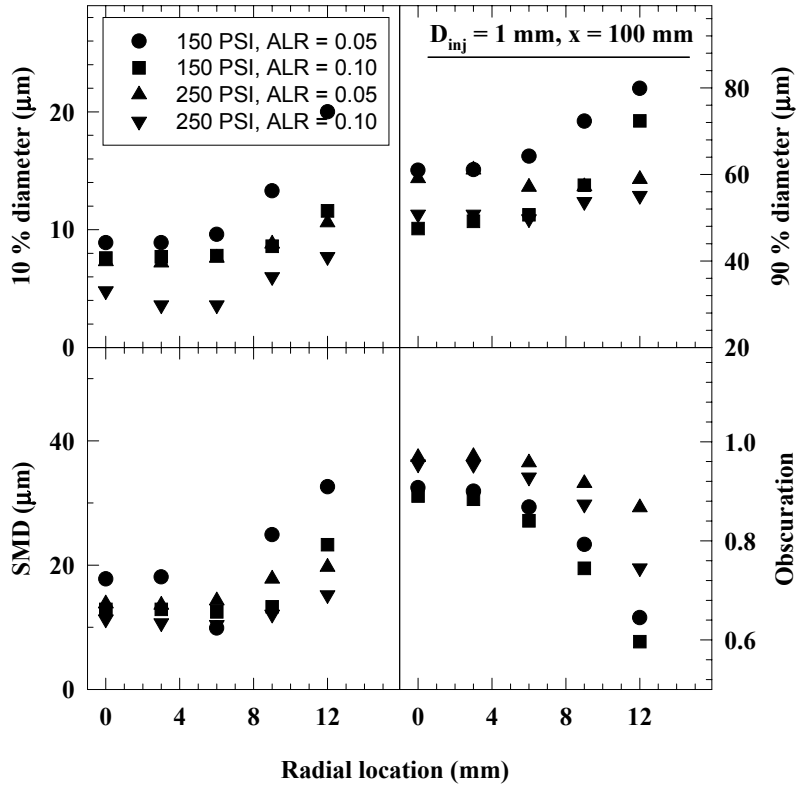


Figure 26. Drop characteristics of the 1 mm nozzle at an axial location of 100 mm.

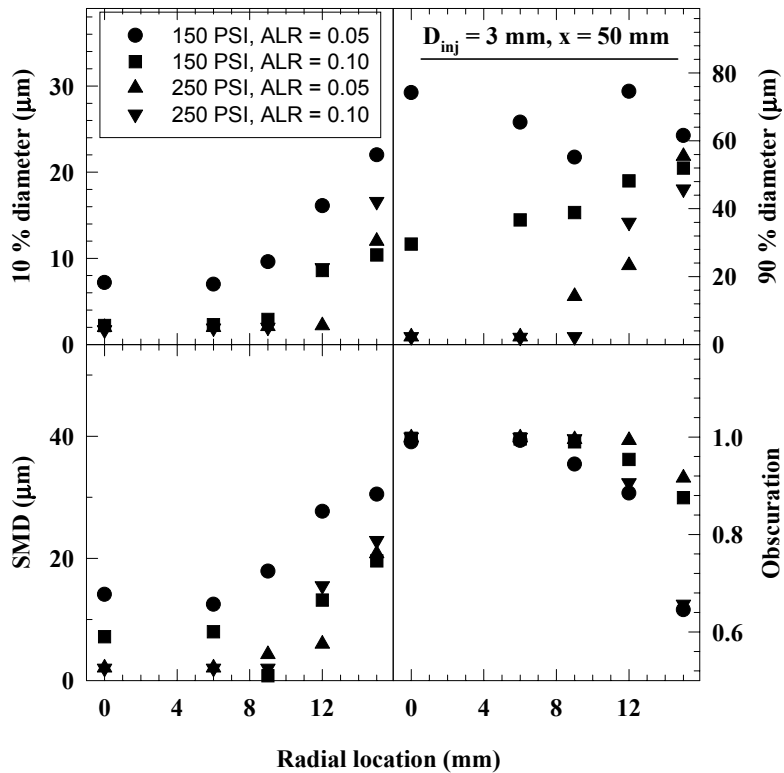


Figure 27. Drop characteristics of the 3 mm nozzle at an axial location of 50 mm.

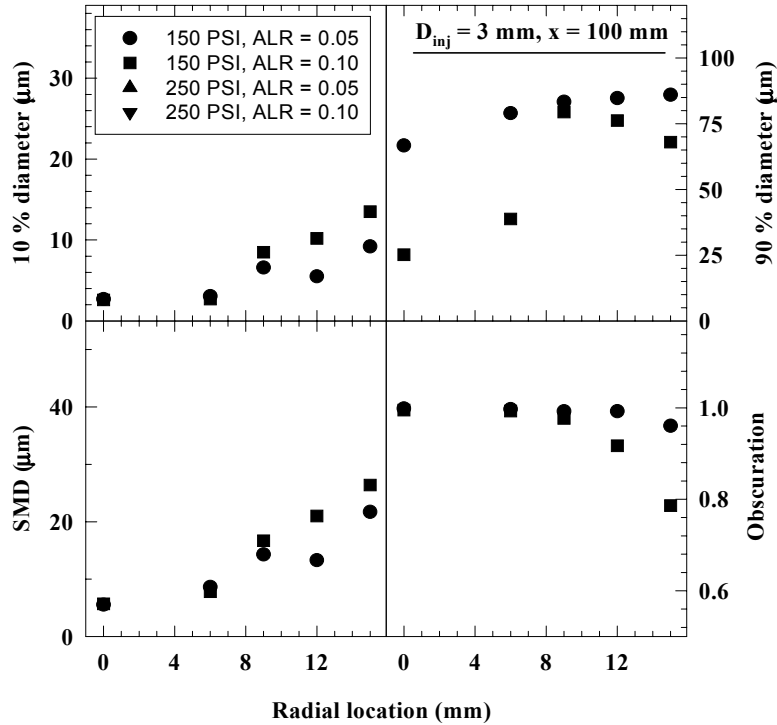


Figure 28. Drop characteristics of the 3 mm nozzle at an axial location of 100 mm.

For the 1 mm diameter nozzle, the results obtained at the centerline for 150 psi (0.1 ALR) and 250 psi (0.05 ALR) injector pressures show SMDs below 15 microns. The probability density functions (PDFs) of the drop sizes for these two conditions are shown in Figure 29. Approximately 50% of the drops are smaller than 25 microns for both these conditions, and 20% of the drops are larger than 50 microns. However, the maximum size of the drops in these sprays is smaller than 100 microns.

Similarly, for the 3 mm nozzle, sub 10-micron SMDs were obtained using injection pressures of 150 psi (ALR of 0.10) and 150 psi (ALR of 0.05) at a distance of 12 mm from the centerline of the spray. The PDFs of drop sizes for these two conditions are shown in Figure 30. In both cases, approximately 50% of the drops are smaller than 10 microns. In addition, there are very few drops with diameters larger than 25 microns, and almost no drops larger than 50 microns. The SMD in both cases is below 10 microns.

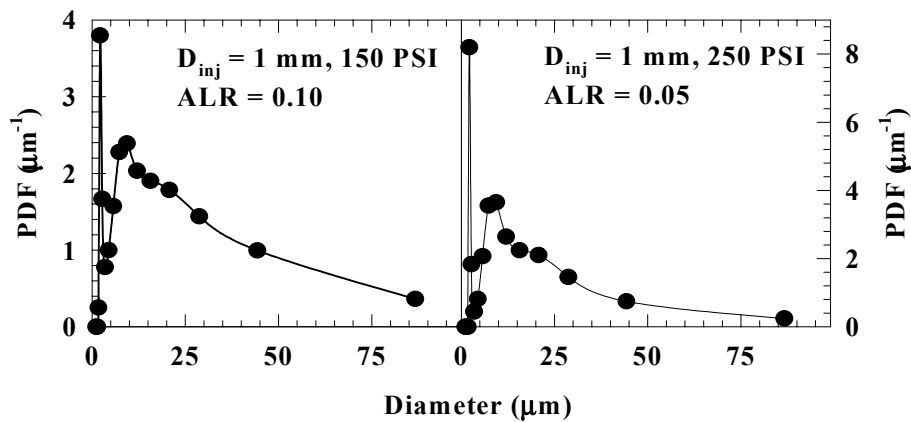


Figure 29. PDFs of the droplets obtained using a 1 mm diameter effervescent spray.

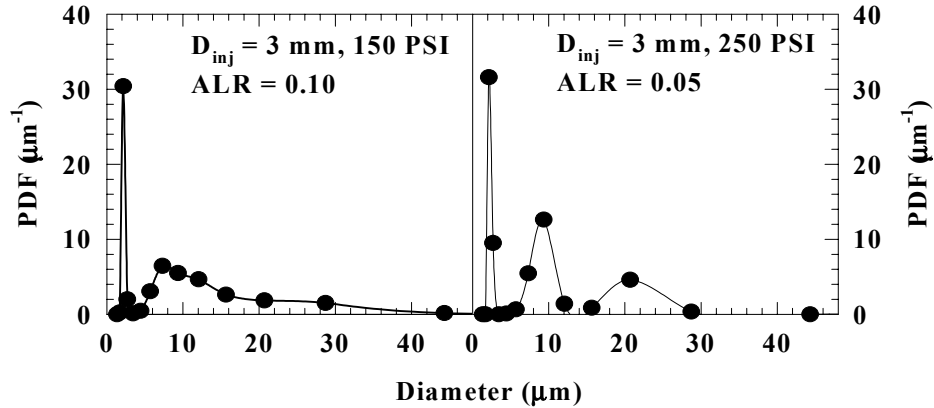


Figure 30. PDFs of the droplets obtained using a 3 mm diameter effervescent spray.

The feasibility of obtaining water sprays with an SMD of below 10 microns (with less than 250 psi injection pressure and less than 0.10 ALR) using effervescent atomization is conclusively demonstrated.

All of these measurements were obtained in a stagnant atmosphere. In the presence of a cross flow, the particle sizes are not expected to increase. These measurements can be used as the inlet conditions for approximate drop trajectory calculations. For drop trajectory calculations, the initial conditions of the spray (radial profiles of mass and momentum flux) are needed in addition to the cross-flow velocity. The next section details the momentum flux measurements obtained using a laboratory scale during this project.

**Momentum Flux for the Water Sprays** The mean force exerted by the spray was measured using a laboratory scale. The results of the measurements are provided in Table X.

All the sprays obtained in this study were too dense to use the obscuration profiles to obtain radial mass flux profiles; however, for trajectory calculations, both top hat and parabolic inlet mass flow profiles can be used. The mean trajectory of the spray is not expected to be sensitive to the specific inlet mass flow profile used. Supply pressures and orifice diameters are clearly the dominant factors in the momentum of the spray; therefore, the momentum can be controlled independent of the SMD using different ALR. Thus, the drop penetration is somewhat decoupled from the specific mass flux profile.

Table X. Momentum flux of the effervescent atomizer.

Injector diameter—mm	Liquid flow rate—gm/s	ALR	Nominal pressure—psi	Area integrated momentum flux—gms
3.0	45.2	0.097	150	500
3.0	64.8	0.052	150	520
3.0	63.9	0.100	250	800
3.0	94.4	0.053	250	940
1.0	13.0	0.100	150	130
1.0	19.8	0.047	150	130
1.0	22.8	0.097	250	260
1.0	30.2	0.050	250	270

**Drop Size Characterization of Methanol/Water Sprays** The final task undertaken during this project was to measure the drop sizes for sprays containing 30% methanol with 70% water by weight. To prevent too high obscuration rates for these measurements, the 1 mm diameter injector nozzle was used. The drop size characteristics of the methanol/water spray are shown in Figure 31. For comparison purposes, the results obtained using water sprays having the same flow rate and injection pressure are also shown in Figure 31 as closed symbols. The addition of methanol lowers both the surface tension and the viscosity of the fluid; therefore, the drop sizes are smaller for all the test conditions.

SMDs below 10 microns were obtained consistently for both injection pressures and ALRs. The centerline obscuration rate with methanol is higher; however, the radial profiles are very smooth and in some cases SMDs of approximately 10 microns were obtained with relatively low (0.91 and 0.83) obscuration rates. PDFs of drop sizes for two locations (CL for 150 psi injection pressure and 9 mm from the CL for 250 psi injection pressure) that had obscuration rates of 0.91 and 0.83, respectively, are shown in Figure 32.

Approximately 50% of the drops are smaller than 20 microns and 90% of the drops are smaller than 45 microns. The major conclusion that can be drawn from these results is that SMDs below 10 microns can be obtained even with very low injection pressures and very low ALRs.

### 4.3 Turbine Bypass System Requirements

When the water/methanol is injected into the engine, a reduction in surge margin is a concern. It was thought a turbine bypass system would be required to overcome this effect; however, after conducting the performance cycle analysis, it became apparent sufficient surge margin is maintained and a turbine bypass system was not necessary.

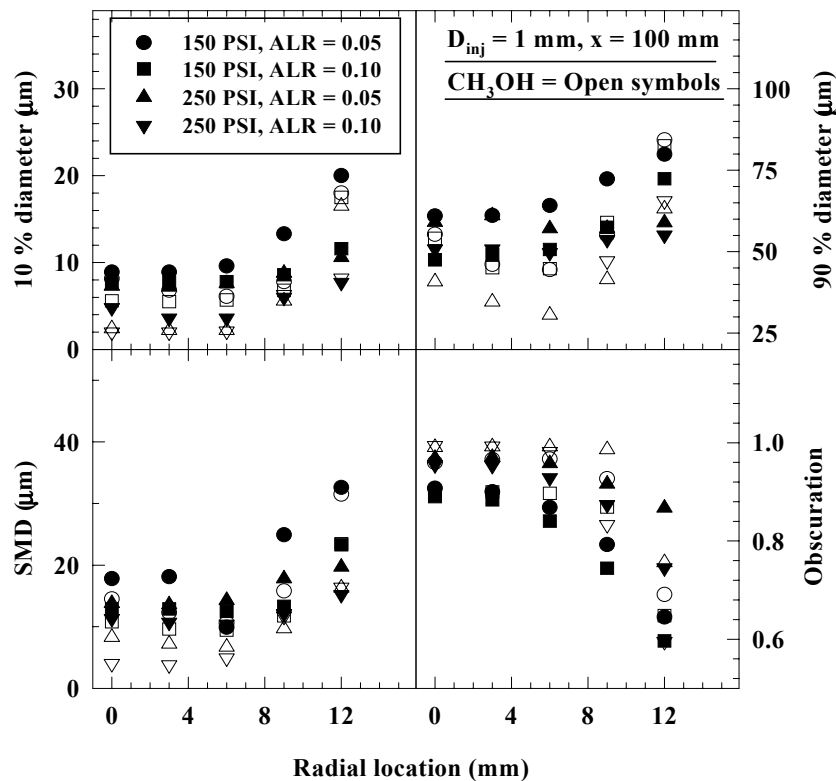


Figure 31. Change in the spray characteristics with the addition of methanol.

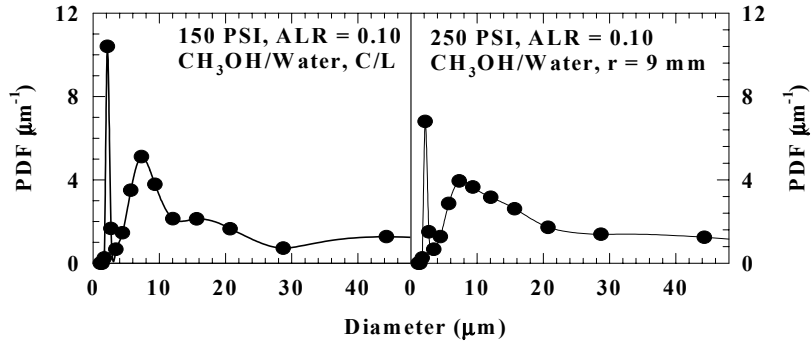


Figure 32. PDFs of the droplets obtained using methanol/water mixture.

## 5.0 Task 3—Preliminary Design

### 5.1 Compressor Preliminary Design

#### 5.1.1 Baseline Aerodynamic Design

The compressor selected for the preliminary design configuration is an eight-stage unit having a corrected airflow of 42 lb/sec, a pressure ratio of 18.1:1, and a corrected rpm of 17,580. This design is scaleable within the airflow range for both the baseline and injected engines. The polytropic efficiency and surge margin are 89% and 20%, respectively. The design is characterized as having high stage loading and relatively small airflow size. Average stage work for example is some 20% higher than that for the GE Energy Efficient Engine (EEE) compressor, while the exit corrected airflow (a size parameter) is 56% smaller than that of the EEE machine. At this flow size, the polytropic efficiency goal of 89% is aggressive as illustrated in Figure 33, which shows state-of-the-art axial compressor technology in terms of polytropic efficiency versus exit corrected airflow with average stage pressure ratio as a parameter.

At the smaller flow size blade tip clearance is a larger percentage of the blade span and endwall boundary layers predominate; airfoil thickness and edge radii have lower limits, which in turn impacts aspect ratio selection; and fillet radii occupy a larger portion of the airfoils.

Mechanical constraints guiding the compressor preliminary design include:

- Rpm set by turbine mechanical limits
- Airfoil maximum thickness held to a minimum of 0.040 in.
- Minimum leading/trailing edge radii value is 0.005 in.
- Minimum exit annulus height set at 0.500 in.

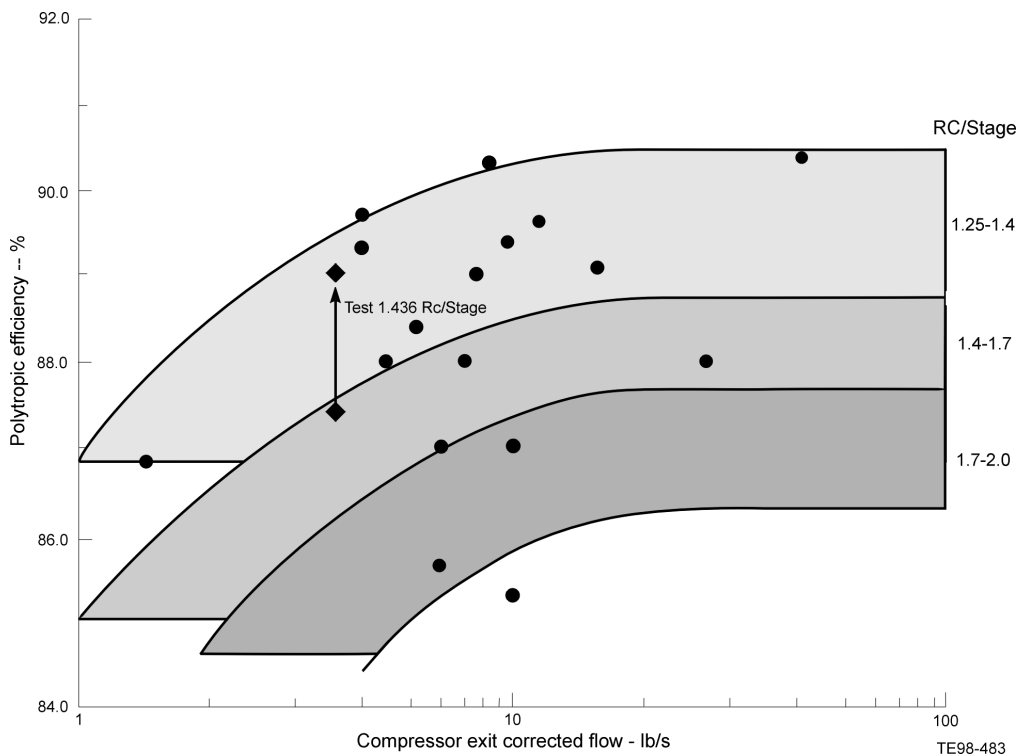


Figure 33. Compressor efficiency is aggressive compared with state of the art.

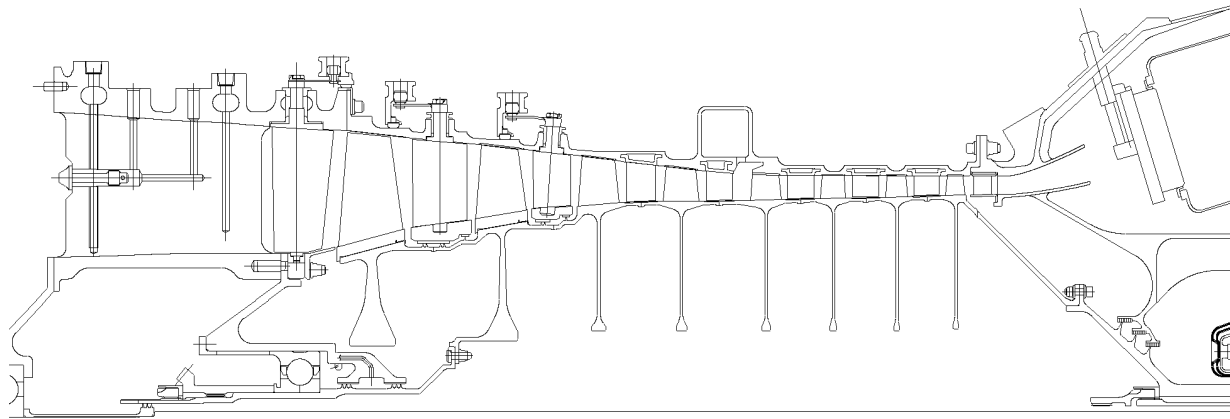
Figure 34 shows a flow-path cross section of the preliminary design configuration.

Variable geometry is used in the inlet guide vane plus the first two stator rows, and an interstage bleed is placed at the exit of stage four. The compressor airfoil count is 1272, which is a reduction of 38% relative to the AE 1107C 14-stage compressor.

Table XI further compares this compressor with the AE 1107C compressor. The preliminary design is 4.2 in. shorter than the AE 1107C with 43% fewer stages with a significant increase in the average stage pressure ratio.

### 5.1.2 Effect of Water/Methanol Injection on Compressor Performance

Generally, the compressor map is the means by which the compression process is represented in engine cycle decks. It is assumed the working fluid is “dry air” alone and corrections are applied for humidity effects. Water/methanol injection at compressor inlet, however, cannot be treated in the same way as humidity. Its benefit to engine output power results from the heat transfer to the fluid in its liquid phase, which results in evaporation and makes the compressor look more efficient, and by the simple addition of working fluid mass flow. The resultant reduction in compressor delivery temperature also permits more fuel to be added to restore RIT, which increases rotor rpm and further increases engine



TE98-498

Figure 34. Compressor flow-path cross section.

Table XI. Compressor design parameter comparison.

	Preliminary design	AE 1107C
Number of stages	8	14
Corrected airflow—lb/sec	42.00	37.50
Pressure ratio	18.10	16.60
Average stage pressure ratio	1.436	1.222
Corrected rpm	17580	15265
Length—in.	18.61	22.81
Average diffusion factor	0.455	0.395
Number of airfoils	1272	2063

airflow and power. The most direct means of modeling the compression process with entrained water/methanol is to modify a dry air compressor map for the presence of the water/methanol so the resultant map can still be used in the customary fashion in the cycle deck. The procedure adopted for modifying the map involves an adaptation of the notion of stage stacking.

The overall map for the proposed eight-stage compressor was generated by stacking 3 subcomponent (2- or 3-stage) maps scaled from the experimentally defined subcomponent maps of a similar compressor, each responding to a prescribed addition of water. The proportion of water, in both liquid and gaseous phases, relative to the “dry air” through-flow and the distribution of gas (air/water/methanol vapor mixture) temperatures through the compressor were prescribed by the heat transfer model described in subsection 4.2. Each subcomponent map was then scaled (relative to its respective dry air submap) for the combined effects of reduced inlet temperature, increased blockage (associated with the amount of liquid water/methanol still entrained), and altered gas mixture (air/water/methanol vapor) properties.

Once the maps for each subcomponent block have been scaled, they are restacked to produce a new overall compressor map that is unique for a given volume flow rate of inlet water/methanol, such as that shown in Figure 35. Typically, the rematching produces little change in the pressure ratio-flow map. Here, there is a marked increase in flow at speed which is the result of introducing the water/methanol well upstream of the compressor. Fully 14% of the water/methanol injected is predicted to have evaporated upon reaching the compressor inlet, causing it to run 17°F cooler than it would dry. As a result, a greater airflow of increased density is drawn in through the same inlet despite the added volume of water. The indicated corrected flow is the sum of both this flow of air and the water/methanol already vaporized.

A difficulty with this approach is its apparent effect on stall line. Since pressure ratio at speed is little changed with the increase in flow, the stall line appears shifted to the right, thereby reducing stall margin relative to a given operating line. In reality stall lines do not scale. Some small loss in stall margin has been observed in past compressor tests with water/methanol injection, but this loss correlates with deterioration in tip clearances. If there is insufficient atomization of the water, it is centrifuged to the case, which runs cooler and so does not grow as designed with the rotor, and causes severe rubs. The proposed water/methanol delivery system has been designed for very fine atomization that circumvents this. There is, otherwise, no reason to expect any discernable reduction in stall line.

The most dramatic change to the map with water/methanol injection shows in the efficiency contours at the top of Figure 35. Since the presence of the water/methanol has little impact on pressure rise through the compressor, but vastly reduces temperatures, efficiencies considerably greater than 100% are calculated. While this would seem to violate the Second Law of Thermodynamics, it results from using the definition of efficiency to suit a process other than the one from which it is derived. Compression with water/methanol injection involves heat transfer between constituents in a two-phase flow system, whereas classical efficiency is defined for a single homogeneous working fluid. The water/methanol is effectively an additional heat sink the engine cycle has no other way to recognize.

The two extra speed lines with water/methanol injection for 105 and 110% corrected were added after scaling the dry map to expedite overspeed calculations in the cycle deck. They were scaled based on trends observed in the original dry map data associated with choke.

### 5.1.3 Trade Study Options

The starting point for the compressor preliminary design was a defined engine cycle and aerodynamic flow path. The preliminary aerodynamic design resulted in an eight-stage compressor configuration, based on the latest advanced compressor technology. Several main configurations were analyzed as alternatives for the basic mechanical design of the compressor.

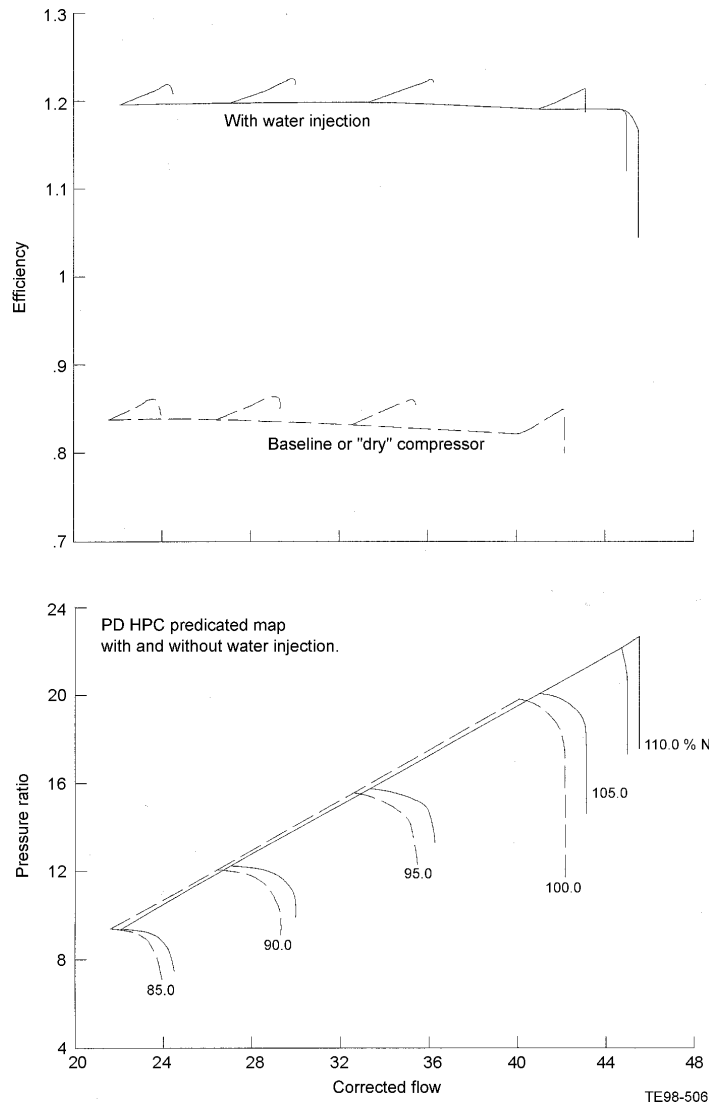


Figure 35. Overall compressor map.

A stacked rotor construction, similar to the AE 1107C/AE engine series designs, using splines at the disc rims to transmit the torque between rotor stages, with a tiebolt clamping the whole rotor together, was used as the baseline configuration. The blades all have axial type attachments, based on our current experience on the AE 1107C. The static structure here is basically the same as on the AE 1107C/AE engine series with a reduction in the number of variable guide vanes (VGVs) in relation to the reduction in the number of stages from the baseline AE 1107C engine. The stationary vanes are all of a fixed-fixed construction with a solid inner vane band, again similar to the AE 1107C engine.

Several design variations were studied to determine an optimal configuration. The various configurations included the following design features: welded rotor, circumferential attachments, cantilevered vanes, and bladed disks (blisks). These features were integrated into various compressor mechanical arrangements as described in Table XII. The result of this evaluation is the determination that configuration F is the optimal design.

Table XII. Trade study option summary.

Option	Rotor style	Axial attachments	Circumferential attachments	Blisk	Cantilevered vanes
A	Stacked	1-8	—	—	—
B	Welded	1-8	—	—	—
C	Welded	1-2	3-8	—	—
D	Welded	1-2	3-8	—	3-8
E	Welded	1-2	—	3-8	—
F	Welded	1-2	—	3-8	3-8

### 5.1.4 Mechanical Design Considerations

Once the basic aerodynamic blading was designed, then the airfoil volumes were obtained for preliminary sizing of the blade attachments and discs. Preliminary attachment sizes for the axial style attachments were determined for the appropriate configurations. Simple stalk and bearing stress calculations were performed to size the circumferential attachments.

After a downselect of the most promising configurations, disc sizing was performed in detail for the axial attachment versions of the rotor (options A and B) and for the blisk versions (options E and F). These two basic design configurations usually have the greatest change in disc size and hence engine weight. The circumferential attachment discs (options C and D) were assumed to be the same size as the axial attachment discs. However, it must be stated the rotor rim speed is higher for the NASA SHCT than previous designs and it is possible the circumferential attachment options may indeed result in heavier discs than has been assumed.

The use of a welded rotor is a critical improvement to the existing design philosophy. The disc rims would be electron-beam (EB) welded together to form a compressor drum that could then be fitted with blades using either axial or circumferential attachments. The advantage of an EB-welded construction is that it is relatively simple, lightweight, and removes the necessity of having the splines at the disc rims to transmit the torque between stages. It is cheaper than the baseline rotor construction. The only disadvantage of a welded disc construction is that if any particular stage is damaged or its low cycle fatigue (LCF) life is used up then the complete rotor has to be replaced. Industry experience has shown the risk of disc/drum damage due to foreign object damage (FOD) to be minimal. Even with severe bird strikes causing damage to the first few stages of blades and vanes, damage to the discs typically does not occur. Any other forms of FOD, such as stones, nuts, and bolts, can cause damage to more stages of blades and vanes and will possibly cause some damage to the compressor discs/drum. Usually, the disc damage tends to be small nicks and dents that can be blended out within approved service limits, but damage that caused a disc to be scrapped has been observed on occasion. If discs are welded together to form a compressor drum, then there is the option of machining out the damaged stage from the drum and EB welding a new disc in place. This repair is sometimes used on new parts during manufacture to replace discrepant stages, and could easily be adapted for repairing parts in service.

Blisk technology, as in stages 3-8 of the final chosen option for the NASA SHCT (Option F), is more advanced than the welded drum technology. A blisk removes the requirement for blade and disc attachments and therefore is lighter in weight and less costly than the conventional equivalent. The biggest risk to blisks is that any FOD or handling damage would require the replacement of the whole rotor.

Handling damage should be a minor concern, as rotor assemblies on existing engines (with their airfoils exposed in the same way as the blisk proposal) do not tend to suffer from handling damage because of the use of protective assembly stands, fixtures, and covers during assembly and overhaul. Bird strike damage is usually only seen in the first few airfoil stages of a compressor, as after that the bird is

sufficiently fragmented to pass through the rest of the compressor without damaging the airfoils. Disc/drum damage due to bird ingestion is not typically experienced, and for this reason, the first two stages of the NASA SHCT proposal have been configured with standard axial attachments, to allow easy blade replacement due to bird ingestion damage. FOD type damage due to nuts, bolts, and stone ingestion is more of a concern to the blisk airfoils. Typically, if a small hard object is ingested by an engine, then there will be a trail of damage to most stages of airfoil throughout the length of the compressor. Often this damage can result in airfoils being blended within acceptable blend limits, but with major FOD several stages of blade and vane will require component replacement.

The biggest positive factor for accepting the risk of FOD damage is that FOD is greatly affected by engine intake design and positioning. In the AE 1107C engine, where the intake is positioned on the underside of the main wing, close to the runway, FOD is a relatively frequent occurrence. However, the AE 1107C engine has never had an incidence of compressor FOD because the engine inlet is positioned high above the wing with the rear mounted engine design on this aircraft.

To further substantiate the fact that the risk of FOD would be very low in a civil tiltrotor, it is of note that the V-22 aircraft (having similar intakes to the NASA SHCT design) has never had an occurrence of FOD due to the ingestion of hard objects from the landing areas (several instances of engine intake nuts/screws/hardware have been observed, but this will be reduced for production engines by design improvements in the intake area).

The final design option under study for this proposal was the use of cantilevered vanes. This type of vane is mounted simply from the engine casing and does not have an inner band or platform. The advantage of this configuration is that the efficiency of the compressor can be superior to a typical design, with its rotating knife seals sealing under the inner band of a fixed-fixed vane. The higher rim speeds of the NASA proposal will also result in a greater temperature rise of the recirculating air through the knife seals of a fixed-fixed design due to windage effects. The increased heating of the disc rim is undesirable and a cantilevered vane style will serve to reduce the heating.

The major design concern with a cantilevered vane is that the clearance under the vane hub between the vane and the rotor must be maintained at a minimum or the performance improvement will be reduced. This clearance can be maintained by matching the mechanical and thermal growths of the rotor and stator in much the same way as the clearance at the rotating blade tip is matched to the growth of the casing. The only difference between a blade tip and a cantilevered vane hub is that the casing should have an abrasible coating where the blade may contact, whereas the rotor should have a slightly abrasive coating in areas where the vane may come into contact with the rotor. It is preferable for the blades to cut into the casing where the rotor and stator are not centered correctly, but it is preferable for the rotor to actually remove material from the vane hubs at the equivalent vane locations. The removal of excess material from the stator minimizes the performance reduction as the material is only removed from a local area, whereas if the same material is removed from the rotor it is removed from around the whole circumference at this location.

A fixed-fixed vane does not require such careful matching of the growths of the rotor and the stator because the vane inner platform has an abrasible coating on it and the knife seals on the rotor are designed to deliberately rub into the coating, thereby optimizing their clearance. It must be emphasized that by matching the rotor and stator growths, the magnitude of the rub at this location will be minimized.

The weights for the six options under consideration are given below in Table XIII. These weights are compared with the current AE 1107C for reference and are the basic weights for the compressor discs/blades, casing, vanes, VGVs, and inner VGV support ring hardware. Any additional VGV actuation ring hardware is not included because it will remain the same for all options.

Table XIII. Compressor trade study—weight comparisons.

Option	Weight index—%
AE 1107C baseline	100
A	94.3
B	90.6
C	90.6
D	89.4
E	82.9
F	80.2

### 5.1.5 Manufacturing and Cost Analysis

The manufacturing cost assessment for the six options under study is based on existing engine AE 1107C cost studies. Cost reduction factors for known process improvements currently being implemented are included in this study. Where processes were changed from the existing manufacturing methods, the appropriate correction was made. Simple reductions were made for parts reduced in length/size from their equivalent AE 1107C part. A cost increase was assumed for the discs/blades and vanes based upon the increase shown in airfoil axial chord/width. It was assumed a circumferentially attached blade cost is 1.25 times the cost of an equivalent axial style attachment blade, based upon Rolls-Royce Allison manufacturing experience. The cost for a cantilevered fixed vane also was assumed to be 1.25 times the cost of a fixed-fixed vane stage due to the increased machining cost. The results of the trade study for the manufacturing costs are shown in Table XIV. These costs are competition sensitive, so they are shown as a percentage of the current costs for an AE 1107C compressor. These costs were also used as an internal index to indicate the relative merits of each design style. A whole engine detailed cost estimate as calculated by the Price-H program is included in subsection 5.6.3.

### 5.1.6 Materials Considerations

The temperatures and general operating conditions of the NASA SHCT proposal are within the experience of existing AE 1107C engine series, so the materials for the components were generally picked based upon the existing experience. The major change from the current Rolls-Royce Allison experience base is to use titanium airfoils for the rotor blades, as our existing blades use 17-4 PH or IN 718 blades. The current blade material was picked based upon the military requirement to avoid titanium blades from rubbing into a titanium case and possibly causing a titanium fire. The use of steel/nickel blades does not work with a blisk-type configuration because the blade/airfoil material *must* be the same as the disc portion and steel/nickel blisks would have an unnecessary weight penalty.

Table XIV. Compressor trade study—relative costs.

Option	Cost index—%
AE 1107C baseline	100
A	63.40
B	62.10
C	62.40
D	63.60
E	54.00
F	55.20

Many commercial engine compressors use titanium blades and the possibility of a compressor fire is avoided by ensuring the abradable coating in the compressor casing is thick enough to prevent blade tip-to-casing contact under the most severe rub. With the use of cantilevered vanes, the initial clearance plus the abrasive coating depth will be set to prevent titanium-to-titanium contact between the rotor and the vane airfoil hub under worst case conditions.

Once the decision was made to accept titanium blading for the blisk options, it was then decided to also keep the same material for all of the bladed options, as the reduction in rotor weight due to the reduction in blade rim load is significant. The blisk/disc materials were chosen to be titanium 6-4 for stages 1 through 5 and titanium 6-2-4-2 for stages 6 through 8.

The abrasive coating on the rotor is Metco 104, which has been used widely in the industry. The compressor case is titanium 6-2-4-2 with an XPT 268 abradable coating based on AE 1107C use. The VGVs and actuation hardware are also made of similar materials to AE 1107C hardware. The fixed vane materials are 17-4 PH for stages 1 through 5 and IN 718 for stages 6 through 8. A full listing of component materials is included in subsection 5.6.

### 5.1.7 Recommendations for Further Work

Further work should include more detailed design/stressing for the chosen configuration, along with more detailed work on the promising alternative options for a back-up design. If development of this size of engine is initiated, then compressor rig testing should be performed as a first priority to ensure the success of the project. The first manufacturing based work would be to conduct trials for the EB-welding process proposed. Rolls-Royce and other companies successfully perform such operations on similar components, so the technology has already been proved but it is important to conduct trials to set up usable parameters for the manufacturing equipment available. Repair development for weld buildup of titanium airfoils would be a priority. Trials are currently under way for proposing weld repair of steel/nickel airfoils, but this NASA proposal uses titanium blades and the early development of weld repairs would be beneficial.

Future work for blisk design would be the testing and approval of design parameters ensuring that if an airfoil, for instance, suffered from cracking then the cracks would tend to grow in the airfoil only and not progress into the blisk rim area. Similarly, if the blisk rim area suffered a crack initiation, then the crack growth should only tend to turn and release a small section of blisk rim rather than grow down the blisk web into the bore area. If cracking did grow down the blisk web, then uncontained failure would be the result. It is obviously beneficial to design parts so cracks tend to turn in the rim area and testing/design rules should be set up to ensure this is the probable result.

## 5.2 Combustor Preliminary Design

The proposed combustion system for the SHCT is based on technology being developed under NASA Advanced Subsonic Transport (AST) (*Low Emissions Combustor Development for Regional Airlines*, NAS-27725). Although no requirements currently exist addressing emissions for tiltrotors, it is reasonable to assume introduction and growth of this market in the year 2003 and beyond would rapidly require compliance with emissions standards comparable to those being established for turbofan engines. This is especially likely when considering the market niche being addressed by the civil tiltrotor involves short trips in urban areas and often to major airports. Because of the expected demands for low emissions combustion, the combustion system will be similar to those being developed by Rolls-Royce Allison in the NASA AST program. The key elements of the system allowing it to operate with low emissions levels are a lean direct injection (LDI) fuel module and circumferential fuel staging.

Reduction in oxides of nitrogen (NO<sub>x</sub>) is proposed through lean well mixed combustion. Since NO<sub>x</sub> is known to be exponentially dependent on temperature, significant reduction can be achieved through

reduction in the maximum local combustion gas temperatures, which is accomplished through better mixing of fuel and air prior to combustion. The LDI module achieves this reduction by introducing significantly more air through the dome of the combustor and providing a prechamber to allow partial evaporation and mixing. Circumferential fuel staging is used to keep modules operating over an optimum range of fuel/air ratios in terms of emissions. Significant enhancement of lean blowout limits has also been demonstrated with circumferential fuel staging.

### 5.2.1 Injection Fluid Selection

A 70/30 mixture of water and methanol is proposed as the injected liquid for power augmentation during the OEI condition. Ideally the injectable fluid will have a low freezing point, atomize and evaporate completely in the compressor, and be low cost. It is also desirable the augmenting fluid be combustible so the fuel delivery system need not be sized for the OEI condition. Key fluid properties of possible fluids are shown in Table XV. Both methanol and ethanol water mixtures have the prerequisite fluid properties. Higher order methanols don't suppress the freezing point sufficiently to be considered. Although methanol is toxic, it is much more effective as an antifreeze than ethanol. It should be noted that ethylene glycol has poor atomization and evaporative characteristics. An added benefit of the 70/30 mixture of water and methanol is that RIT is nearly independent of the injection rate. Methanol water mixtures have previously been used for augmentation of the T56 and methanol has been used on a 501-K industrial engines as the primary fuel for 1000 hr of operation.

### 5.2.2 Airflow Analysis

Key design requirements of the combustor were determined as follows. Consideration was first given to the noninjected cycle with the assumption the combustor for the methanol/water injected engine could easily be scaled based on the reduction of corrected engine airflow. The LDI fuel module design is based on module AST-6b, which has been extensively tested in a single module combustor rig and is currently being evaluated in a three-module sector rig under the NASA AST program. AST-6b was scaled based on a 25% reduction in corrected airflow as compared to the NASA AST cycle. Combustor volume is approximately twice that of a conventional combustor to provide additional time for carbon monoxide burnout. This is achieved almost exclusively by increasing the annulus height. Basic combustion design parameters are listed in Table XVI.

Table XV. Injection fluid characteristics.

	Methanol	Ethanol	$\eta$ -propyl	Ethylene glycol
Caloric value—MJ/Kg	19.57	21.84	30.54	—
Viscosity— $10^{-3}$ Pa.s	0.57	1.1	2	17.2
Surface tension— $10^{-3}$ N/m	22.6	22.3	23.8	47.7
Boiling point—K	337.8	351.5	371	470.3

Table XVI. Combustion design parameters for baseline and methanol/water injected engine (length, aspect ratio, nozzle spacing/annulus height, and system pressure drop).

	L—in.	L/H	tres—msec	Theta	$\Delta P/q$	S/H	$\Delta P/P$ sys
Baseline cycle combustor	7.71	1.71	17.9	0.021	84.3	1.05	0.0675
H <sub>2</sub> O/CH <sub>4</sub> O injected cycle combustor	6.28	1.73	14.8	0.041	120.8	0.99	0.0675

The module (Figure 36) consists of an outer main fuel circuit and an inner pilot nozzle. Fuel is introduced into the main nozzle through 12 plain jet atomizers oriented radially inwards. The main circuit consists of an outer axial swirler and inner air passage without a swirl component. The distribution of swirling and nonswirling air is found to directly affect the distance the flame establishes from the module exit plane. This parameter is determined based on a tradeoff between emissions and combustion stability. The length of the premixing section of the nozzle is relatively short to reduce the likelihood of autoignition. The center portion of the module consists of a centrally located pressure atomizer surrounded by an axial swirler.

Figure 37 shows a schematic of the baseline cycle combustion system. Approximately 85% of the combustor air passes through the LDI modules, while 15% is used for liner cooling. The combustion gases are swirl stabilized and no primary or dilution holes are required. Temperature profile is expected to be relatively flat because of the degree of fuel/air mixing at the front of the combustor. Because fuel/air ratios are relatively high for the SHCT cycle, a significant amount of air is needed to achieve large NO<sub>x</sub> reductions.

Rolls-Royce Allison is also working on alternate designs under NASA AST funding that use significantly less dome air (~50%) and have primary and dilution holes and simplified staging schemes but achieve smaller reductions in NO<sub>x</sub>. Ultimately, the liner flow distribution will be optimized to achieve the conflicting requirements of adequate lean blowout, ignition, and acceptable emissions.

The proposed layout of fuel modules and fuel staging is shown in Figure 38. Ten main modules and two pilot-only modules are equally distributed. The pilot-only modules are separated from the main module air for easy ignition. The pilots on the main modules serve primarily for flame stabilization and operate at all times. The ten main modules are divided into four different fuel circuits whose operation is determined base on engine fuel flow. At all times, the fuel/air ratio at the dome of the combustor for all fueled modules (including pilot-only modules) is nearly the same. Beyond 82% power all circuits are fueled.

A single- and a tri-passage diffuser were both considered. The tri-passage diffuser provides the benefit of shorter length, but was impractical in this size system due to splitter blockage. A single dump diffuser is proposed based on consideration of performance, package size, and cost. Estimated dump diffuser performance based on flow and size characteristics suggests the goal pressure drop can easily be met while providing adequate margin from separation and reasonable length (5:1, length:channel height).

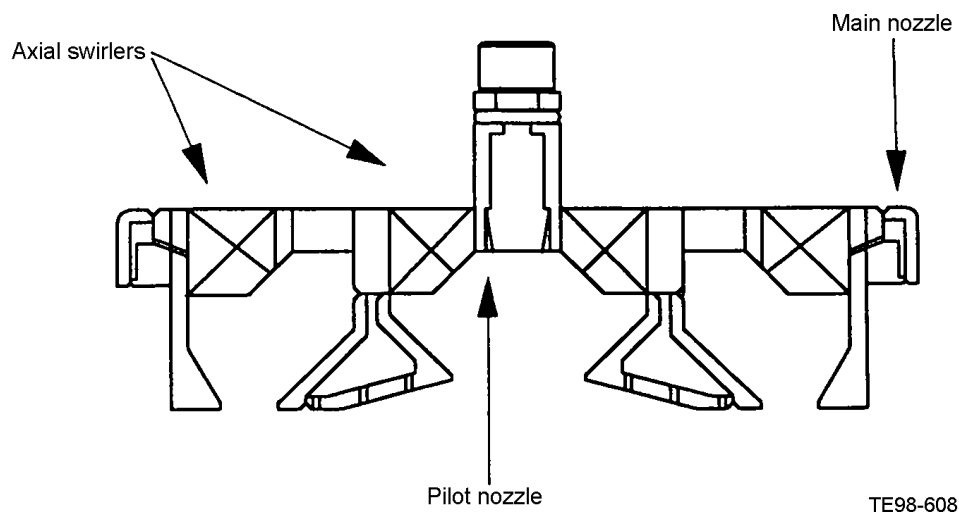
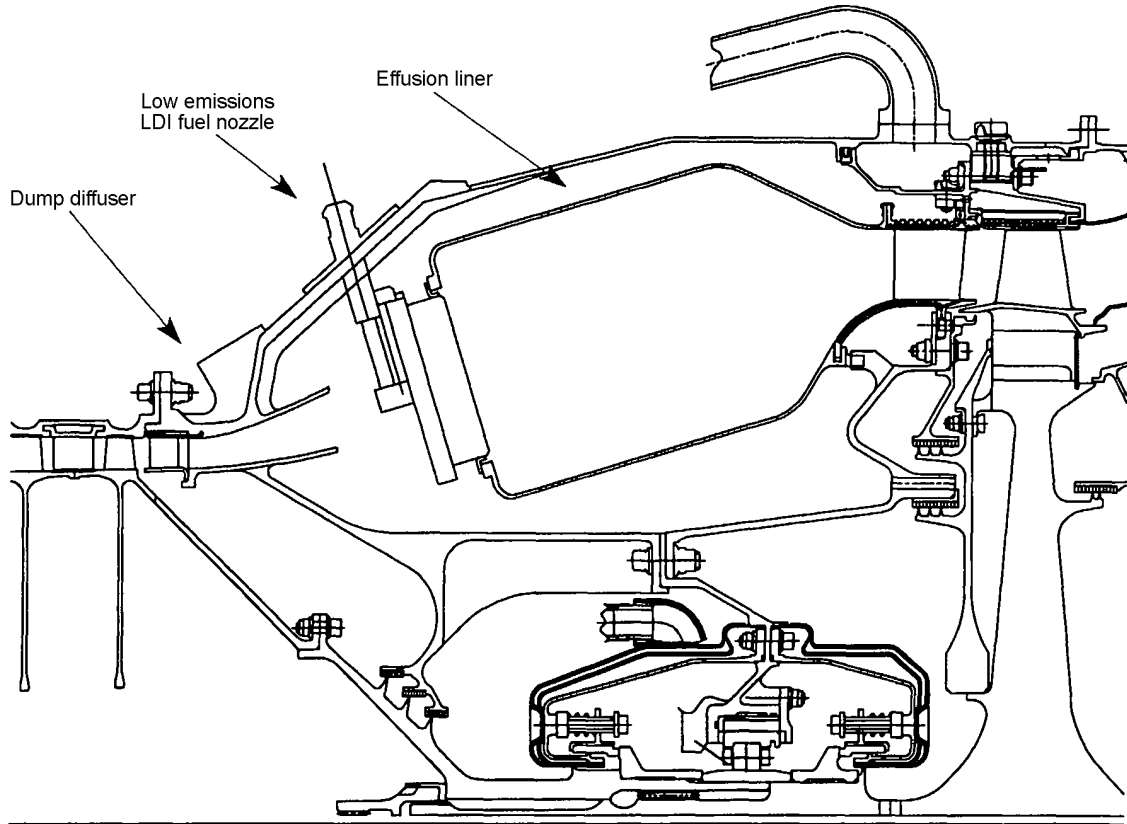
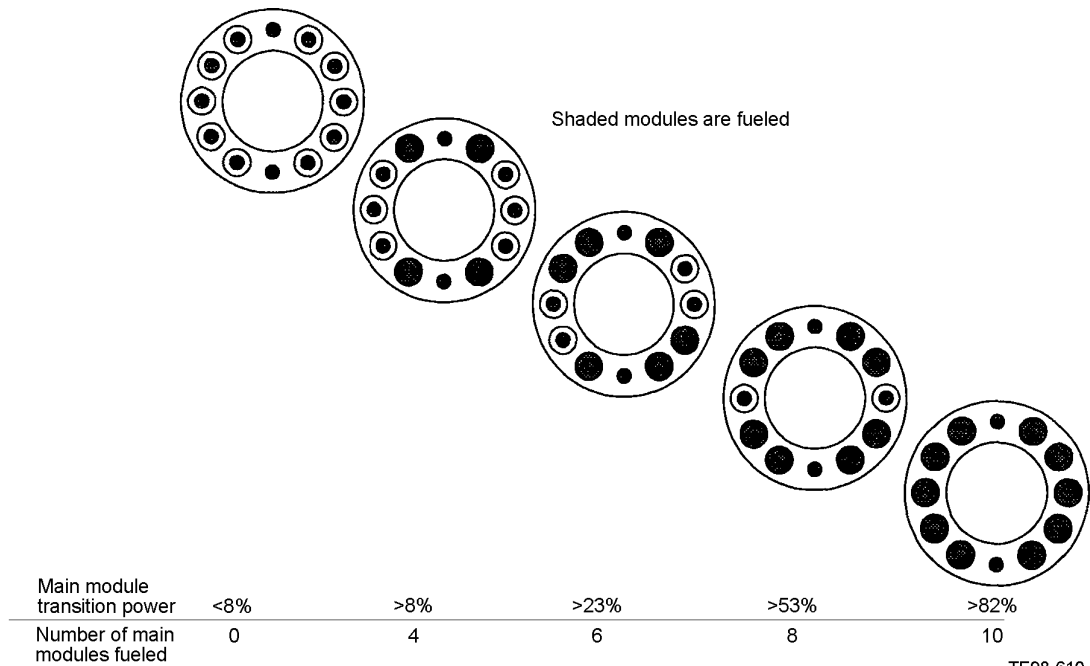


Figure 36. Schematic of lean direct injection fuel module AST6-b.



TE98-609

Figure 37. Schematic of baseline cycle combustion system.



TE98-610

Figure 38. Circumferential fuel staging scheme for SHCT combustor.

### 5.2.3 Heat Transfer

A one-dimensional (1D) heat transfer analysis was performed to predict both inner and outer liner wall temperatures. The relatively high burner outlet temperatures and goal to achieve low emissions requires an efficient wall cooling scheme. Single module combustor rig tests with as little as 12% cooling air have shown the combustor liner temperature is less than 300°F above burner inlet temperature using effusion cooling. Videotapes of LDI module AST-6b in an optically accessible combustor rig at NASA LeRC indicate a blue nonluminous flame resulting in low radiant heat flux to the liner. A second factor reducing cooling air requirements is the burner cross section is large, reducing gas velocity and convective heat transfer on the hot side.

An effusion liner was chosen for both performance and cost considerations. One-dimensional heat transfer calculations were made with an in-house combustion heat transfer code at various axial stages of the combustor assuming 15% of the combustor air is allocated for wall cooling. The inner and outer liners are both assumed to be made of 0.080-in. Haynes 230 and were analyzed without thermal barrier coating. Calculated inner and outer liner temperatures are shown in Figure 39 for the baseline cycle. Because burner inlet and outlet temperatures are nearly the same for the injected combustor, the predictions are believed to be representative for this case as well. The key finding is that 15% budgeted air cooling is adequate to keep wall temperatures lower than 1550°F for LDI type lean combustion where hot side temperature and radiation are significantly lower than in a conventional combustor.

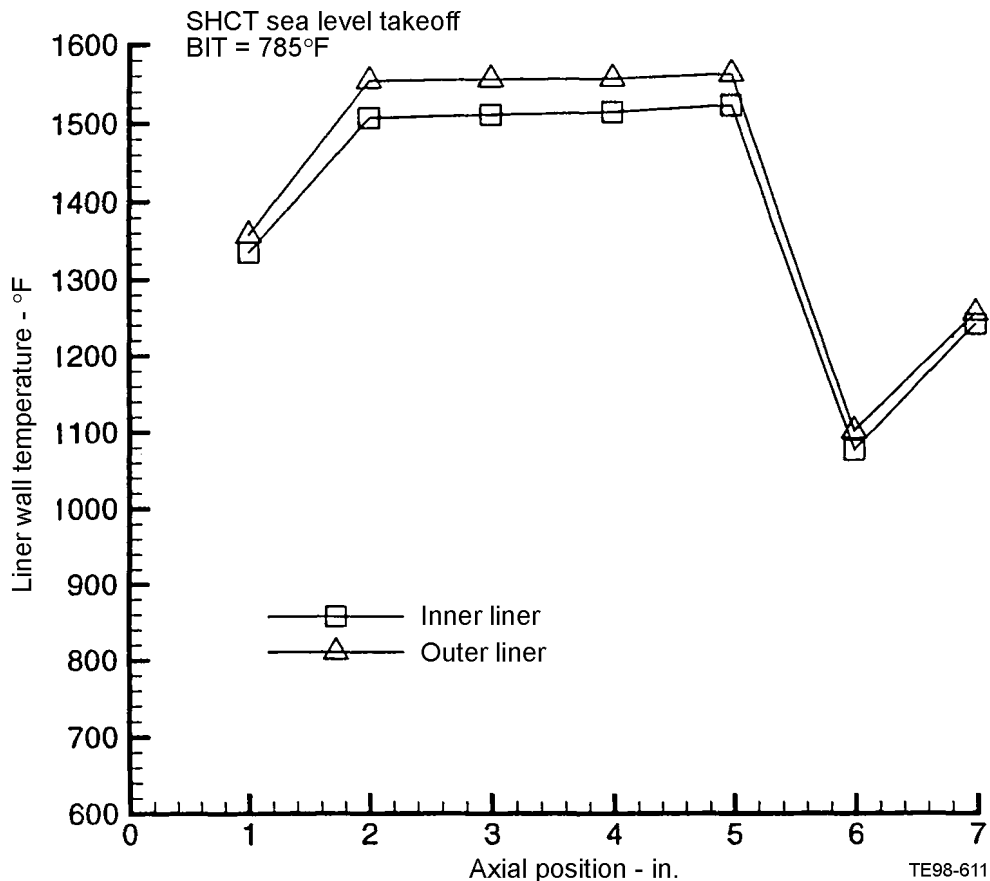


Figure 39. Predicted inner and outer liner wall temperatures at maximum power condition for baseline cycle SHCT combustor.

## 5.2.4 Emissions

Emissions estimates were made for the LDI combustor operating over a landing takeoff (LTO) cycle derived from a typical civil tiltrotor mission. The LTO shown in Table XVII is composed of idle, cruise, maximum cruise, and takeoff conditions weighted by the appropriate time period. The estimates of emissions for the SHCT combustor are determined from single module rig tests at similar operating conditions. Carbon monoxide (CO) measurements were corrected by the inverse ratio of combustor residence time because the combustor rig residence time was approximately half the SHCT combustor residence time. Comparisons are made with a conventional diffusion flame combustor operating over the same cycle.

NO<sub>x</sub> estimates for the conventional diffusion flame combustor are from the Rolls-Royce Allison probability density function based NO<sub>x</sub> model, which accounts for realistic distributions of fuel/air ratio in the combustor based on design parameters. Carbon monoxide (CO) and unburned hydrocarbon (UHC) estimates for the conventional combustor are based on AE 1107C measurements at comparable operating conditions corrected for differences in inlet temperature and pressure using a calibrated 1D performance model.

Table XVII summarizes the predictions in terms of emission indices at individual operating conditions as well as total weight of pollutant produced over the assumed LTO cycle. The SHCT combustor is predicted to have 45% lower NO<sub>x</sub> and nearly the same levels of CO and UHC as a conventional diffusion flame combustor. Emissions for the water/methanol injected engine were not considered since this is only an emergency condition. Equilibrium temperature calculations at this condition do however support that combustion temperatures will be sufficiently high to stabilize a flame.

*Table XVII. Landing takeoff cycle emissions estimates for baseline cycle low emissions combustor and typical diffusion flame combustor.*

Power	Flight condition	Time—min	NO <sub>x</sub> EI—g/kg		CO EI—g/kg		UHC EI—g/kg	
			LDI	Diff flame	LDI	Diff flame	LDI	Diff flame
Idle	Taxi	6	2.8	5.37	12.77	15.83	1.91	0.89
Cruise	Descent	1.5	5.88	5.8	2.73	3.09	0.02	0.19
Max cruise	Convert climb	4	9.76	11.51	0.21	1.82	0.22	0.44
Takeoff	Takeoff	1	7.72	27.51	0.39	0.39	0.04	0.35
LTO sum—g			976.5	1754.09	486.3	631.81	70.688	65.68

## 5.2.5 Recommendations for Further Work

Further work needs to be done to address several issues before an LDI-based circumferentially staged low emissions combustor technology can be used in a practical application. Currently, these modules have only been demonstrated in single module tests. The effect of module-to-module interactions on emissions and carbon monoxide quenching specifically can only be studied in sector or full annular combustion rig tests.

Sector rig tests under funding from NASA AST are currently in progress, while future plans include full annular combustion rig tests as well as engine testing. Additional work needs to be directed toward the implementation and demonstration of low cost fuel staging control strategies.

Staging can be accomplished through flow divider valves and careful selection of fuel nozzle flow numbers. This approach however introduces a "dead band" where modules are being fueled insufficiently to support combustion. The goal of fuel staging scheme and valve development must be to minimize this "dead band" and keep all modules fuel operating over an optimum band of fuel/air ratios. Alternatively,

solenoid valves that are located near the module could be used. This eliminates the "dead band" but introduces more cost and size to the fuel manifold system. Finally, water/methanol injection increases the tendency towards autoignition in the LDI module. Although the equivalent enrichment (in terms of heat content) by JP fuel is small, demonstration of autoignition margin with water/methanol should be demonstrated in rig tests.

### **5.3 Turbine Preliminary Design**

This section describes the preliminary aerodynamic and mechanical design of the gas generator and power turbines for the baseline and water/methanol-injected engines. The objective of this task was to design a high performance hot section that would also be cost-effective for the customer. Preliminary design trade studies were performed to determine the best aerodynamic and mechanical system configuration. Detailed information relating to turbine performance, weight, cost, mechanical integrity, and life are included in this section.

The SHCT gas generator turbine and power turbine incorporate much of the design experience from the Rolls-Royce Allison AE engine family. Each turbine is designed as a module for ease of maintenance with simple static and rotating structures. The materials selected for the turbines are well characterized and readily available and fabrication techniques are proven and incorporated in current production engines.

#### **5.3.1 Aerodynamic Design**

##### **5.3.1.1 Baseline Engine**

The gas generator turbine (GGT) is a single-stage, air-cooled, axial-flow machine. The power turbine (PT) is a two-stage axial-flow machine with air-cooled components in the first stage. The PT rotates in the opposite direction of the GGT, thus reducing the turning and the associated secondary losses in the PT first-stage vane. The two turbines are connected aerodynamically by a short transition duct. The design of the two turbines was coordinated so the exit conditions of the GGT would be properly used as inlet conditions for the PT. The selected configuration represents a reasonable compromise between turbine performance, acquisition cost, maintainability, and life cycle costs.

A trade study was done to determine whether the PT should be a two- or three-stage design. The primary advantage of the three-stage turbine was a significant reduction in exit Mach number and swirl, which would provide more favorable inlet conditions to the downstream exhaust-diffuser across the operating range, thus improving the performance of the system. The three-stage design benefited from lower stage loadings, but the improvement in turbine efficiency was less than +0.5%. This slight improvement in performance was more than offset by the higher acquisition costs, increased weight, and engine length. Therefore, it was concluded that for this application the PT should be a two-stage configuration.

An operating condition at 25,000 ft, 350 ktas, ISA, maximum cruise was selected as the aerodynamic design point for the GGT and PT. The design parameters are summarized in Table XVIII.

The GGT airfoils, nozzle endwalls, and blade tracks are air cooled to accommodate rotor inlet temperatures up to 2650°F for takeoff conditions and 2800°F for OEI conditions. The PT first-stage vanes and blades require a small amount of cooling air to meet mission life requirements.

A meridional view of the GGT and PT flow paths is shown in Figure 40, and the hot flow-path corner point dimensions are shown in Table XIX. The axial airfoil spacings were selected to satisfy dynamic stress criteria. All flow-path dimensions are described at design point conditions.

Table XVIII. Gas generator turbine and power turbine aerodynamic design point parameters.

	GGT	PT
Rotor inlet equivalent flow— $W\sqrt{\theta_{cr}}\epsilon/\delta$	5.810 lbm/sec	19.900 lbm/sec
Equivalent work— $\Delta h/\theta_{cr}$	34.1 Btu/lbm	45.3 Btu/lbm
Equivalent speed— $N/\sqrt{\theta_{cr}}$	7097 rpm	5676 rpm
Overall expansion ratio— $Re_{TT}$	3.546	5.137
Goal efficiency— $\eta_{TT}$	86.7%	91.2%

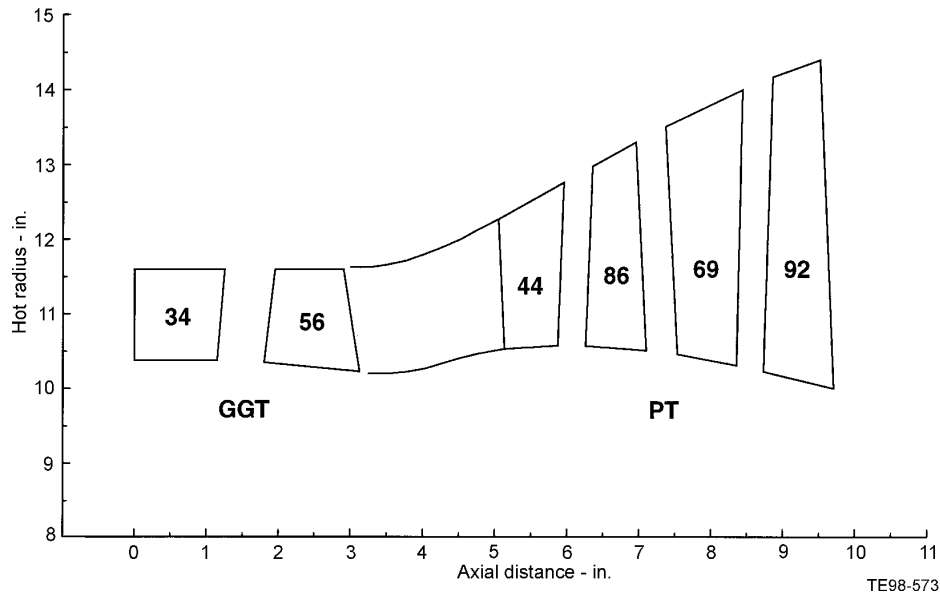


Figure 40. Gas generator turbine and power turbine flow path schematic at design point.

Table XIX. Turbine flow-path hot corner point dimensions at design point conditions.

Location	Hub X	Hub R	Tip X	Tip R	Annulus area
GGT stator inlet	0.000	10.375	0.000	11.600	84.5697
GGT stator exit	1.150	10.375	1.250	11.600	84.5697
GGT rotor inlet	1.800	10.350	1.950	11.600	86.1974
GGT rotor exit	3.125	10.225	2.900	11.600	94.2772
PT first stator inlet	5.125	10.530	5.040	12.270	124.6333
PT first stator exit	5.870	10.575	5.950	12.760	160.1803
PT first rotor inlet	6.260	10.570	6.350	12.980	178.3027
PT first rotor exit	7.100	10.510	6.950	13.300	208.6957
PT second stator inlet	7.530	10.460	7.360	13.510	229.6771
PT second stator exit	8.350	10.310	8.430	14.000	281.8131
PT second rotor inlet	8.730	10.225	8.850	14.170	302.3415
PT second rotor exit	9.700	10.000	9.500	14.400	337.2814

The radial location and size of the GGT were dictated by several factors, including hub turning and blade tip speed. The annulus area was sized so the exit axial Mach number at design point was less than 0.50, while keeping the vane exit absolute gas angle greater than 12 degrees. These constraints determined the placement of the GGT and gave a maximum untapered blade stress parameter of  $AN^2 = 2.7 \times 10^{10}$ . The PT placement was influenced by the location of the GGT. The PT exit area was sized for a maximum exit Mach number of 0.55 at design point conditions. The maximum tip speed of the PT second blade is 1720 ft/sec with an exit  $AN^2 = 6.4 \times 10^{10}$ .

A controlled-vortex velocity diagram calculation was generated featuring a complete axisymmetric radial equilibrium solution using the combustor exit profiles as inlet boundary conditions. For this analysis and for the generation of interstage data, the temperature profile shown in Figure 41 was assumed.

The effects of blade tip leakages are included in the velocity diagram model. The GGT has unshrouded rotor blades, and the PT first and second blades are shrouded. In the controlled-vortex velocity diagram analysis, the tip leakage flow is extracted from the primary flow at the rotor inlet station and reintroduced at the first station downstream of the rotor exit. The mean-line controlled-vortex velocity diagrams are shown in Figure 42 (velocities are shown in terms of Mach number and angles are shown in degrees). A summary of some important velocity diagram parameters is listed in Table XX.

After the velocity diagrams for both turbines were completed, the turbine airfoils were designed. The airfoil section contours were developed along conical surfaces defined by the design mean streamline. Each airfoil was designed interactively and analyzed using a 2D inviscid blade-to-blade flow analysis. The airfoil sections were modified until aerodynamically acceptable surface velocities were achieved and mechanical design criteria were satisfied.

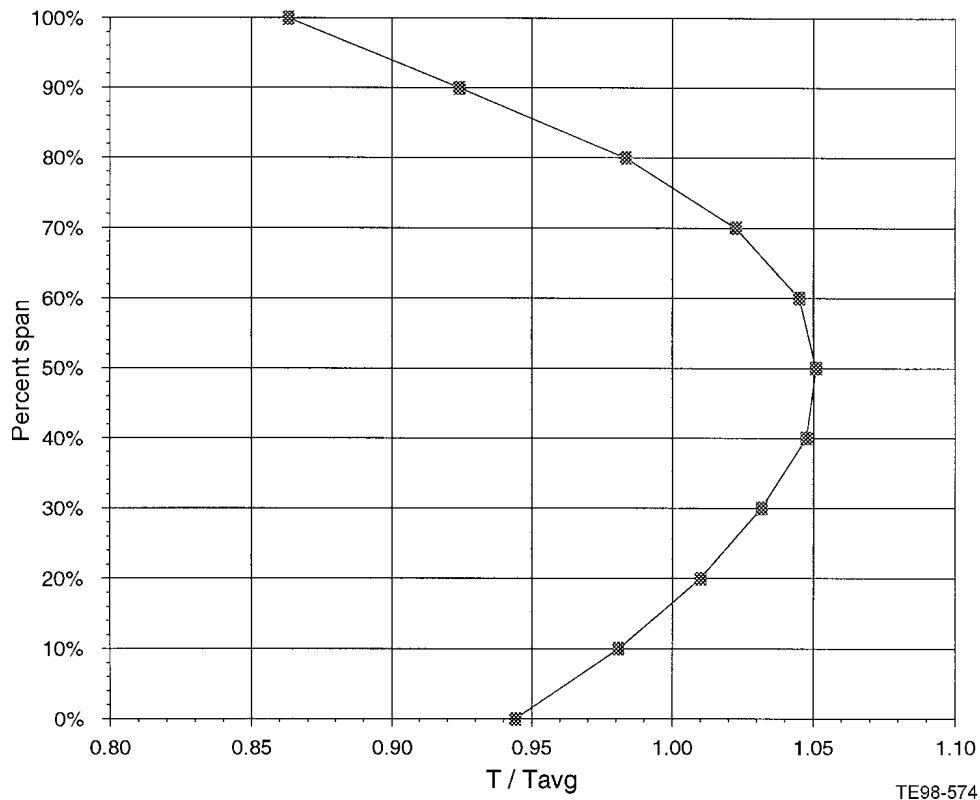


Figure 41. Gas generator turbine inlet temperature profile at design point conditions.

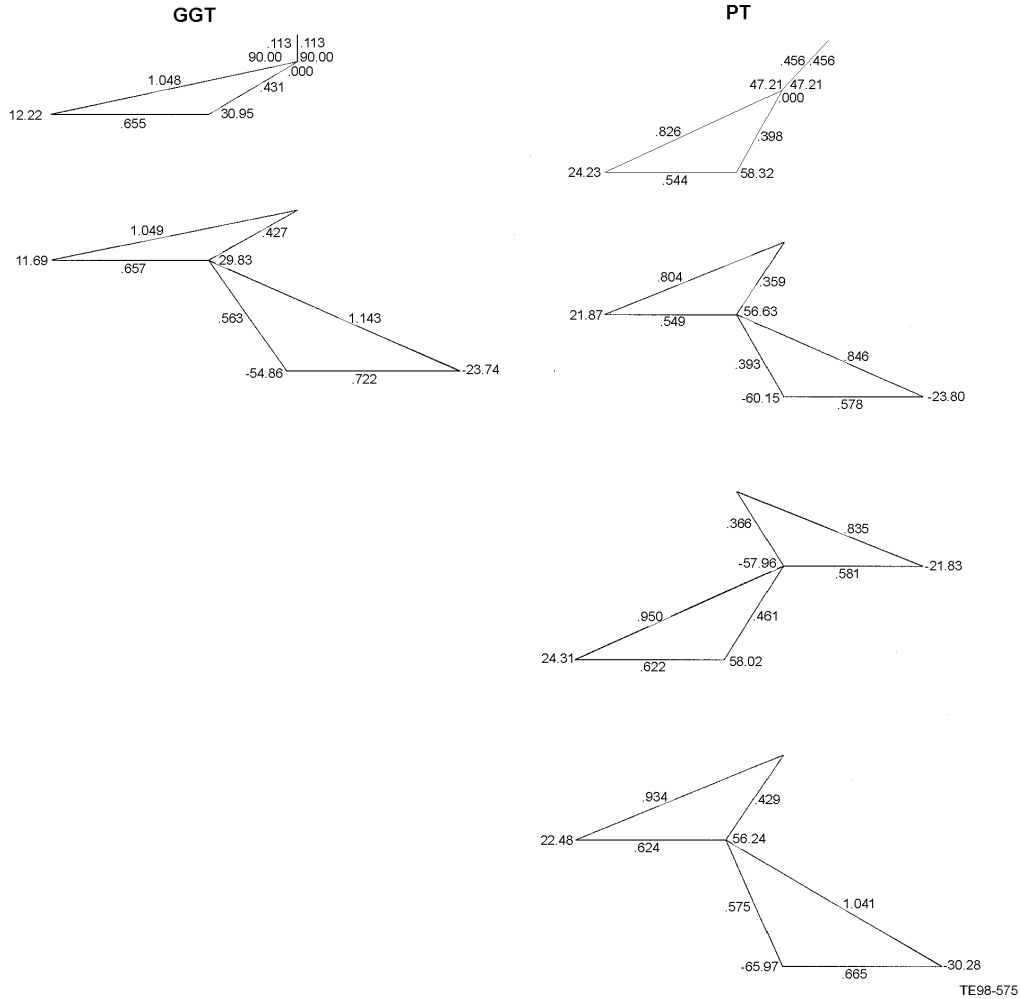
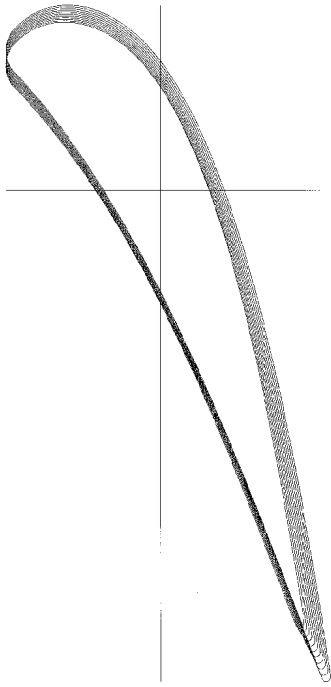


Figure 42. Gas generator turbine and power turbine design point controlled-vortex velocity diagrams.

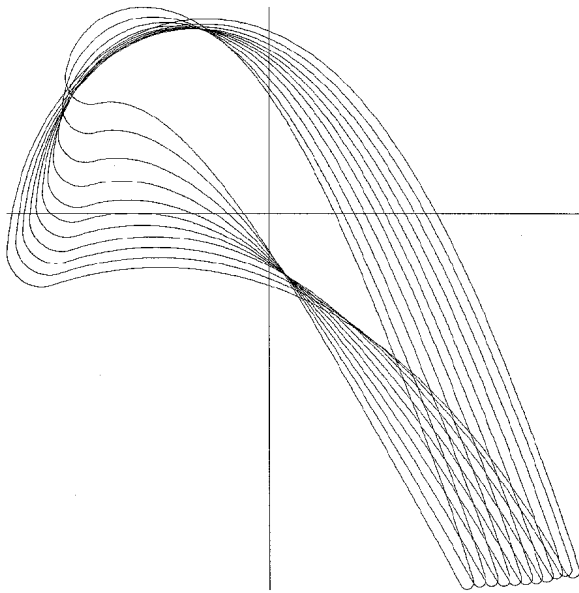
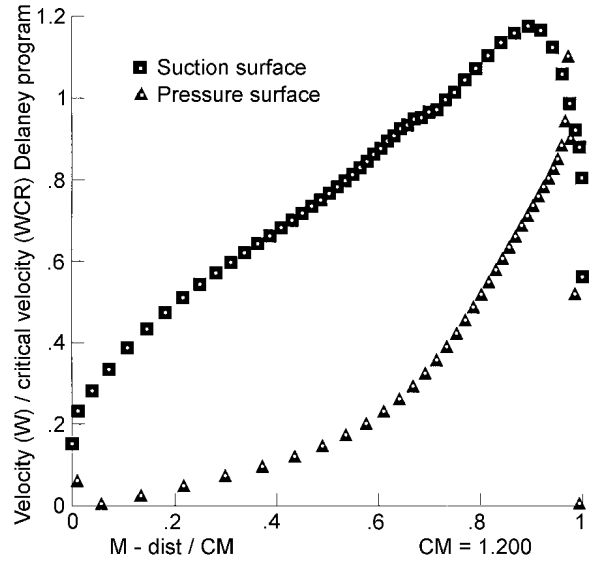
Table XX. Gas generator turbine and power turbine velocity diagram parameters at 25,000 ft, 350 ktas, ISA, maximum cruise design point conditions.

	GGT	PT stage 1	PT stage 2
<b>Load coefficient—<math>gJ\Delta h/U_m^2</math></b>	1.924	1.578	1.664
<b>Flow coefficient—<math>V_x/U_m</math></b>	0.460	0.536	0.664
<b>Work split</b>	—	47.0%	53.0%
<b>Stage reaction—<math>(W_{tr\ ex}^2 - W_{tr\ in}^2)/2gJ\Delta h</math></b>	0.505	0.500	0.562
<b>Mean-line exit Mach Number—<math>M_v</math></b>	0.563	0.393	0.575
<b>Average exit swirl—<math>\alpha_{ex}</math></b>	-32.1 deg	-26.5 deg	-21.6 deg

The airfoil design process was iterative, with the proposed airfoils having to satisfy aerodynamic, structural, and mechanical design criteria. Extensive work was applied to the GGT and PT first-stage airfoils so they could accommodate appropriate cooling schemes while meeting goal mission lives. The airfoil leading and trailing edge regions were sized so there was sufficient room for all the cooling passages, pins, fins, and film holes. Wall thicknesses were selected to satisfy allowable stress and mission life criteria. The final GGT and PT airfoil mean-line sections and their respective surface velocities are shown in Figures 43 and 44. A summary of the airfoil geometric parameters is listed in Table XXI.



GGT Vane



GGT Blade

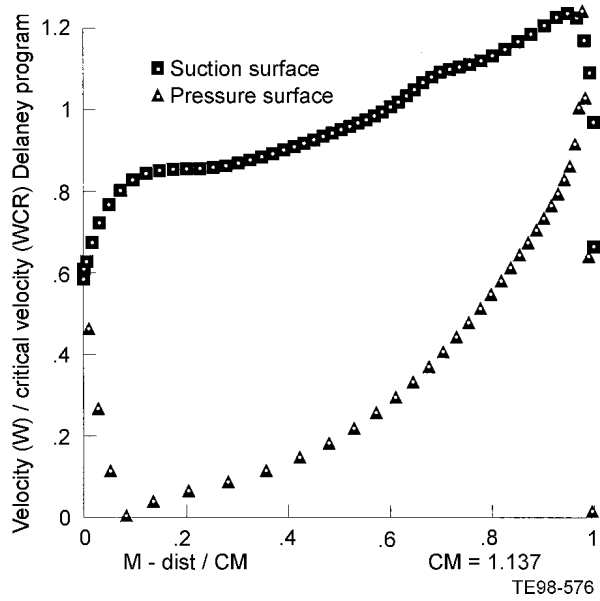
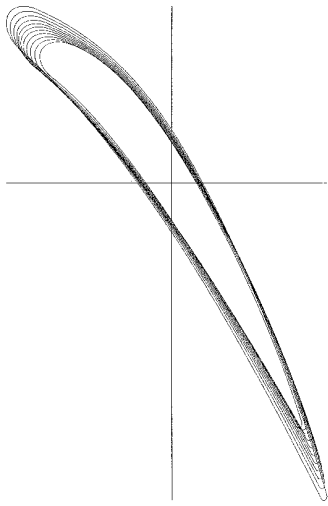
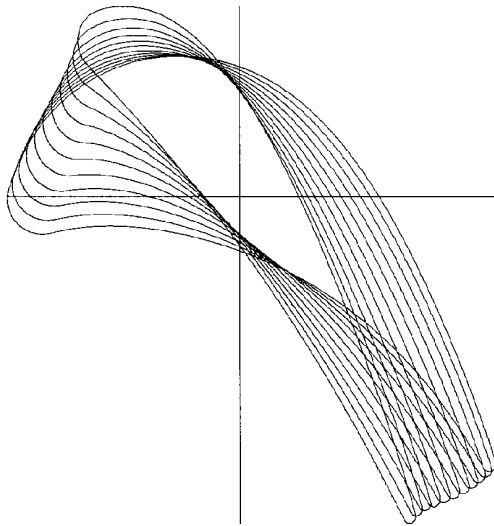
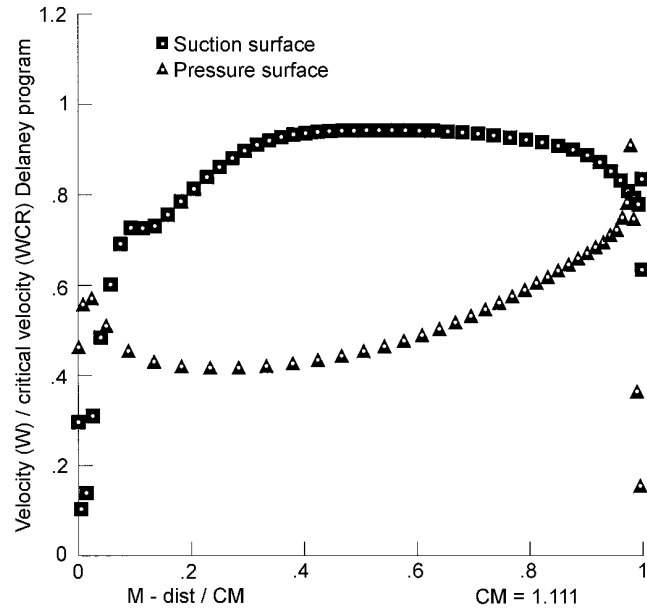


Figure 43. Gas generator turbine airfoils and surface velocities.



PT 1st Vane



PT 1st Blade

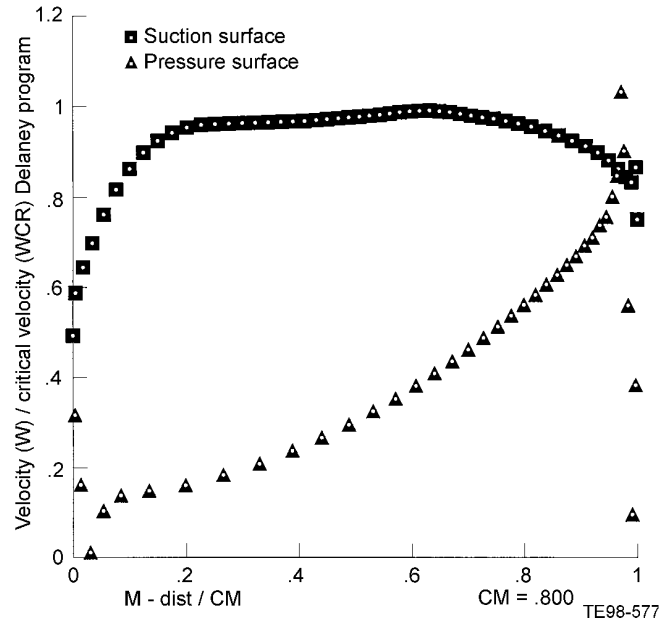
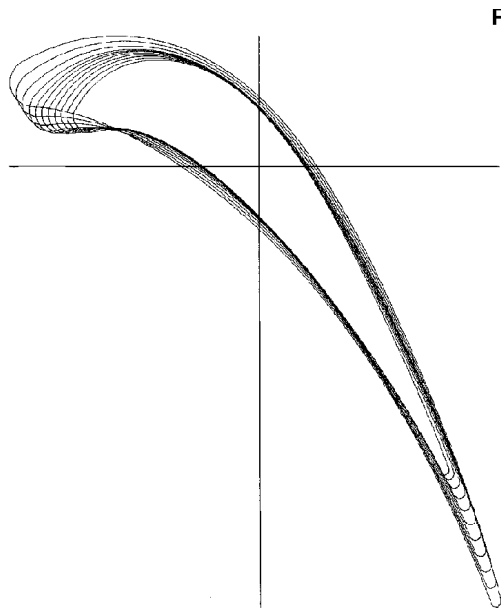
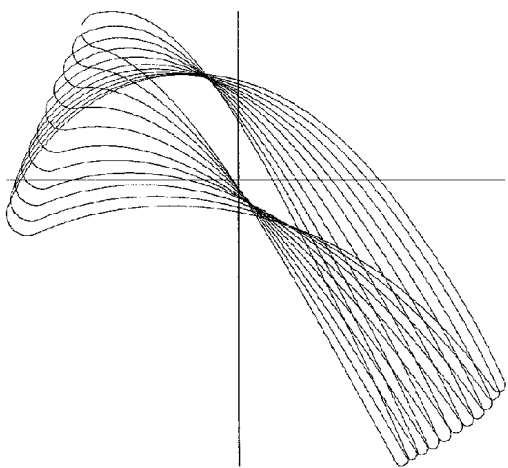
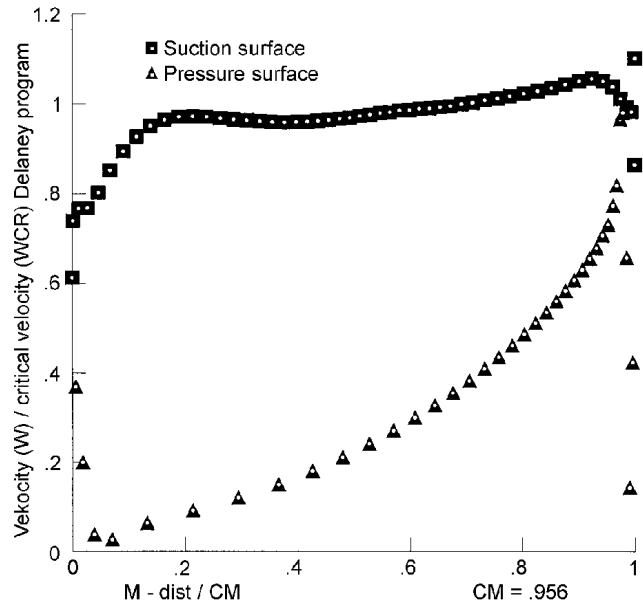


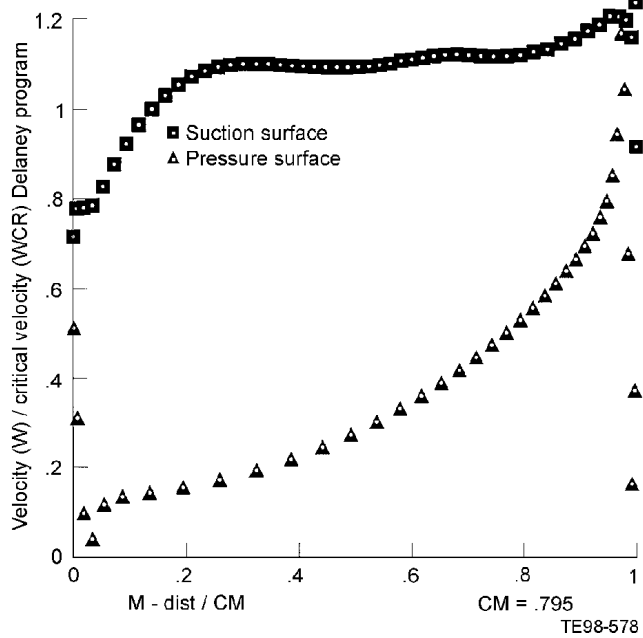
Figure 44. Power turbine airfoils and surface velocities (1 of 2).



PT 2nd Vane



PT 2nd Blade



TE98-578

Figure 44. Power turbine airfoils and surface velocities (2 of 2).

Table XXI. Gas generator turbine and power turbine mean-line geometric blading parameters.

	GGT vane	GGT blade	PT first vane	PT first blade	PT second vane	PT second blade
Number of airfoils	34	56	44	86	69	92
Meridional chord— $C_m$ -in.	1.200	1.137	1.112	0.800	0.957	0.795
True chord— $C_t$ - in.	2.576	1.391	1.859	1.005	1.287	0.942
Blade length— $h$ - in.	1.225	1.225	1.963	2.600	3.370	4.173
Hub/tip ratio— $D_{hub}/D_{tip}$	0.894	0.894	0.843	0.802	0.755	0.708
Solidity— $C_t/Sp$	1.268	1.128	1.127	1.161	1.166	1.133
Aspect ratio— $h/C_m$	1.021	1.077	1.765	3.250	3.523	5.248
Thickness/chord— $T/C_t$	0.174	0.315	0.105	0.236	0.148	0.179
Trailing edge diameter— $D_{te}$ - in.	0.035	0.030	0.025	0.025	0.025	0.025
Blockage— $D_{te}/(\Theta+D_{te})$	0.077	0.061	0.033	0.065	0.051	0.056
Rotor tip shroud	-	No	-	Yes	-	Yes

The performance maps for the GGT and PT were generated using the 25,000 ft, 350 ktas, ISA, maximum cruise condition as the design point.

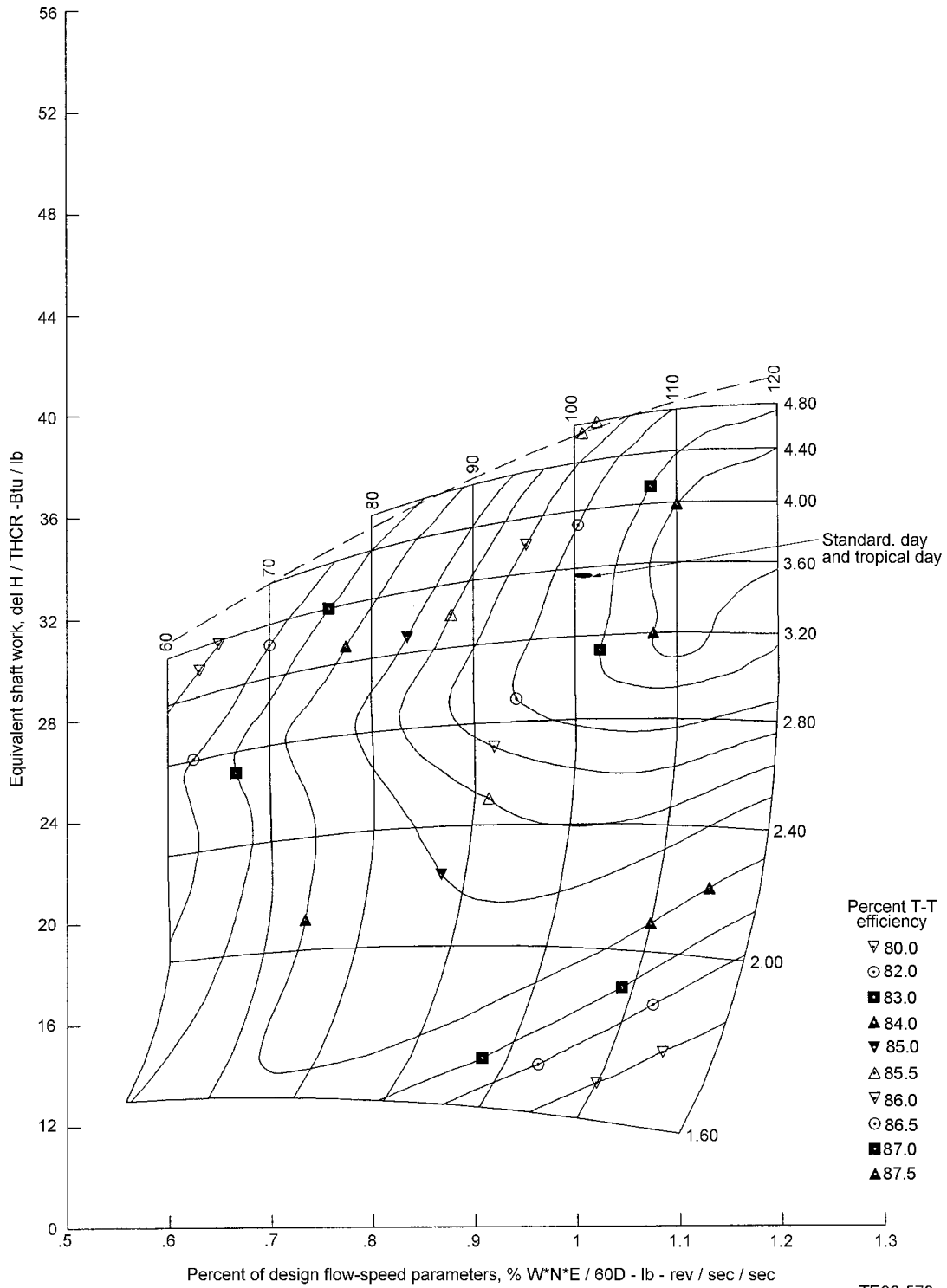
While the GGT operates at roughly a fixed point on the turbine map, the PT runs at a constant mechanical speed and must operate over a wide range of conditions and power settings. This is shown on the overall turbine maps shown in Figures 45 and 46.

### 5.3.1.2 Water/Methanol Injected Engine

The turbines in the injected engine are much like those of the baseline engine, though there is a difference in inlet and exit flow capacities. At the aerodynamic design point conditions, the GGT of the injected engine has an 8.9% higher inlet flow capacity while the PT has a 9.1% lower flow capacity relative to the baseline engine. The changes in flow were accommodated by reblading the turbines and maintaining the basic aerodynamics of the baseline engine. Thus, the GGT and PT of the injected engine were essentially photographic scales of the baseline engine and no additional mechanical design work was required. Though the turbines will be rebladed, the airfoil geometric characteristics will only be slightly different from the baseline turbines.

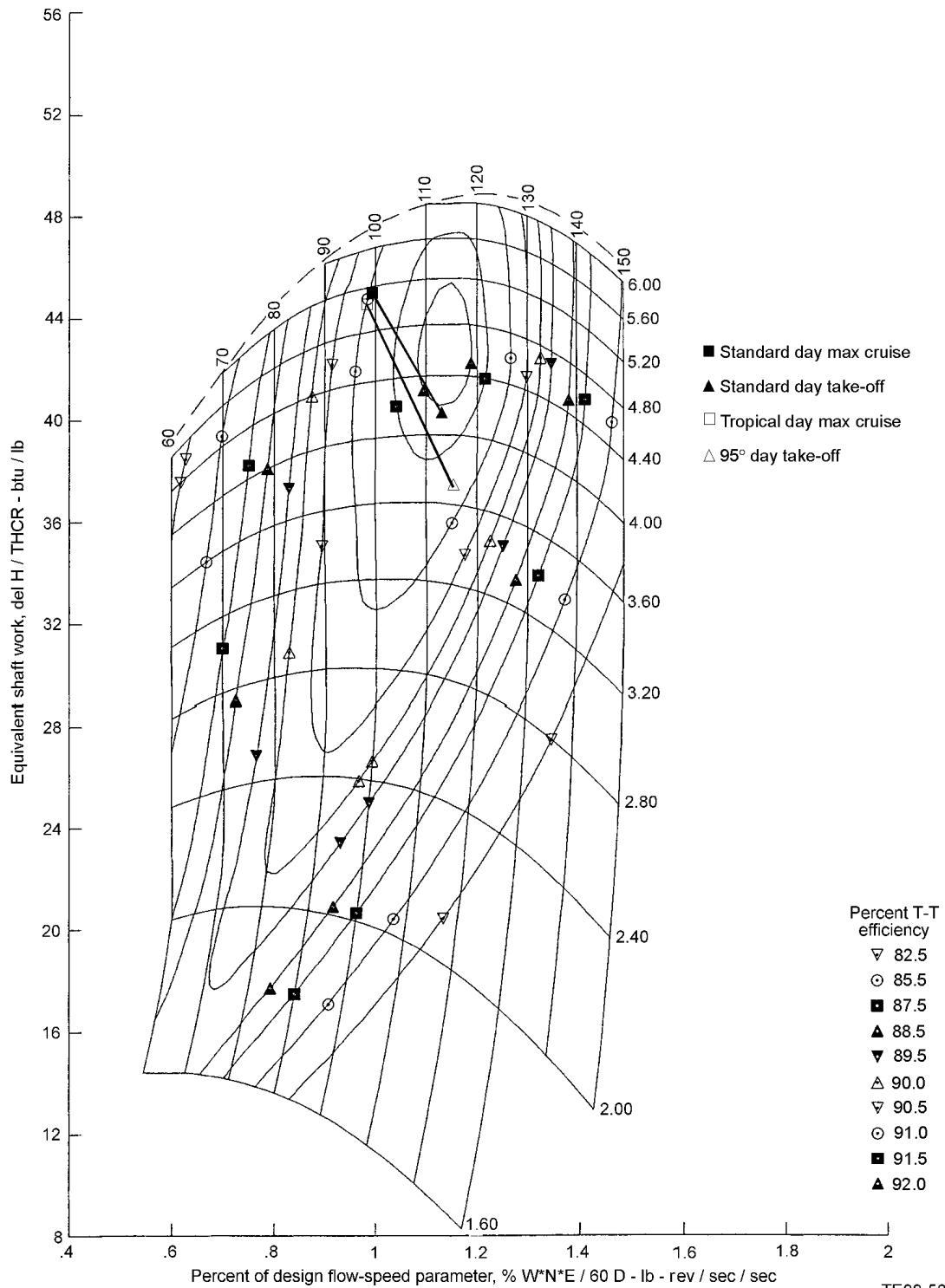
### 5.3.2 Heat Transfer

The anticipated cooling configuration for the GGT vane is an impingement/film-cooled design with pressure side edge discharge and a thermal barrier coating (TBC). The source of cooling air for this vane is compressor discharge. An illustration of the airfoil cross section at the midspan is shown in Figure 47. Two impingement tubes (one forward and aft of the dividing rib) are supplied coolant flow from the outer diameter of the airfoil. The forward impingement tube exhausts coolant flow to a showerhead film-cooled leading edge and after impingement to a row of film holes angled 30 deg from the suction and pressure sides. The aft impingement tube discharges coolant air through impingement holes and aft tube trailing edge holes. Coolant flow continues in the chordwise direction, passing across a pin fin array and discharging through the pressure side exit slot. A row of 30-deg angled film holes on the suction side, fed from the pin fin channel upstream of the last pin row, provides additional cooling of the suction side trailing edge. The required coolant flow for this vane is 6.09% of engine flow.



TE98-579

Figure 45. Gas generator turbine overall map.



TE98-580

Figure 46. Power turbine overall map.

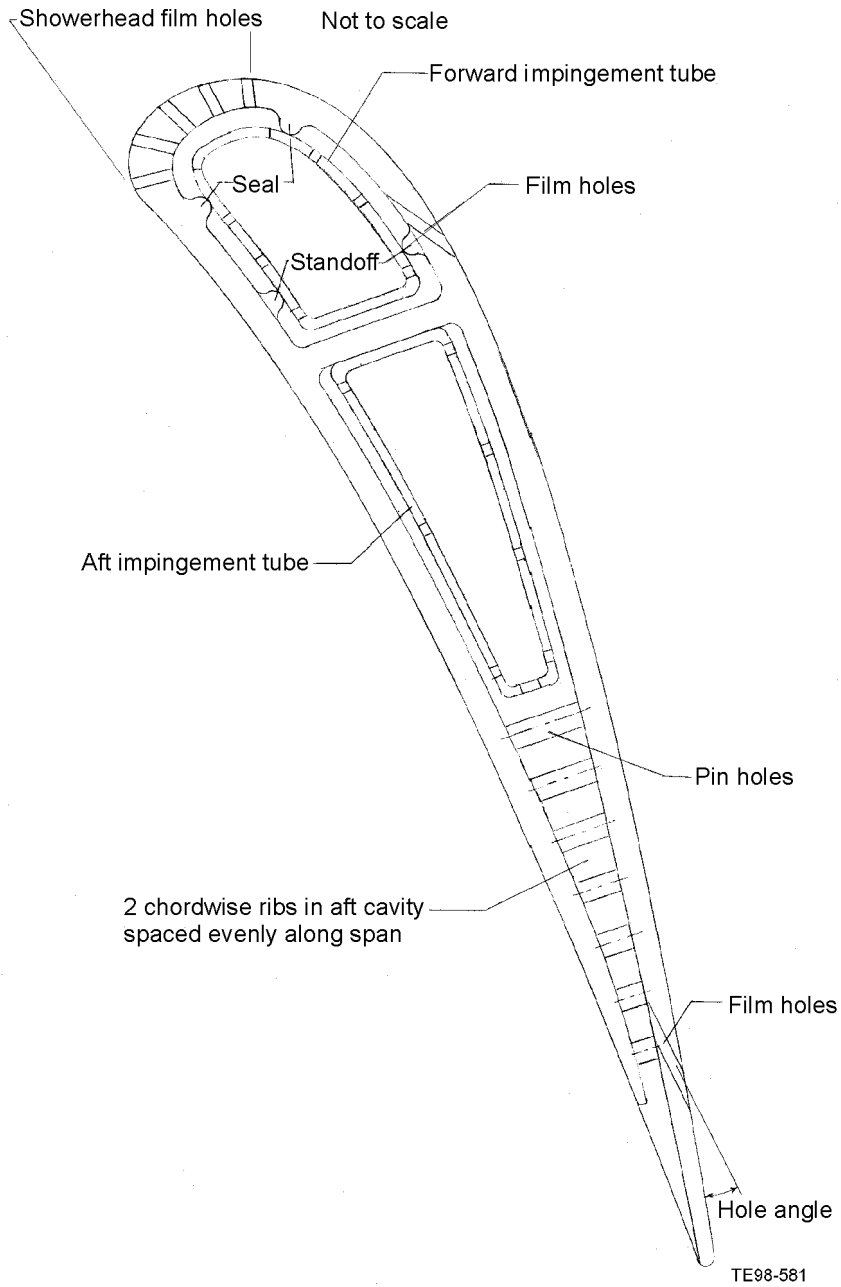


Figure 47. GGT vane cooling scheme.

The inner and outer endwall cooling configuration consists of double wall construction containing pin arrays to augment heat transfer. Coolant flow enters through the backside at the endwall leading edge and exits through the trailing edge. A TBC is used on the endwalls. The required coolant flow for the outer and inner endwalls is 1.92 and 1.22%, respectively.

The anticipated cooling configuration for the GGT blade is shown in Figure 48. The source of cooling air for this blade is compressor discharge. This configuration consists of two separate circuits. First is a leading edge circuit containing three rows of film-cooling holes, two rows near the geometric leading edge and inclined radially outward and a single row of shaped holes angled in the streamwise direction that discharge on the suction side of the airfoil near the crown. The second circuit is a serpentine circuit consisting of three passages connected in series. A single row of film-cooling holes exhausting to the pressure surface is featured in both the second and third passages of the serpentine and a row of trailing edge channels in the third passage discharges on the pressure surface. All passages contain angled (45 deg) rib turbulators to enhance heat transfer. The required coolant flow for this blade is 3.13% of engine flow.

The cooling configuration for the GGT blade track is impingement using compressor discharge air fed through the inner GG turbine case. The blade track also features a TBC (0.010 in. thick) on the gas side of the blade track. The required coolant flow for the blade track is 1.44% of engine inlet flow.

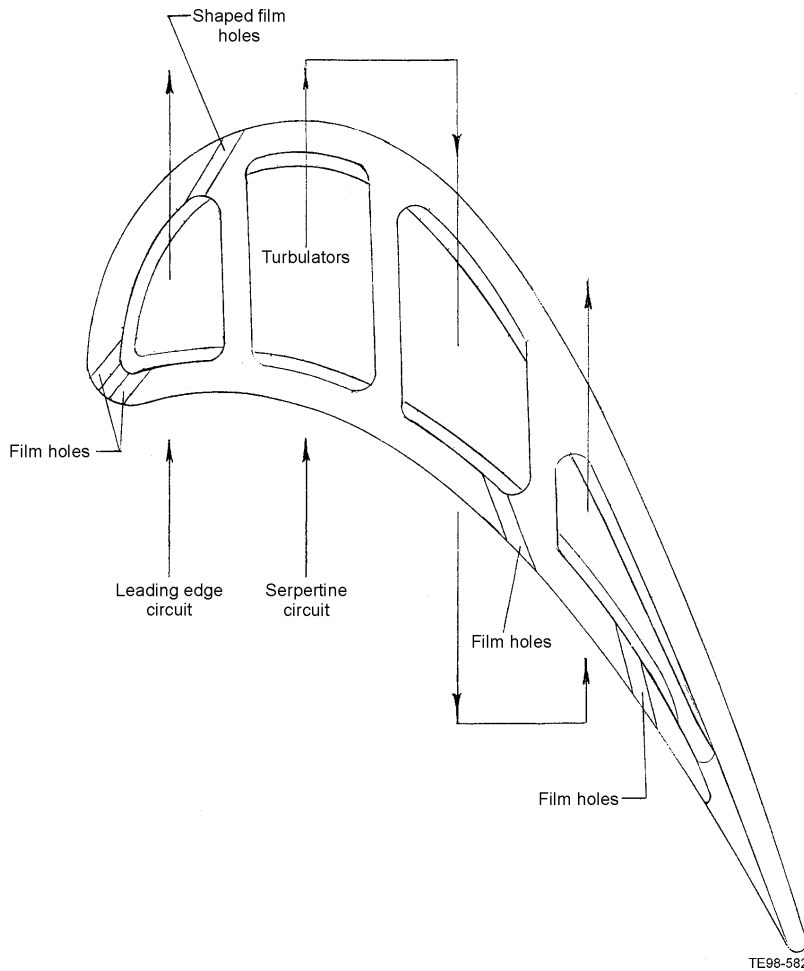


Figure 48. GGT blade cooling scheme.

The selected cooling configuration for the PT1 vane is of the impingement/convection type. The source of cooling flow for this vane is the fifth stage of the compressor. The cooling scheme has holes at the leading edge of the impingement tube delivering cooling air to the backside of the vane leading edge. The coolant flow then proceeds aft through channels formed by the inside surfaces of the airfoil suction and pressure surfaces, the impingement tube and chordwise fins cast into the airfoil. The two coolant flow streams join at the trailing edge of the impingement tube and then flow across an array of pin fins before exiting the vane through a slot on the pressure surface near the trailing edge. The required coolant flow for this vane is 1.80% of engine flow.

The cooling configuration of the PT1 blade consists of three parallel cooling channels with 45 deg rib turbulators for augmentation of heat transfer. The strips are 0.010 in. high, spaced radially at 0.1 in., and are staggered from pressure to suction surface. Cooling air (the source is fifth-stage compressor air) is supplied at the base of the attachment. The flow is metered to the blade by a flow restriction plate at the attachment entrance location. The blade shroud is passively cooled by purging the blade track cavity with spent cooling air from the blade and cooling flow from the surrounding static structure. The required cooling flow for this blade airfoil is 0.57% of compressor inlet.

A summary of the secondary and leakage flows in the GGT and PT at a sea level static, ISA+36°F, takeoff power condition is shown in Figure 49.

The vane and blade cooling requirements were determined using a realistic first-order basis derived from a simple overall energy balance equating the convective heat load on any cooled structural component to the coolant heat absorption. The assumption is made that the external (gas-to-wall) heat transfer distribution can be approximated by fully developed turbulent flat plate heat transfer correlations and the internal cooling circuit heat transfer efficiency can be expressed in terms of simple (infinite hot

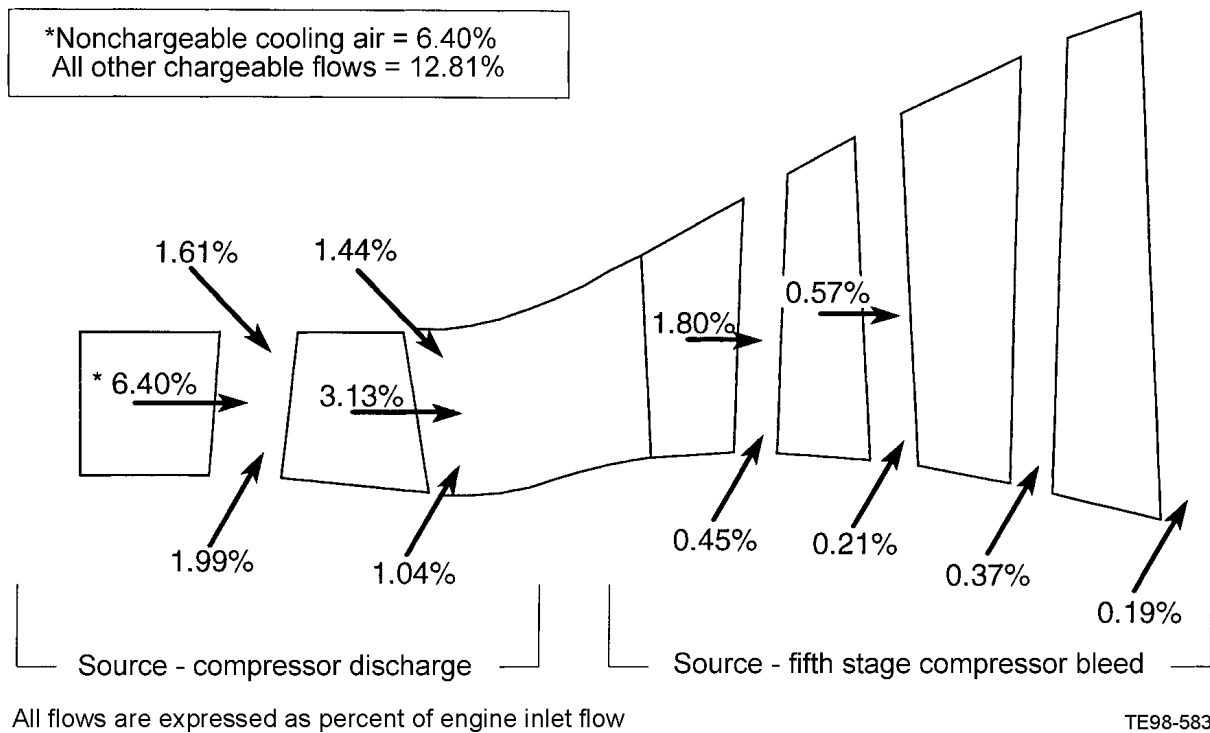


Figure 49. Gas generator turbine and power turbine secondary flows.

fluid thermal capacity) heat exchanger relationships. This results in simple expressions relating cooling flow requirements to basic turbine aerothermodynamic parameters. The general expressions are combined

into a form reflecting global engine geometric and cycle parameters known in the preliminary design stage, thus permitting informed estimates of cooling flow requirements based on limited available design definition.

The derived expressions provide a means of projecting cooling flow requirements reflecting:

- Turbine solidity
- Airfoil row inlet/exit Mach number levels
- Airfoil row Reynolds number
- Cooling system internal efficiency
- Dimensionless level of cooling

The characteristic coefficient of the cooling flow relationship is adjusted so a simple expression correctly predicts a known design for which detailed cooling performance is available. Then realistic projections to off-design operation or alternate aerodynamic configurations are developed.

Since the characteristic coefficient is tied specifically to a previously designed airfoil, the determination of the cooling flow requirements also establishes the basic cooling configuration. The database contains characteristic coefficients for impingement, convection, and combined convection, impingement, and film-cooling designs. To facilitate the estimation of the coolant flow requirements during the preliminary design phase, the scaling technique described previously has been incorporated into the velocity diagram computer program used in the aerodynamic design of the turbine. In addition to cooling requirements, this program also determines realistic first-order estimates of radial distributions of cored metal area consistent with a life and maximum allowable stress constraint. Knowing the required coolant flow and the blade hub coolant flow area allows for the calculation of an inlet coolant Mach number. To satisfy the requirement for sufficient coolant flow area, the inlet coolant Mach number is also constrained to a maximum value.

### 5.3.3 Mechanical Design

Much of the mechanical design of the SHCT turbines was done using an aerodynamic/ mechanical preliminary design model, which used inputs from the heat transfer, stress analysis, and mechanical design disciplines. Airfoils designed during the aerodynamic design phase were scaled and/or cored to meet stress rupture life requirements. In addition, airfoil cooling air requirements were calculated as well as blade weights and centrifugal loadings, which were subsequently used to size the turbine wheels. Specific turbine features are illustrated in the general layout drawing of the SHCT engine shown in subsection 5.6.

The turbine components were designed to meet the following mission life requirements:

- 50% of missions at standard day (59°F) conditions
- 50% of missions at tropical day (95°F) conditions
- Typical mission—total 50 min (see Table XXII)
- Component life:
  - ◆ LCF—30,000 cycles
  - ◆ 1% creep, coating repairable—15,000 hr
  - ◆ Uncoated oxidation, stress rupture—30,000 hr
  - ◆ OEI operation (2 occurrences)—10 min

Table XXII. Typical mission profiles.

Flight condition	Performance point	Time—min
Taxi	Idle	3
Takeoff	Max power	0.5
Convert	Max continuous	1.5
Climb	Max continuous	8
Cruise	Typical cruise	20
Descent	Typical cruise	12
Convert	Max continuous	1.5
Land	Max power	0.5
Taxi	Idle	3

### 5.3.4 Stress Analysis

The preliminary design of the GGT and PT vanes, blades, and wheels was performed using Rolls-Royce Allison-developed preliminary design tools. The vane allowable temperatures were determined on the basis of corrosion/oxidation in and out of a salt environment, while the blades were analyzed with respect to creep/stress rupture, corrosion/oxidation, and thermal fatigue. While these methods are more than adequate for this preliminary design effort, a detailed design phase would incorporate finite element analyses to predict LCF and fatigue crack growth in the various turbine components.

Based on successful Rolls-Royce Allison and industry experience with high-temperature materials, the GGT and PT components meet life and performance goals at minimal risk. Table XXIII summarizes the materials for the GGT and PT vanes, blades, and wheels required to meet the SHCT design goals.

The structural mechanics design point was at a sea level static, ISA+36°F takeoff power condition. The turbines were analyzed at several operating conditions from the typical mission to ensure all components met or exceeded the goal mission life of 15,000 hr. A summary of the GGT airfoil lives is shown in Table XXIV.

Avoidance of dynamic resonances leading to high cycle fatigue failures was examined on a first-order basis for this preliminary design. Failures due to the resonant behavior of the primary modes were avoided by increasing the axial gaps between the vanes and the blades until the dynamic stresses were sufficiently low as compared to existing production engines. The maximum 1T and 2T alternating stresses for the GGT and PT stages at the sea level static, ISA+36°F, takeoff power condition are shown in Figure 50.

Table XXIII. Gas generator turbine and power turbine vane, blade, and wheel materials.

Component	Rpm	RIT—°F	Material
GGT vane	-	2650	CMSX-4
GGT blade	17,850	2650	CMSX-4
GGT wheel	17,850	2650	U-720
PT first vane	-	1890	Mar-M247 DS
PT first blade	13,800	1890	Mar-M247 DS
PT first wheel	13,800	1890	U-720
PT second vane	-	1560	Mar-M247
PT second blade	13,800	1560	Mar-M247
PT second wheel	13,800	1560	U-720

Table XXIV. Gas generator turbine vane and blade life.

<b>Vane</b>					
<b>Condition</b>	<b>Metal temp—°F</b>	<b>No salt life—hr</b>	<b>Salt life—hr</b>	<b>Required hr</b>	<b>% life no salt/salt</b>
SLS, 95°F takeoff	1950	7000	5000	300	0.042/0.060
25,000 ft, trop day max cruise	1882	15,000	6800	3300	0.220/0.485
25,000 ft, trop day cruise	1635	>100,000	15,000	9600	0.096/0.640
SLS, 95°F flight idle	1433	>100,000	30,000	1800	0.0/0.060
<b>50%/50% avg.</b>					<b>0.802</b>
<b>Blade</b>					
<b>Condition</b>	<b>Critical span—%</b>	<b>Metal temp—°F</b>	<b>Life—hr</b>	<b>Required hr</b>	<b>% life</b>
SLS, ISA, takeoff	30	1770	2,133	300	0.140
25,000 ft, ISA, maximum cruise	30	1618	171,673	3300	0.019
2000 ft, ISA+36°F, OEI	30	1880	260	0.67	0.005
SLS, 95°F takeoff	30	1795	1,053	300	0.285
25,000 ft, trop day maximum cruise	30	1715	10,088	3300	0.327
<b>50%/50% avg.</b>					<b>0.388</b>

### 5.3.5 Component Cost Estimates

Completion of the SHCT turbine preliminary design made it possible to estimate the cost of the turbine components. The estimates were based on the number of parts, part complexity, materials used, and the weight of each component. Standard items or items not designed specifically for the SHCT were scaled from the Rolls-Royce Allison AE 1107 production engine. The major turbine assemblies breakdown is shown in Table XXV. The costing methodology and a detailed breakdown appear in subsection 5.6.

### 5.3.6 Recommendations for Further Work

Work in the turbine section of the SHCT beyond this preliminary design phase should include:

- Explore adjustments to the engine cycle temperature so the PT first-stage blade and perhaps the vane would not have to be air-cooled to meet life requirements. This would reduce the complexity and cost of manufacturing the airfoils and would eliminate cooling air, which ultimately degrades the engine cycle. Also, lower cycle temperatures may allow the use of less expensive materials in other parts of the turbine.
- Use 3D passage flow analysis tools to minimize the number of airfoils required in each blade row, potentially reducing acquisition and maintenance costs. Reduced airfoil solidities might also show a benefit in reduced airfoil trailing edge blockages, which should reduce secondary losses.
- Examine the application of a vaneless counter-rotating PT. Though specific conditions must be present for this turbine architecture to succeed, it would eliminate the acquisition and maintenance cost of an air-cooled PT first-stage vane, potentially reducing overall cooling air requirements and engine length. The impact on the overall engine cycle and other engine components must be explored before going forward with this design concept.

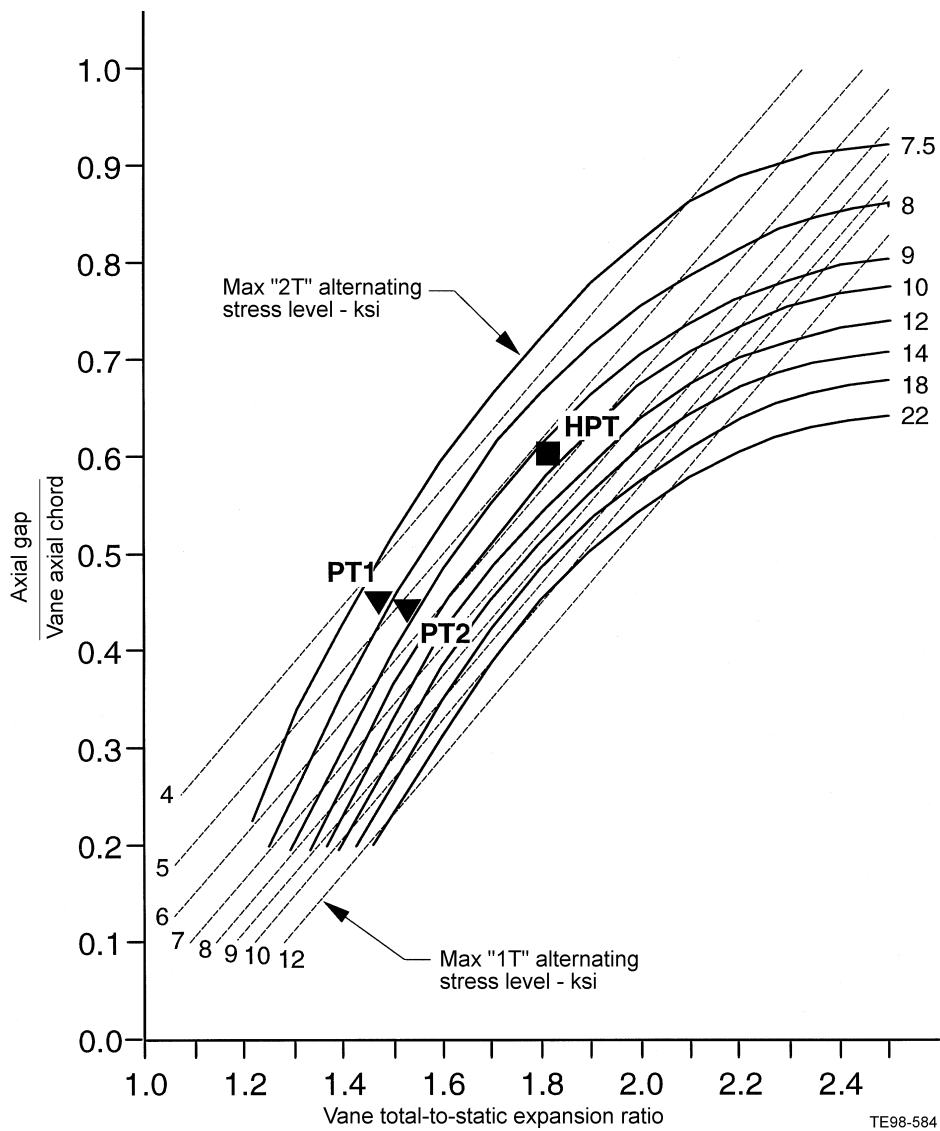


Figure 50. Conservative axial vane-blade spacings result in low predicted dynamic stresses.

Table XXV. Turbine assemblies breakdown.

Module description	Weight—lb	Material and labor cost—\$
GGT first vane and support assembly	28.5	75,450
GGT rotor assembly and second vane	201.7	104,023
PT assembly	403.3	179,992

## 5.4 Mechanical Systems Preliminary Design

### 5.4.1 Sumps

Design of the sumps for this engine is based on simplicity, reliability, and low cost. A novel LP small diameter shaft design allows for very low bearing and seal speeds (Table XXVI). The low speed of the bearings and seals reduces heat generation, resulting in a reduced size lube system, improves reliability, and eliminates the expensive features required for other modern gas turbines, such as out of round bearings and exotic seal designs.

Each of the two rotors is supported by a thrust bearing in front and a roller bearing in the hot section of the engine. Labyrinth seals are used in the front sump, where pressures across seals are low and absolute sealing is not as critical as in the hot section. Labyrinth seals provide the lowest life cycle costs and are extremely reliable. They also allow for simple engine assembly, improving maintainability. This also reduces the amount of lubrication required in the front sump, as carbon seal runners require lubrication. Carbon face seals are used in the two hot section sumps to provide absolute sealing when the engine is in the vertical position and to reduce loss of compressor air used for seal pressurization. The carbon face seal is the only liquid seal; all other types of gas turbine seals, such as labyrinth and circumferential carbon seals, are gas seals only.

The secondary flow diagram for sump pressurization is shown in Figure 51. Front sump pressurization uses second-stage compressor air with the sump vented to atmosphere. This low pressure across the seals allows use of labyrinth seals in the forward sump. Cool fourth-stage compressor air will be ducted to, and surround, the two hot section sumps to keep the sumps cool. This will eliminate the oil coking problems that can occur in hot sumps. CDP air will combine with this cooling air and be used to provide turbine cooling, ultimately returning to the flow path after the first LP turbine stage.

The cooler air will reduce the heat loading into the sump in the hot area of the engine. The bulk of the seals are located inside the sump and are being fed with the cooler air. These features will help to greatly reduce the potential for coke formation on the seals, a major source of seal failure.

Bearings will be made of M50 for low cost, except for the gas generator thrust bearing outer ring, which is integral with the squirrel cage. This part will be made of a case carburized steel such as CBS 600 or M50 NIL.

*Table XXVI. The low pressure, small diameter shaft design allows for very low bearing and seal speeds.*

<b>Bearing</b>	<b>Bore—mm</b>	<b>Rpm</b>	<b>DN</b>
1 - LP thrust	55	16500	907,000
2 - GG thrust	90	17700	1,590,000
3 - GG roller	100	17700	1,770,000
4 - LP roller	60	16500	990,000

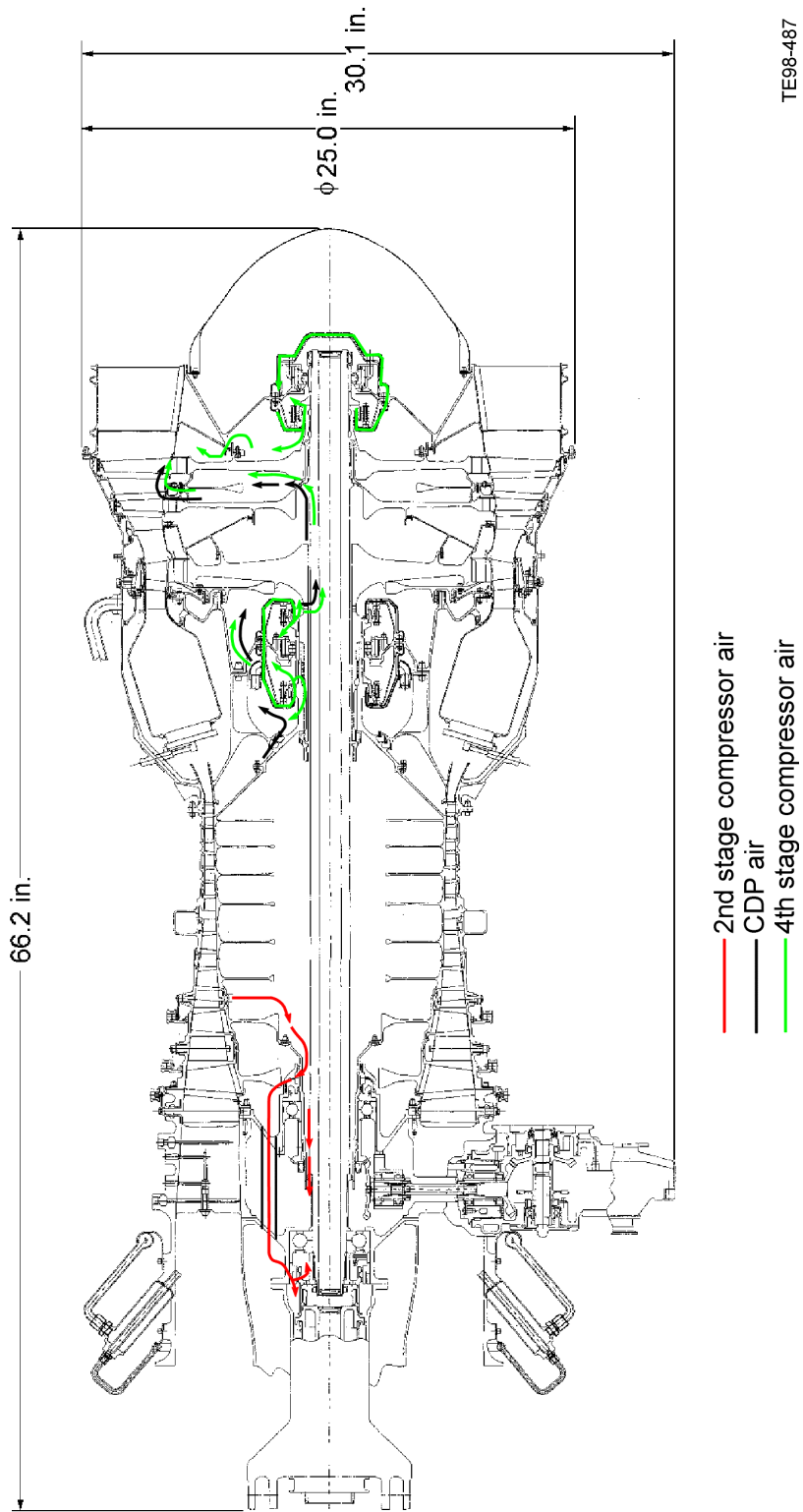


Figure 51. Sump pressurization.

## 5.4.2 Lubrication System

The dry sump lubrication system for the tiltrotor engine will be a conventional hot tank, recirculating closed-loop, oil jet supply type, which will have simple, lightweight, reliable components. All of the system components will be state of the art. This represents the system approach with the greatest reliability and lowest developmental cost because of its very low technical risk.

Rolls-Royce Allison designs and develops the lubrication systems for all of its products. Well established design guides and procedures are in place for the detailed analysis of lubrication systems. SPAN, a Rolls-Royce Allison proprietary steady-state lubrication analysis program, will be used to calculate the supply oil flows and temperatures throughout the engine under a variety of normal and emergency operating conditions. The model predictions will be validated with both individual component and engine testing.

Many of the major components of the lubrication system will be designed and developed to Rolls-Royce Allison specifications by specialized vendors. Good working relationships have been developed with many component vendors during the recent development of many new Rolls-Royce Allison products. Specific lubrication studies will be completed to minimize the weight of the total lubrication system based on lubricant temperatures and flow rates. These tiltrotor mass flows and temperature differences will be related to weight through past correlations for pumps, tanks, and heat exchangers to select the minimum overall system weight.

An auxiliary gearbox-driven supply pump will draw oil from a tank and overcome the variable pressure drop in the filter, fuel-oil cooler, and supply lines to the three sump mainshaft bearings and seals, as well as the gearbox mechanical components. A 3-micron filter will be used to improve engine bearing, seal, and gear life and increase overall engine cleanliness and reliability. The filter will incorporate a pressure bypass valve to accommodate cold start and clogged conditions. The filter element will be sized to achieve 2000-hr operational life before a filter element change. A fuel/oil cooler will regulate the flow of oil through the cooler by means of a thermal bypass valve to maintain a constant oil outlet temperature. This thermal bypass valve will also function as a cold start bypass valve. A pressure regulator, downstream of the cooler, maintains a constant pressure drop across the supply lines and jets to ensure a constant supply of filtered and cooled oil to all the rotating components.

Oil will be distributed through a typical distribution system, with the utilization of internal cast passages as much as possible. Scavenge oil will be collected from the gearbox and output shaft sumps by individual scavenge pumping elements. The combined scavenge flow will flow past a debris monitor to assess the health of the oil-wetted components. The aerated oil is deaerated in a static cyclonic separator in the top of the tank, with the oil gravity drained to the bottom of the tank. The sumps and tank are connected with vent tubes that will maintain a common pressure in all of the sumps. Air entering the system through seal leakage will exit the tank and pass through a rotating separator in the auxiliary gearbox to remove the oil from the air. The separated air will then be vented to ambient. This sump vent system will ensure a low oil consumption rate. The lubrication system will be electrically instrumented with pressure, temperature, oil level, and debris monitor devices to interface with the Rolls-Royce Allison control system.

## 5.4.3 Define Scaled AE 1107C Accessory Drives (Accessory Gearbox and Power Takeoff Gearbox)

The accessory drive gearing is entirely conventional. The power takeoff (PTO) bevel gear is mounted directly to the gas generator shaft, as it is in most new aircraft engines. The bevel gear pinion mounts in its own housing bolted to the gas generator thrust bearing housing; again this is entirely conventional for new engines. The bevel gears can be adjusted and inspected in the open before the front frame is installed. The PTO and accessory gearboxes are connected with a quill shaft, and this shaft has a shear section for

overload protection. At this time the current accessory gearbox can only be scaled based on the new engine's power requirements compared to the AE 1107C. New gearbox technology reducing cost and improving performance can also be addressed.

Rolls-Royce Allison is focusing on achieving an industry-leading position in gearbox technology and production. This work encompasses gears, bearings, seals, lube systems, and housings. It is expected the accessory gearbox will look similar in configuration to the AE 1107C accessory gearbox, but the technology used will result in cost reduction and performance improvements. As with the current AE 1107C, the first mesh will be a pair of bevel gears. All other meshes in the accessory gearbox will be spur gears.

#### 5.4.4 Rotor Dynamics/LP and HP Shafting

The rotor dynamic design objectives for the SHCT engine were:

- Keep the number of rotor and bearing components to a minimum to eliminate as many interfaces as possible. This lowers engine cost, aids assembly, and simplifies rotor balancing with reduced stacking of tolerances.
- Locate all hotter running thrust bearings forward in the engine and keep roller bearings aft because a roller bearing with very small internal diametral clearance can control the HP turbine better than a ball bearing.
- Keep rotor and bearing diameters to a minimum for reduced component weight and reduced bearing heat generation. Reduced bearing diameters simplify the bearing cooling system and enhance bearing reliability.
- Design the rotor geometry and bearing locations to maintain all critical speeds 25% below or 30% above the steady operating speed ranges of the LP and HP rotors.
- Provide sufficient rotor damping to safely transition through critical speeds lower than the steady-state operating speed range.
- Design an effective and straightforward balancing procedure that is consistent and repeatable. At the same time provide a damper system capacity for at least 0.001 in. of rotor unbalance eccentricity.

These design objectives were used to define the bearings and geometry of the LP and HP rotor systems starting from the centerline and working outward.

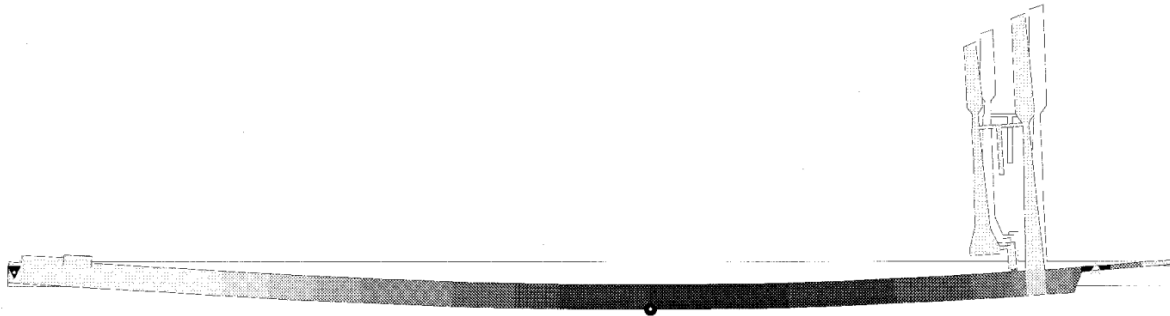
##### 5.4.4.1 LP Shaft Design Description

The length of the LP rotor was set by the combined length required for the compressor, turbines, and combustion system. The design speed is 13,500 rpm, which is 10% lower than the Rolls-Royce Allison AE 1107C LP shaft. The AE 1107C shaft is also longer because the AE 1107C compressor is longer. The AE 1107C LP shaft system currently runs above its first shaft bending mode. The alternatives for the SHCT are to increase shaft diameter to run below the first bending mode or reduce shaft diameter to run above as the AE 1107C.

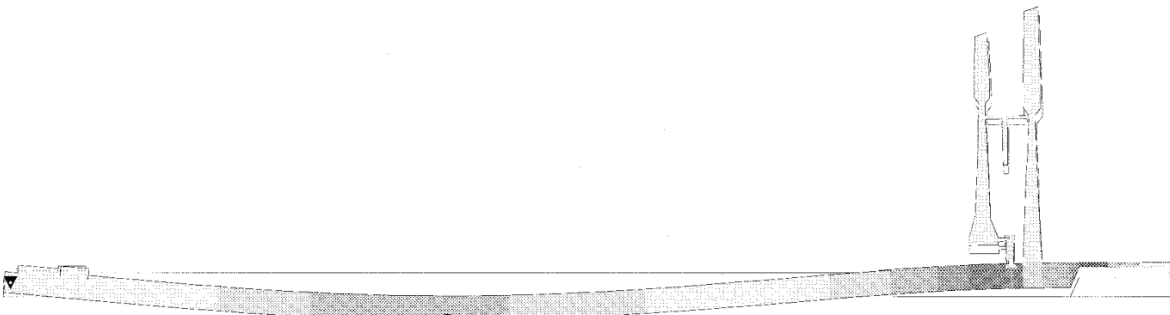
To run below the bending mode the shaft diameter would need to grow to 5 in. in diameter. This high LP shaft diameter would increase the HP rotor bearing and turbine bore diameters to a point violating the design objectives, as gas generator bearings DN would be over 2.7 million. To run above the shaft first bending mode, like the AE 1107C, a reduced 2.5-in. diameter LP shaft would be required. The reduced diameter would lower the first bending mode from the higher speed AE 1107C shaft, while the smaller diameter shaft would meet and exceed the static bending stiffness of the AE 1107C shaft. This is important where gyroscopic moments can bend the shaft during an aircraft maneuver. This shaft can be balanced simply by measuring shaft runout between bearings and then calculating a correction based on influence coefficient methods. The shaft is supported by a ball thrust bearing forward of the compressor

and by a roller bearing aft of the turbine. An oil squeeze film damper supporting the roller bearing provides damping for both the turbine and shaft modes below the steady-state operating speed range.

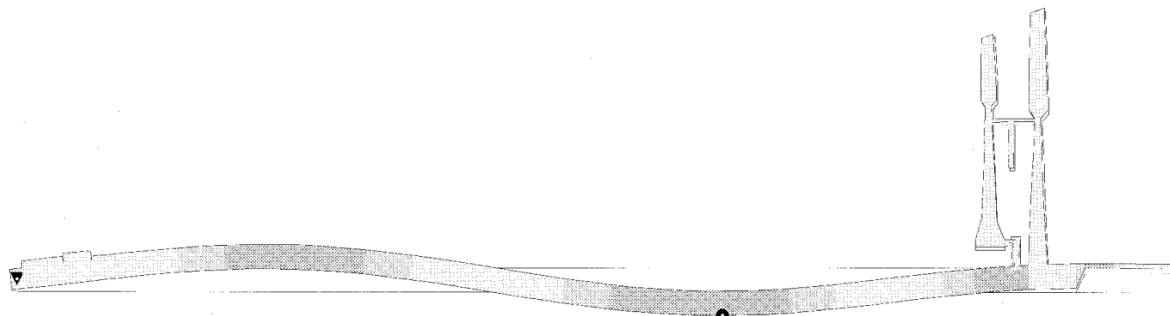
The predicted shaft and turbine critical speeds are shown in the following bulleted list. The rotor damping is expressed as LogDec. Dynamic amplification through the critical speed is approximately  $3.14/\text{LogDec}$ . Rolls-Royce Allison typically requires a LogDec of at least 1 when passing through a shaft bending mode. The deflection mode shape for the modes listed is shown in Figure 52 with only half of the geometry above the centerline shown.



Turbine mode @ 3187 rpm with a LogDec of 1.87



First shaft bending mode @ 8188 rpm with a LogDec of 1.41



Second shaft bending mode @ 23125 rpm with a LogDec of .2

TE98-485

*Figure 52. LP shaft and turbine modal deflections.*

- Turbine mode at 3187 rpm with a LogDec of 1.87
- First shaft bending mode at 8188 rpm with a LogDec of 1.41
- Second shaft bending mode at 23,125 rpm with a LogDec of 0.2

The design allows steady-state operation of the LP shaft down to 10,900 rpm with plenty of margin from the second bending mode at maximum operating speed. This LP shaft design meets all of the design objectives listed. The higher solid shaft weight is offset by reduced weight on other low diameter shaft, turbine bore, housing, and bearing components.

#### 5.4.4.2 HP Shaft Design Description

The HP shafting system is composed of an eight-stage axial compressor and a single-stage turbine to drive it. The compressor stages are welded together into one unified assembly. Both ends pilot on the same diameter as the bearings for effective balancing about the true running center of the compressor assembly. A shaft is attached to the single-stage turbine that includes pilots at the bearings for balancing about turbine running center. The shaft double pilots to the compressor rotor assembly with a locked spline between the pilots to transfer torque between the compressor and turbine. The ball thrust bearing is located in front of the compressor, where the temperatures are lower and the radial loads are less. The thrust bearing is supported by a squirrel cage compliant spring acting in parallel with a squeeze film damper. The squirrel cage reacts the bearing thrust loads and centers the front compressor.

The basic design of the HP rotor eliminates many interfaces required with multiple pieces that complicate rotor balancing. The long turbine shaft provides ample stretch to ensure the turbine does not become loose during thermal transients. This arrangement provides the lowest diameter bearings and turbine bore when compared to other attachment arrangements and therefore best meets the design objectives.

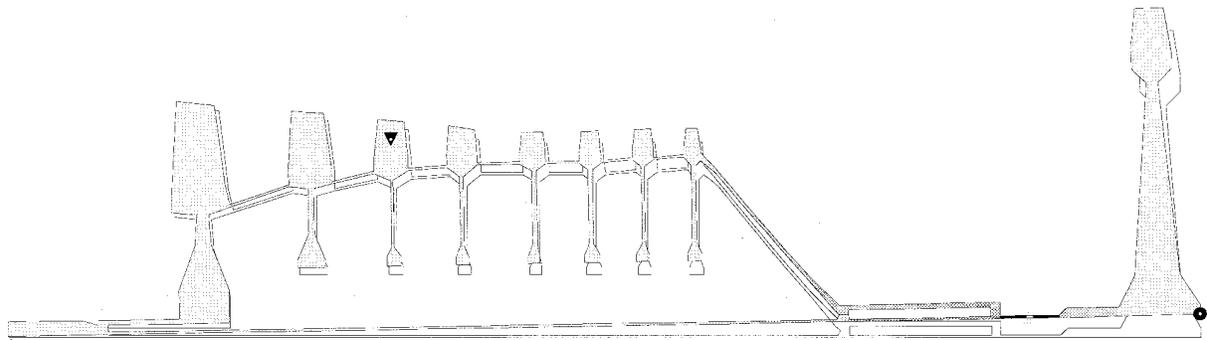
Both the ball bearing in front of the compressor and the roller bearing in front of the turbine are supported by oil squeeze film dampers to provide damping for both the compressor and turbine rigid body modes below steady-state operating speeds. The first rotor bending mode has more than adequate margin above the 17,500 rpm HP rotor design speed. The critical speeds are shown in the following bulleted list. The mode shapes are shown in Figure 53.

- Turbine mode at 3285 rpm has a LogDec of 9.3.
- Compressor mode at 6398 rpm has a LogDec of 1.8.
- First bending mode at 31,989 rpm has a LogDec of 1.6.

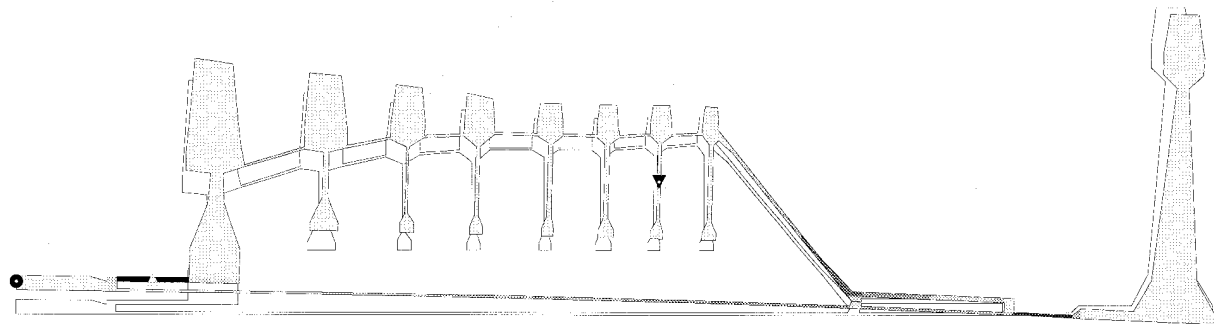
All other shafting configurations considered violated the basic design objectives by requiring higher diameter bearings, had more parts requiring high tolerance interfaces, or would be difficult to balance effectively. These configurations included:

- HP and LP roller bearings between the turbines. This would require an additional damped roller bearing to provide damping for LP shaft mode; otherwise the shaft and bearing diameters would be required to exceed acceptable levels.
- HP turbine supported by intershaft roller bearing. The LP shaft would be excited by the higher speed HP rotor, which would require an unacceptable increase in LP shaft diameter.

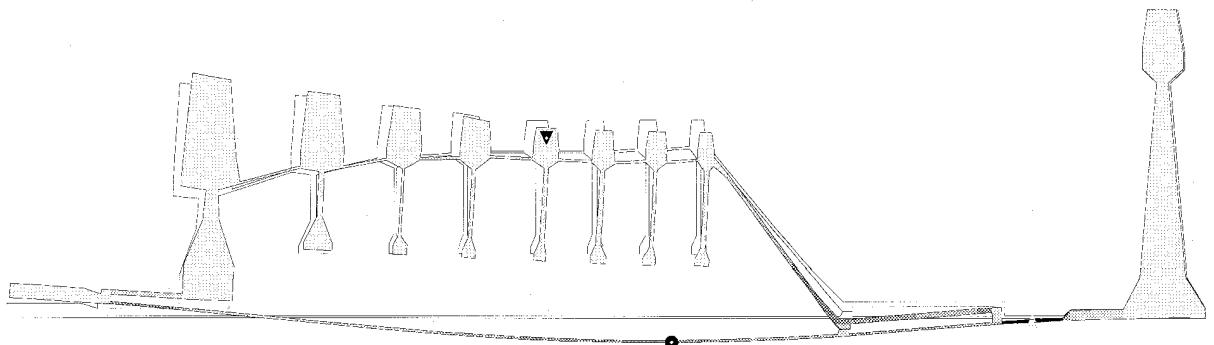
The dampers supporting both the LP and HP turbine roller bearings may be provided with a continuous supply of oil or may be sealed if the bearings are vapor lubed. Rolls-Royce Allison has tested such sealed dampers in the past as part of a high-temperature bearing and damper effort contract with the Air Force.



Turbine mode @ 3285 rpm has a LogDec of 9.3



Compressor mode @ 6398 rpm has a LogDec of 1.8



First bending mode @ 31989 rpm has a LogDec of 1.6

TE98-486

*Figure 53. HP rotor modal deflections.*

#### 5.4.5 Recommendations for Future Work

The Rolls-Royce Allison AE 1107C engine has a specification oil consumption rate of 0.08 gal/hr. Oil is lost due to sump vent air with oil entrained in the air and not 100% separated. Oil is also lost due to leakage across seals, including mainshaft and accessory gearbox seals. One way to reduce the loss of oil to the atmosphere and to reduce cost and weight and improve reliability is to go to a once-through oil system. While this may seem to be a contradiction, the amount of oil required for an optimized once-through system is very small. Rolls-Royce Allison has successfully tested a high-speed mainshaft bearing with only 0.01 gal/hr of oil supplied in a very hot environment. With optimization, it may be possible to

further reduce this flow. The bearing had ceramic rollers, and it would be logical to apply this type of lubrication to the roller bearings in the hot sumps. This would also allow the use of labyrinth seals in place of the carbon face seals, further reducing cost and heat generation. Self-contained dampers could be used.

Using the once-through system a total of 0.0002 gpm of oil would be supplied to the mid sump, compared to the approximately 2 gpm currently required. This mist would be routed to the turbine exhaust after lubricating the bearings, and the fire hazards of oil leaking from the hot sumps would be eliminated. Scavenge lines and pump elements would be eliminated and the supply pump could be reduced in size. This is especially desirable for a tiltrotor engine. All the required technology has been demonstrated; it now needs to be successfully applied. The greatest benefit would be achieved if a once-through system were applied to all the lubricated components. This would necessitate the development of gears that could operate with a small amount of mist. Rolls-Royce Allison is working on the technology necessary to achieve this goal.

Past successful engine oil mist lubrication has demonstrated the feasibility of once-through lubrication systems on NASA helicopter test bearings, the J99 lift engine design, the T800 emergency lubrication system, and many other commercial applications.

A dry sump lubrication system improvement program increasing system reliability and reducing engine operating costs would promote the commercial development of a more sensitive oil debris health monitoring system. While adequately lubricated, properly designed rolling-element bearings, seals, and gears theoretically have very long operating lives, but manufacturing flaws, improper installation, unexpected service loading, and lubricant starvation can result in the need for premature component failure identification. However, existing, commercially available debris monitoring systems are limited in identifying particle sizes greater than 200 micro-inches. Smaller particle size identification would allow much earlier detection of impending component failure. One emerging technology capable of reliably detecting both metallic and nonmetallic oil debris particles from 50 to 200 micro-inches in size is claimed by a small business concern that is in contact with Rolls-Royce Allison. This technology, however, requires a development program to validate the claims of the inventor. Coupled with this more sensitive oil debris size transducer, component thermal measurements and individual jet flow identification should be pursued to augment the early identification of component problems.

Health monitoring of the bearings, gears, and seals would be accomplished with a combined vibration and acoustic technique that is progressing at a small company currently in contact with Rolls-Royce Allison.

## ***5.5 Water/Methanol Injection System Preliminary Design***

### **5.5.1 Water/Methanol Injection System Description**

To meet the aero/thermal design requirements a fine mist of water/methanol spray is needed. This is accomplished with ten water injection nozzles located symmetrically around the front of the engine. The water/methanol mixture and eighth-stage air pressure are distributed to the fuel nozzles through separate manifolds. The nozzle spacing is based upon 12 equally distributed positions with position 1 being at the top of the engine (Figure 54). Fuel nozzles occupy positions 2, 3, 4, 5, 6, 8, 9, 10, 11, and 12. The centers of the manifolds are connected to distribution lines at position 1 with a tee. The manifolds end at the nozzles in positions 6 and 8. Position 7 is vacant.

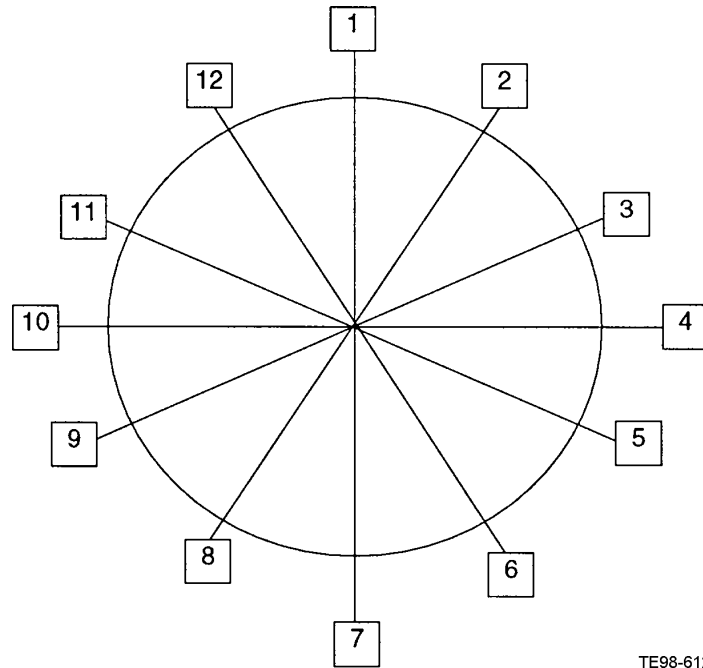


*Figure 54. Schematic of nozzle spacing.*

Nozzle pressure is regulated by the eighth-stage bleed air pressure. The water/methanol mixture is stored in a tank in the aircraft. The system is precharged to provide a rapid response capability. This is achieved by providing a continuous pressure and flow via a pump located near the tank.

### 5.5.2 Front Frame Design

As originally conceived, the water/methanol injection system would be incorporated into the engine front frame design; however, rig tests demonstrated the need to inject ahead of this major engine structure and this resulted in a significant simplification of the task.

The baseline engine front frame is similar to that used on the AE 1107. The core flow path was resized to match the aerodynamic design requirements. Engine mounts, water wash, sensor pads, anti-ice, and oil-in boss were not changed except as required to match the new flow-path diameter. The bearings were resized for the new loads, which caused a change in the bearing mount surfaces, strut width, and cast in oil passages. The number of struts were not changed from the AE 1107.

### 5.5.3 Water/Methanol Injection Preliminary Design Scheme

The water-injected engine incorporates a front frame with an extended front outer wall and a shortened inlet duct. The extended front outer wall incorporates integrally cast mount pads to attach the water/methanol injection nozzles and the manifold distribution systems. The baseline eighth-stage compressor bleed coupling is changed to a tee fitting to route bleed air to the injection nozzles. An aircraft-mounted water/methanol tank and pumping system complete the water injection system.

### 5.5.4 Recommendations for Further Effort

Further effort in the areas listed in the following subsections would improve the water/methanol injection system.

#### 5.5.4.1 Optimize Number of Spray Nozzles

The current design utilizes ten spray nozzle locations. A trade study should be conducted to optimize the number of spray nozzles required relative to the position of the nozzle in the intake. This is obviously installation dependent, but it appears intuitive that as the injection system is moved upstream, then fewer nozzles would be required. If this characteristic is validated during tests, it should be exploited to minimize overall system cost.

#### 5.5.4.2 Redesign Nozzles to Reduce Size, Cost, and Weight

The existing nozzles are approximately 6-in. long and are made from stainless steel tubing and machined fittings. Different materials and resizing combined with the above may yield further cost benefits.

#### 5.5.4.3 Conduct Additional Testing to Define Nozzle Parameters

The key to the nozzle injection system is the difference in pressure between the flow path, the water/methanol mixture, and the eighth-stage compressor bleed air. The limits of these variations that will still provide adequate spray patterns need to be explored by rig testing.

#### 5.5.4.4 Evaluate Replacement of Tank/Pump System with a Pressurized Tank

Cost, weight, and reliability would be improved if the pump and associated wiring and mounting could be replaced by a single pressurized tank. This should be reviewed prior to the definition of any test hardware.

### 5.6 Whole Engine Preliminary Design

#### 5.6.1 Engine Life Requirements

To conduct a valid preliminary design of any engine, it is important that engine life expectations are known against specific missions anticipated for the engine. At Rolls-Royce Allison these requirements are usually captured in a product requirements document (PRD). This section describes the life requirement using the 200 nautical mile mission outlined in Table XXVII.

The desired engine life is 30,000 missions with the following component lives:

- Hot flow path
  - ◆ 30,000 cycles      low cycle fatigue
  - ◆ 15,000 cycles      fracture crack growth
  - ◆ 30,000 hr          stress rupture and uncoated oxidation
  - ◆ 15,000 hr          1% creep (repairable coating)
  - ◆ 10 minutes        OEI operation (2 occurrences)
- All others
  - ◆ 30,000 cycles      low cycle fatigue
  - ◆ 15,000 cycles      fracture crack growth
  - ◆ 30,000 hr          0.2% creep
  - ◆ 10 minutes        OEI operation (2 occurrences)

Table XXVII. Parameters for 200 nautical mile mission.

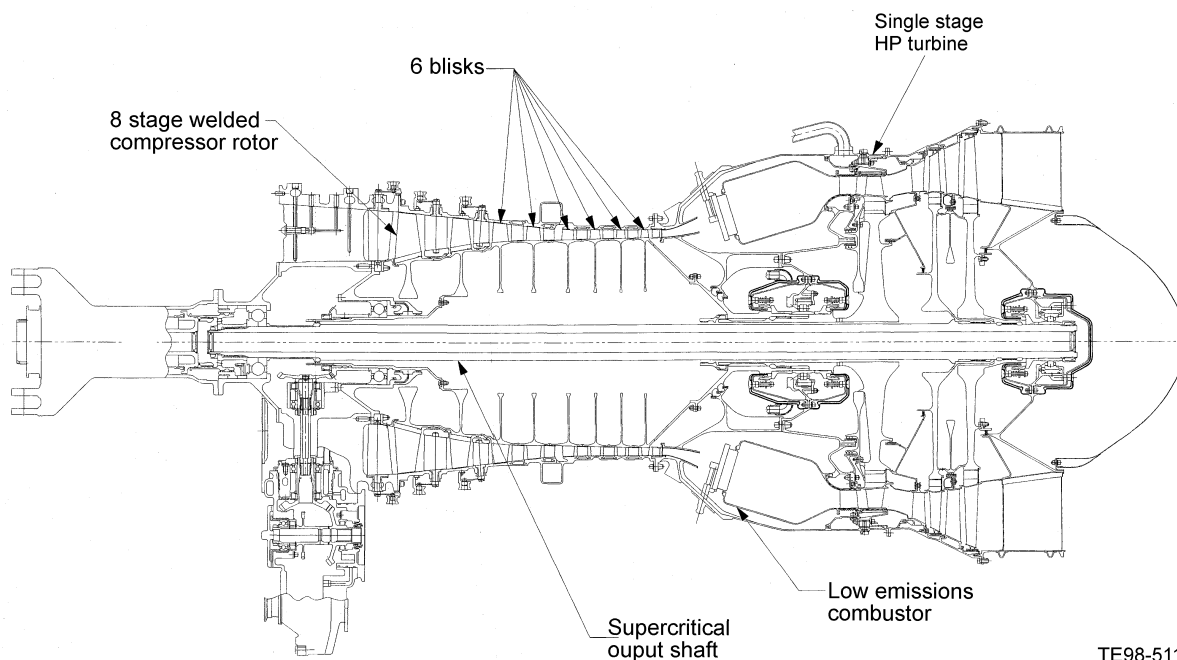
Condition	Time—min
Taxi	3.0
Takeoff	0.5
Convert	1.5
Climb	8.0
Cruise	20.0
Descent	12.0
Convert	1.5
Land	0.5
Taxi	3.0
Total	50.0

## 5.6.2 Baseline Engine Preliminary Design

### 5.6.2.1 Baseline Engine General Arrangement

The baseline engine defined for this study was designed with state-of-the-art technologies and manufacturing techniques consistent with a 2005 entry into service date. A schematic of the engine is shown in Figure 55. The cycle chosen has a takeoff turbine RIT of 2650°F.

An attempt was made to reduce cost by reducing the part count and complexity of the engine, and an eight-stage axial compressor was designed. A welded drum design was chosen for the compressor rotor to reduce both cost and weight. Moreover, the welded drum rotor design was further enhanced for weight and cost through the use of integrally bladed disks. The first two stages, however, have removable blades to permit replacement in case of FOD. In addition to the rotor improvements, cantilevered vanes were chosen to eliminate the vanes' inner rings and thereby reduce weight and cost. Titanium alloys were used extensively throughout the compressor for weight benefits.



TE98-511

Figure 55. Baseline engine generator arrangement.

The combustor was designed with the knowledge that low emissions will become increasingly important in the 2005 time frame. This led to a combustion system designed to meet emissions regulations comparable to those for turbofan engines in the year 2003 and beyond.

The turbine section was identified as an area where cost could be reduced by using a single-stage axial turbine in the gas producer section. This decision eliminated an entire stage of expensive air-cooled turbine blades and vanes. However, the single-stage turbine requires a higher rim speed to maintain the turbine efficiency, and as a result, the wheel increases in size and weight to carry the increased rim load. To minimize the weight impact, it was desirable to reduce the wheel's bore diameter. To accomplish this, the turbine's spanner nut was moved from beneath the turbine and placed at the back of the compressor. This makes assembly more difficult but reduces the weight. To further reduce the cost of the turbine wheel, a steel shaft could be welded onto the turbine wheel, thereby reducing the cost of both the Udimet 720 forging and the machining of splines and threads. These welding techniques, however, need to be refined for this type of application, so a one-piece U720 forging will be used for the turbine wheel and stub shaft.

Another way the bore diameter of the HP turbine wheel was reduced was through the use of supercritical shafting on the LP turbine rotor. In the case of a supercritical shaft, the engine's operating range is above the first bend mode harmonic of the shaft but it is acceptable because bearing dampers minimize the effects. The supercritical shafting, therefore, allows the shaft diameters to be smaller than the shafting for a subcritical design. The low diameter shafting also helps the bearings through a reduction in the race velocities, which makes oil mist lubrication a possibility for the two bearings in the turbine section. Oil mist lubrication in these two sumps reduces weight and expense by eliminating scavenge lines and scavenge pump elements, but this technology needs further development before being incorporated into a commercial application so the general arrangement shows oil jetted bearings in the two turbine sumps.

Overall, this engine is representative of an engine that could be fielded in the 2005 time frame without large investments in immature technologies.

#### *5.6.2.2 Baseline Engine Weight*

The weight of the candidate 40 lb/sec class engine was determined by the Weights group at Rolls-Royce Allison. The AE 1107 used in the V-22 tiltrotor aircraft was the starting point for weight calculations and items not newly designed were scaled appropriately from the AE 1107. This weight was scaled based on the correct flow size for the SHCT; the calculated weight is 1209 lb. A breakdown of the engine weight by module is shown in Table XXVIII.

#### *5.6.2.3 Baseline Engine Size*

The overall carcass dimensions of the engine are shown in Figure 56. The engine accessories and mounting brackets are not included and would have to be added appropriately depending upon the specific installation.

#### *5.6.2.4 Baseline Engine Mission Fuel Burn*

The engine has a fuel burn of 1865 lb when flown over the prescribed 200 nautical mile mission and 4566 lb when flown on the 600 nautical mile mission.

Table XXVIII. Weight summary.

Module description	Baseline engine—lb	Injected engine—lb
Water injection system	0	81
Basic engine assembly	72	51
Torquemeter assembly	25	18
Compressor assembly	329	242
Gearbox assembly	37	26
Turbine first vane and support assembly	26	18
HP turbine rotor and second vane	182	130
Power turbine assembly	364	260
Fuel system assembly	63	45
Electrical systems assembly	25	18
Lube system assembly	37	26
Air data system assembly	21	15
Engine monitoring system	18	13
Actuator assembly, compressor var, vane CAM	11	8
Integration and assembly	0	0
Total unit weight	1209	952

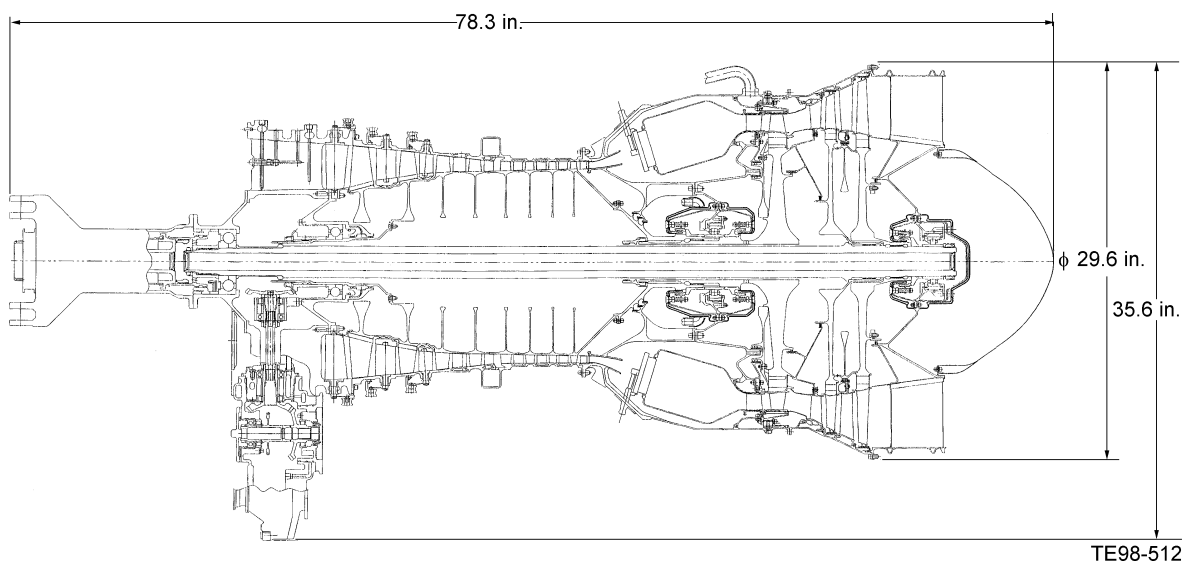


Figure 56. Baseline engine size.

#### 5.6.2.5 Baseline Engine Acquisition Cost

In determining the DOC of the airframe, it is important to have a good estimate of the engine's initial acquisition cost. The factory costs were determined by the Lockheed Martin Price-H computer program using both weight and complexity as input. This program has been validated from actual costs associated with Rolls-Royce Allison production engines. The AE 1107 production engine used in the V-22 tiltrotor aircraft was used as a baseline for this cost study. Items such as electrical harnesses, accessories, and other hardware not designed under this contract were scaled from the AE 1107. The expected acquisition cost for the baseline engine is \$1,047,068 per engine. A breakdown of the costs is shown in Table XXIX.

Table XXIX. Cost summary.

Module description	Baseline engine—\$	Injected engine—\$
Water injection system	0	58,378
Basic engine assembly	94,552	70,758
Torquemeter assembly	12,226	9,149
Compressor assembly	227,212	171,169
Gearbox assembly	33,198	24,844
Turbine first vane and support assembly	85,825	64,227
HP turbine rotor and second vane	118,326	88,550
Power turbine assembly	204,741	153,218
Fuel system assembly	102,387	76,621
Electrical systems assembly	20,460	15,311
Lube system assembly	43,998	32,926
Air data system assembly	19,688	14,733
Engine monitoring system	17,226	12,891
Actuator assembly, compressor var, vane CAM	13,054	9,769
Integration and assembly	54,175	43,932
Total unit cost	1,047,068	846,476

#### 5.6.2.6 Baseline Engine Maintenance/Reliability

The SHCT engine maintenance program is based on an on-condition maintenance philosophy and would be established in conjunction with the operator and the Airworthiness Authorities using MSG-3 guidelines. The MSG-3 process would be employed to develop an efficient and cost-effective maintenance program based on the inherent safety and reliability levels of the engine. In establishing the MSG-3 process, details of the maintenance program would be developed through coordination with specialists from the airlines, manufacturers, and regulatory authorities.

Typically, this process uses working groups consisting of members from major system manufacturers, operators, and regulatory authorities, who establish the logic analysis and choose the most appropriate tasks and task intervals based on the analysis.

Based on prior MSG-3 analysis of the AE engine family, the overall reliability goals for the baseline engine are:

- The engine-caused premature removal rates shall be less than 0.2 per 1000 engine flight hours, based on a 12-month rolling average.
- The engine line replaceable units (LRUs) or engine accessories shall have an inherent premature removal rate of less than 0.38 per 1000 engine flight hours, based on a 12-month rolling average.
- The engine-caused in-flight shutdown rate shall not exceed 0.02 per 1000 engine flight hours.
- The fleet cumulative schedule interruption due to a mechanical malfunction of the engine shall not exceed 0.06%.
- The engine's cumulative mean time for flight line maintenance associated with removal and installation of LRUs shall be less than 0.5 hr.

Additionally, life limits will be established for certain parts (assuming, 1 cycle/hour):

- Inlet housing            30,000 cycles
- Compressor
  - ◆ Case                    30,000 hr
  - ◆ Vanes                  30,000 cycles
  - ◆ Blades                30,000 cycles
  - ◆ Wheels                30,000 cycles
- Diffuser/combustor
  - ◆ Diffuser               30,000 cycles
  - ◆ Combustion liner    15,000 hr (coating repair)
- Turbine
  - ◆ Cases                 30,000 cycles
  - ◆ Vanes                 15,000 hr (coating repair)
  - ◆ Blades                15,000 hr (coating repair)
  - ◆ Wheels                30,000 cycles
- Accessory gearbox    30,000 cycles
- Torquemeter           30,000 cycles

The engine will feature fully modular construction, single-tier line replaceable unit (LRU) replacement, quick disconnect accessories, borescope provisions, and other maintainability characteristics designed to minimize cost and maximize dispatch reliability.

Those parts of the propulsion system requiring service, checking, adjustment, or replacement with the powerplant installed on the aircraft will be accessible for servicing/maintenance without teardown of the engine or removal of any major nacelle, engine component, or accessory. The engine maintenance program will be assisted by on-the-wing based diagnostics. Routine inspection of the engine for FOD, wear, thermal distress, and metal release will be accomplished by using walk-around visual inspection, cowl-up borescope inspection, and inspection of oil debris detectors.

Electrical connectors will be selected so misconnection is virtually impossible. This will be achieved through careful selection and location of the electrical connectors. To further aid in the prevention of misconnection of electrical wiring, separate color codes will be used for the full-authority digital engine control (FADEC) and for the engine monitoring harnesses.

The FADEC system will incorporate extensive built-in test (BIT) capabilities. The FADEC will detect and accommodate most single and many multiple electrical failures. Fault bits indicating the faulty LRU or associated LRUs will be continuously transmitted by the FADEC to the aircraft, and the fault data will be stored in nonvolatile memory within the FADEC. An engine life computer will also provide additional fault detection and engine health monitoring functions.

Quick disconnect “v-band” clamps will be utilized for engine-mounted accessories whenever practical. This feature facilitates line replacement of engine external components. Accessories mounted externally on the engine will be readily accessible through cowling doors for rapid testing, servicing, removal, inspection, or replacement, if required. The engine accessories will be designed for a periodic inspection or scheduled replacement maintenance program and designed with quick disconnect features, tool clearances for bolted connections, and self-locking nuts, if required. In addition the compressor VGV will not require adjustment or rigging.

The following LRU engine components will be readily accessible and are listed with their expected mean time between removal intervals:

• Oil filter	1000 hr
• Fuel filter	2000 hr
• Fuel nozzles	5000 hr
• Igniter plugs	15,000 hr
• Bleed control valve	15,000 hr
• Fuel pump and metering unit (FPMU)	30,000 hr
• FADEC	30,000 hr
• Acceleration bleed valve	30,000 hr
• Thermocouples	50,000 hr
• Exciter box	50,000 hr
• Thermocouple harness	75,000 hr
• Igniter leads	100,000 hr
• Oil pump	100,000 hr
• Oil cooler	100,000 hr
• Compressor variable geometry actuator	100,000 hr
• Oil filter unit assembly	200,000 hr
• Electrical harnesses	200,000 hr
• Sensors, transducers, and accelerometers	200,000 hr

The direct maintenance costs calculated for a mature SHCT (>1,000,000 flight hours) engine are estimated to be \$134.91 per flight hour.

### 5.6.3 Injected Engine Preliminary Design

#### 5.6.3.1 *Injected Engine General Arrangement*

The injected engine general arrangement is a scaled-down version of the baseline engine as a function of core mass flow. Consequently, for a detailed explanation of the component features, refer to subsection 3.6.1.1. The appropriate injection equipment has been added to the general arrangement as shown in Figure 57.

The water/methanol injection system is composed of an aircraft-mounted supply tank, a filter, a delivery pump, supply lines, fluid metering valves, manifolds, and atomizer nozzles. A schematic of the system is shown in Figure 58. The supply tank is not pressurized and is vented to the atmosphere. A filter downstream of the tank has a bypass valve in the event the filter becomes clogged. Downstream of the filter is a 250 psid, 2 gpm pump that maintains a constant supply pressure in the delivery lines. A flexible line (Figure 59) is used between the fixed wing and the rotating nacelle to accommodate the relative motion. Two solenoid valves attached to the engine control the flow of air and water/methanol to their respective manifolds. The two manifolds then unite at the atomizing nozzles where the air enters the fluid stream and a fine mist sprays into the engine inlet. In this design, the ten nozzles are mounted in the inlet of the engine.

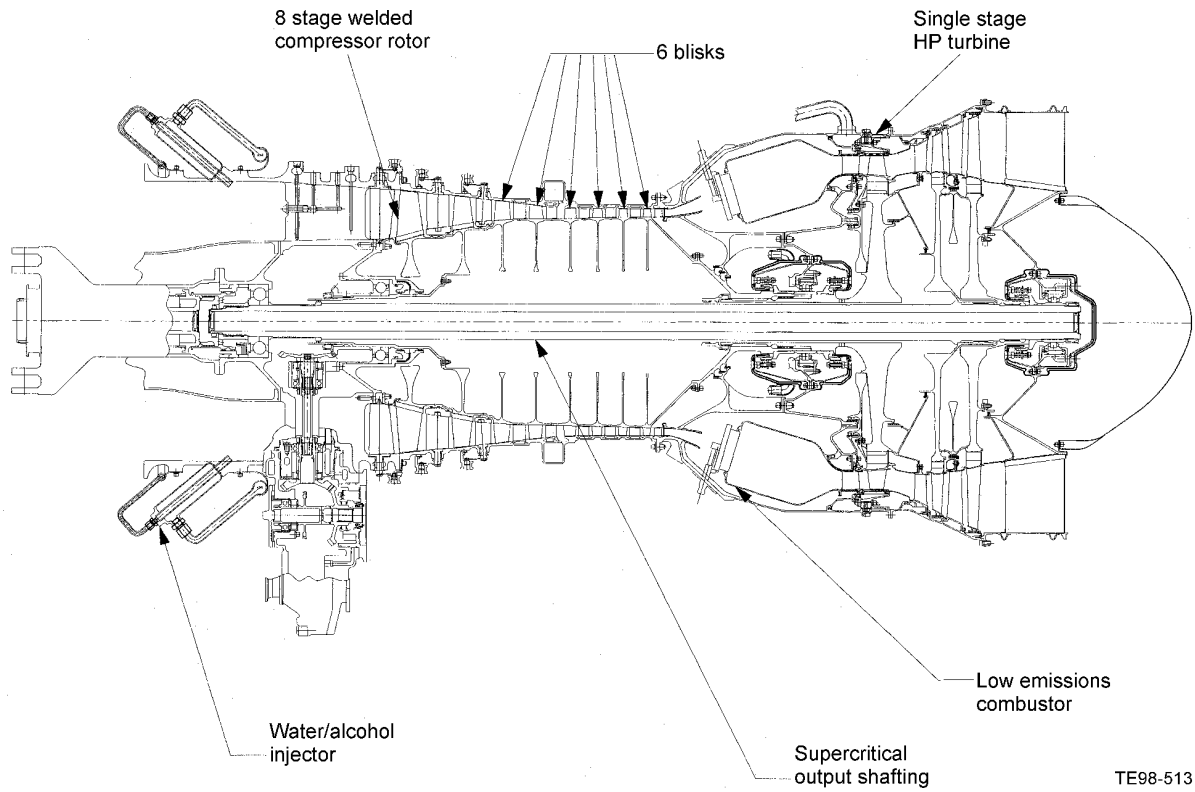


Figure 57. Injected engine general arrangement.

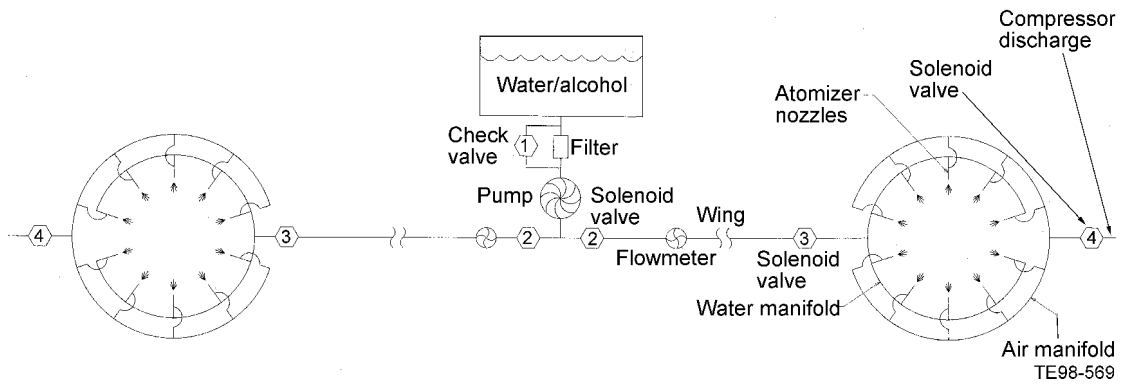


Figure 58. Injection system schematic.

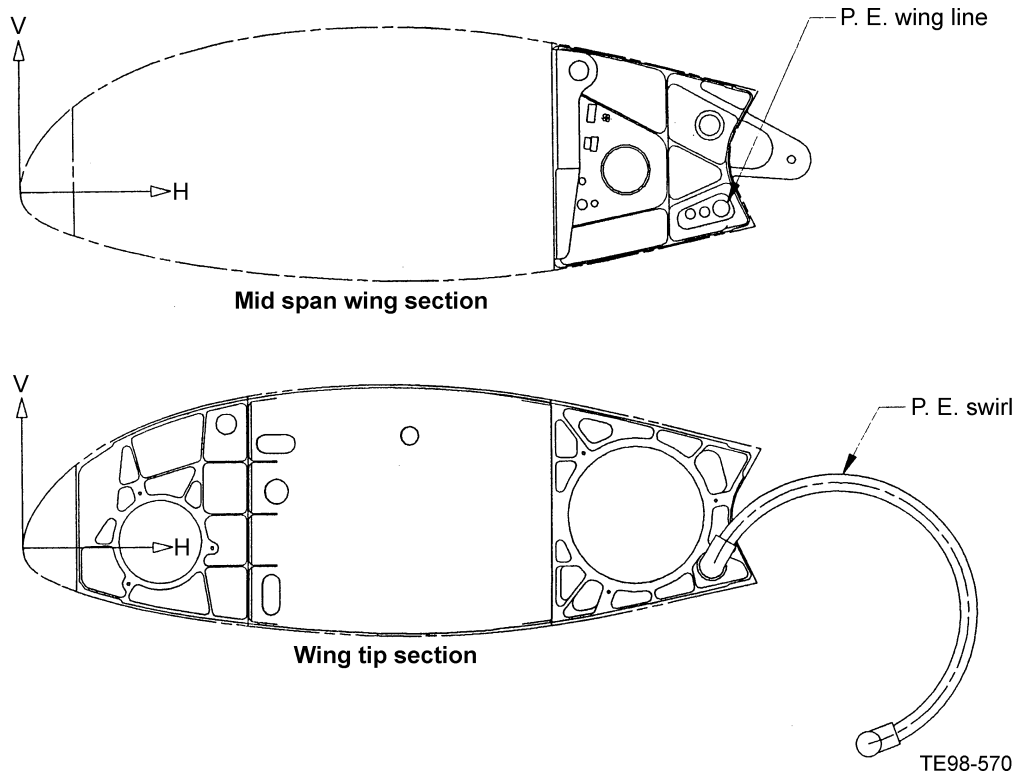


Figure 59. Line locations in wing.

### 5.6.3.2 Injected Engine Weight

The weight of the injected engine is the sum of the core engine and the water/methanol injection system weights. The dry weight is 952 lb per engine and this includes half of the aircraft mounted hardware. The weight of the fluid in the lines and the tank for 2.5 minutes of operation add another 194 lb to the system, so the total weight of the system is 1049 lb per engine as compared to the baseline (unaugmented) engine weight of 1209 lb. The propulsion system weight for a two-engine aircraft can be reduced by a total of 320 lb by using the water/methanol injection system. For a breakdown of engine weights, refer to Table XXVII.

### 5.6.3.3 Injected Engine Size

The injection system does not increase the size of the overall dimensions of the engine because the engine plumbing falls within the outermost case diameter and the torque meter housing extends beyond the nozzles. Since the inlet housing was increased in length to accommodate the injection system, the inlet duct will however be reduced in length. A better option is to incorporate the injection nozzles and manifolds onto the inlet duct. This permits the system to remain mostly intact with the aircraft when the engine is removed. The only piece having to remain with the engine is the compressor discharge bleed tube. For simplicity within this study the injection system was added to the inlet housing. The overall dimensions of the injected engine are shown in Figure 60. The engine accessories and mounting brackets should be added to the size shown.

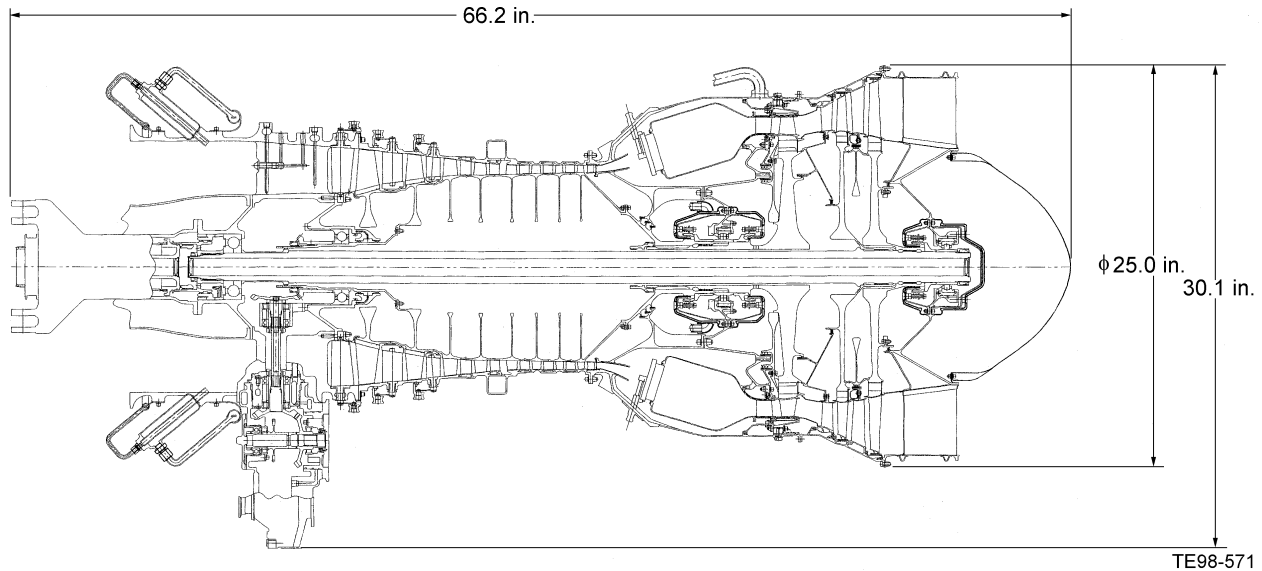


Figure 60. Injected engine size.

#### 5.6.3.4 Injected Engine Mission Fuel Burn

The injected engine's fuel burn is 1588 lb when flown over the prescribed 200 nautical mile mission and 4117 lb over the 600 nautical mile mission.

#### 5.6.3.5 Injected Engine Acquisition Cost

The engine componentry is the same as for the baseline except for the size difference and the injection system. According to the Price-H costing program and scaling for weight, the acquisition cost is \$846,476. A breakdown of the costs is shown in Table XXVIII.

#### 5.6.3.6 Injected Engine Maintenance/Reliability

The maintenance program for the water/methanol injected engine will be the same as for the baseline engine. It will be an on-condition maintenance philosophy. For an explanation of the predicted maintenance and the desired reliability of the core engine, refer to subsection 5.6.2.6.

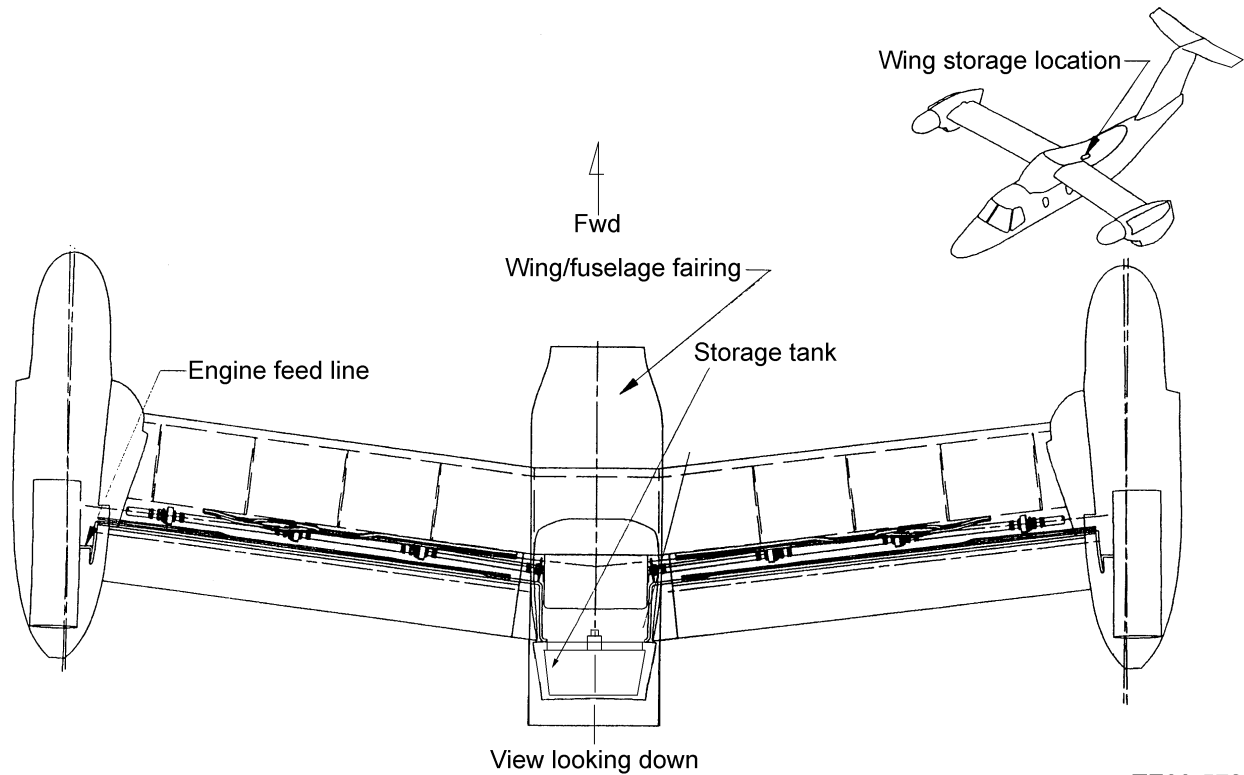
In addition to the core engine, the injection system will also have on-condition maintenance. The following LRU injection system components are listed with their expected mean time between removal intervals:

- Pump 100,000 hr
- Valves 100,000 hr
- Nozzles 100,000 hr

The direct maintenance cost for the injected engine is anticipated to be \$136.08 per flight hour as compared to \$134.91 per flight hour for the baseline engine.

#### 5.6.3.7 Tank Volumes, Line Runs, and Pump/Valve Locations

A schematic of the water/methanol injection system for the scaled-down engine is shown in Figure 58. The system delivers 1.35 lb/sec of a 70% water and 30% methanol mixture to the engine during OEI operation for 2.5 minutes. This requires a 26 gal supply tank located in the aft wing fairing at the top of the fuselage (Figure 61). A filter with a bypass valve is located in the line between the supply tank and a



TE98-572

*Figure 61. Water/methanol tank location.*

pump located in the aft wing fairing. The pump has a capacity of 2 lb/sec at 250 psid and is energized when the aircraft engines are started. The filter has a bypass valve for safety in the event the filter becomes clogged and an OEI situation occurs.

After the pump, the system branches to each engine. Each branch begins and ends with a solenoid valve. These valves serve to control the flow of fluid during OEI operation. Normally, the valve closest to the pump is open and the valve at the end is closed. This allows the lines to be pressurized from the pump out to the nozzle manifolds at all times, and limits the time required to fill empty delivery lines. When OEI power is demanded both valves in the running engine branch are open. This supplies the required water/methanol mixture to the nozzles. A third valve also opens and delivers compressor discharge air to the nozzle manifold. These two fluid streams meet at 10 atomizing nozzles equally spaced around the inlet of the engine. For the atomizing nozzles to operate properly, the liquid and air pressures must have a small difference in pressure. As a result, the valve at the end of the water/methanol line also serves to meter the flow to match the pressure of the compressor air entering the nozzle.

In the case of the failed engine branch both valves are closed, preventing the loss of water through a broken water line in the wing. This could occur if the wing was damaged and both the fuel line and also the water/methanol line were severed.

To check the injection system functionality, a flowmeter is placed in each branch of the system. With the engines running, the valve at the end of the branches can be opened and the flow of liquid can be measured to determine if all 10 valves are open and operating properly.

## 5.6.4 Economic Analysis

### 5.6.4.1 Description of Method

The figure of merit for this study is the DOC comparison of the injected engine with the baseline tiltrotor engine. DOC is calculated by the VASCOMP II V/STOL design and analysis program. With the exception of engine maintenance cost, the components constituting DOC are obtained directly from the VASCOMP II output. The pieces making up DOC are:

- Crew
- Fuel and oil
- Insurance
- Airframe maintenance
- Engine maintenance
- Dynamic system maintenance
- Maintenance burden
- Depreciation
- Interest

The distance for the DOC calculations is 200 nautical miles. This represents the distance of a typical commercial operation of the aircraft as envisioned by NASA for this study, and can be contrasted to the design range of 600 nautical miles. The design range helps to size the aircraft as it will set the requirement for the amount of fuel to be carried, while the economic range is used as typical operational distance for the aircraft that will meet the design range. To compare DOC values, an economic analysis of the two aircraft configurations of the baseline and the aircraft with the injected engine was performed for the specified economic range.

The engine-related cost input to VASCOMP II, in addition to the performance inputs, is engine acquisition cost. Using the CKENGCOST input as a modifier to the internal engine cost calculation, a variation was used to get the unscaled engine cost to match the value determined by in-house Rolls-Royce Allison cost prediction methods. This method was used for both the baseline and injected engine configurations, and in this way, the unscaled engine costs were kept consistent while allowing the correct scaled engine cost to be determined as an output of the VASCOMP II program.

Another important engine-related cost input to DOC is engine maintenance cost. In this parameter there were irreconcilable differences in the way Rolls-Royce Allison calculates and applies maintenance cost and the way the same task is performed by the VASCOMP II program. The engine maintenance cost calculation was performed independent of the VASCOMP II calculations. Rolls-Royce Allison maintenance costs are calculated on a per-flight-hour basis, as if being prepared to quote a commercial Power-By-The-Hour™ value. Scaled engine size was determined by the sizing solution in the VASCOMP II program results and this value was used to scale the maintenance cost. The scaled maintenance costs were then multiplied by the flight hour value, also obtained from the VASCOMP II results, to calculate the engine maintenance costs for the flight. All other components of DOC are obtained directly from the VASCOMP II output.

DOC measures the cost of operation for the economic mission. It is influenced by the design mission, the assumptions for the aircraft design, and engine performance and weight. After the aircraft is sized, the sized aircraft and engine results are used to determine the inputs to the DOC calculation. Table XXX gives the aircraft design parameters determining the values for the components of DOC.

*Table XXX. Main drivers on the DOC components.*

<b>DOC component</b>	<b>Predominant drivers</b>
Crew	Aircraft speed, since crew costs are a fixed value per flight hour
Fuel and oil	Fuel burn, which is determined by aircraft size, engine SFC
Insurance	Aircraft price, which is determined by aircraft size
Airframe maintenance	Aircraft size
Engine maintenance	Engine size
Dynamic system maintenance	Maximum torque, which is determined by aircraft size
Maintenance burden	Other maintenance costs
Depreciation	Aircraft price, which is determined by aircraft and engine size
Interest	Aircraft price, which is determined by aircraft and engine size

With the exception of crew costs, all of the constituents of DOC are influenced to varying degrees by the size and efficiency of the engine. Crew costs are a fixed value multiplied by the flight time. The cost actually increases slightly for the injected engine since the injected engine results in a slightly lower cruise speed. This is due to the fact that the injected engine was much smaller than the baseline engine and resulted in a slightly smaller aircraft. The injected engine configuration's climb was slower, and therefore, the overall mission took longer. All other DOC components were reduced for the injected engine configuration compared to the baseline. The predominant reason for these changes is that as the engine gets smaller, due to the water/ methanol power boost, the aircraft size as expressed by gross weight is also reduced. Changes in aircraft size have a bigger effect on DOC than any other parameter. Engine size also has a direct effect on some of the DOC components in addition to its effect on aircraft size. Table XXXI shows the DOC change direction, baseline to injected, and the reason for the change.

#### *5.6.4.2 Economic Analysis Results*

Applying the foregoing method to the NASA SHCT yields the results shown in Table XXXII. These results show that the injected engine results in a 6.48% reduction in DOC for the 200 nautical mile mission and a 7.32% DOC reduction for the 600 nautical mile mission. Table XXXIII compares the two engines for the 200 nm mission and shows the main DOC cost drivers are maintenance costs and fuel burn.

*Table XXXI. Injected configuration DOC cost trends, injected compared to baseline.*

<b>DOC component</b>	<b>Trend</b>	<b>Reason</b>
Crew	Higher	Flight time increases slightly
Fuel and oil	Lower	Aircraft is smaller and engine SFC is lower, so less fuel burn
Insurance	Lower	Aircraft and the engines are smaller, so the price is lower
Airframe maintenance	Lower	Aircraft is smaller
Engine maintenance	Lower	Engines are smaller
Dynamic system maintenance	Lower	Aircraft is smaller, so less maximum torque is required
Maintenance burden	Lower	All the maintenance components are reduced.
Depreciation	Lower	Aircraft and the engines are smaller, so the price is lower
Interest	Lower	Aircraft and the engines are smaller, so the price is lower

Table XXXII. Economic analysis summary.

	Baseline engine aircraft		Injected engine aircraft	
	200	600	200	600
Distance—nm	200	600	200	600
Time—min	0.804	1.953	0.826	1.975
Crew	\$160.74	\$390.59	\$165.01	\$394.45
Fuel and oil—\$	187.32	458.63	159.55	413.53
Insurance—\$	279.40	678.95	269.53	644.29
Airframe maintenance—\$	210.07	304.14	204.69	295.54
Engine maintenance—\$	195.73	475.46	144.90	346.45
Dynamic system maintenance—\$	67.46	172.63	66.33	166.62
Maintenance burden—\$	370.94	647.93	348.50	606.62
Depreciation—\$	359.73	874.15	346.29	827.79
Interest—\$	290.05	704.83	279.22	667.45
Total DOC	\$2,121.44	\$4,707.31	\$1,984.02	\$4,362.74
DOC per nm, \$/nm	\$10.607	\$7.846	\$9.920	\$7.271
DOC per ASM, \$/seat-nm	\$0.26518	\$0.19614	\$0.24800	\$0.18178
Delta operating cost			<b>-6.48%</b>	<b>-7.32%</b>
Number of seats	40	40	40	40
Engine scale factor	0.902269	0.902269	0.644545	0.644545
Engine maintenance cost, \$/fhr	\$134.91	\$134.91	\$136.08	\$136.08

Table XXXIII. Cost benefits.

	Baseline engine aircraft	Injected engine aircraft	Change in cost—%
Distance—nm	200	200	
Time—minutes	0.804	0.826	
Crew	\$160.74	\$165.01	2.66
Fuel and oil—\$	187.32	159.55	-14.82
Insurance—\$	279.40	269.53	-3.53
Airframe maintenance—\$	210.07	204.69	-2.56
Engine maintenance—\$	195.73	144.90	-25.97
Dynamic system maintenance—\$	67.46	66.33	-1.68
Maintenance burden—\$	370.94	348.50	-6.05
Depreciation—\$	359.73	346.29	-3.74
Interest—\$	290.05	279.22	-3.73
Total DOC	\$2,121.44	\$1,984.02	-6.48
DOC per nm, \$/nm	\$10.607	\$9.920	-6.48
DOC per ASM, \$/seat-nm	\$0.26518	\$0.24800	-6.48

### 5.6.5 Future Work

Testing of the water/methanol injection system should begin in the next phase of currently unfunded work. Rolls-Royce Allison proposes to add this system to the AE 1107 turboshaft engine.

Since these tests could benefit both military and civil tiltrotors, it would be sensible to address both applications at once. The current AE 1107 is optimized to give best fuel consumption during specific portions of its mission at relatively low altitude. The current V-22 customer would not want the addition of a water/methanol system to affect this engine match point. His interest is likely to be to validate the developed prediction techniques by demonstrating the maximum power increase possible by adding water/methanol injection to an unmodified AE 1107C. However, for the SHCT community the interest for these proposed tests will be to validate the developed prediction techniques by demonstrating the maximum power increase possible with full rematch using a modified AE 1107 engine. These engine tests should therefore be preceded by a performance study addressing both of these interests.

The engine tests should incorporate every subsystem from the tank to the atomizing nozzles. The purpose of this testing is to validate the system's functionality. The nozzle design will have to be optimized along with the manifolding. This will be followed by full-scale rig testing of the nozzles with the engine simulated downstream to ensure proper mixing. The injectors would then be added to the AE 1107 inlet for engine testing. The tank will be designed and tested to verify the usable volume of liquid and the required vent size to avoid depressing the tank pressure. The pump must be tested to ensure it will function on demand and will maintain the pressure in the supply lines. The length of supply lines should be appropriate to verify the pressure loss in the lines leading to the distribution manifold. The valves are critical to characterize their opening and closing rates as they are commanded by the FADEC. The software for the FADEC will have to be modified to control the valving and the system functionality checks. It will be necessary to confirm the system functions properly prior to each flight. This will range from a pressure check in the system for a hot start to a water/methanol flow check. Furthermore, it is important to determine the time delays that may occur in the system from valve repositioning and manifold filling.

Some engine hardware will be modified for the system. The diffuser will have to be modified to accommodate the compressor discharge air bleed tube. The manifolds and atomizing nozzles can be added to the inlet bell. Other engine hardware may have to be modified or replaced to accommodate rematching of the engine if this is desired. Some analysis work will have to be done to ensure the rotating hardware is not overstressed because of the horsepower increase from the water injection. It may be necessary to operate the AE 1107 at a horsepower level less than its normal takeoff power to prevent over stressing or over heating engine hardware.

## **6.0 Task 4—Meetings and Reporting**

This final task included all of the NASA required reporting activities. It also included the meetings required to track the reprogrammed effort using the newly acquired Rolls-Royce earned value analysis program management procedure. The earned value approach to program management has been demonstrated to be effective at tracking customer value against expended cost.

### ***6.1 Weekly Progress Meetings***

The Rolls-Royce Allison SHCT program manager held weekly progress meetings during which the control account managers presented progress in their areas of responsibility. The objective of these meetings was to identify and implement any corrective action necessary to ensure customer satisfaction. The program manager chaired these meetings and ensured that minutes and action items were recorded. The minutes and action items were usually published on the same day as the meeting and were distributed to all team members.

### ***6.2 Monthly Written Reports***

Rolls-Royce Allison submitted the following monthly reports, technical progress reports, contractor financial management reports (NASA Form 533M), and contractor financial management performance analysis reports (NASA Form 533P).

### ***6.3 Prepare Final Report Outline***

At an early stage in the program, the program manager defined a final report outline. All reporting subtasks used this format to facilitate the final report preparation process.

### ***6.4 Document Completed Work***

All work performed under the NASA SHCT contract prior to this reprogrammed effort was documented ready for inclusion in the final report.

### ***6.5 Prepare Final Report***

The final report prepared for this program is intended to deliver to NASA all elements required under this reprogrammed effort. The final report also describes the activities performed prior to the reprogramming effort.



## 7.0 Conclusions

This program has defined affordable baseline and injected engines for future SHCT aircraft. The main conclusions are:

- An affordable SHCT baseline engine suitable for 2005 EIS has been defined.
- A simple, low cost SHCT OEI concept has been identified.
- Improved analytical techniques have been applied to predict OEI power boost.
- An improved water/methanol injector has been demonstrated on a rig.
- Improved water/methanol injection techniques yield a 35% power boost.
- A resized SHCT using the injected engine yields a 6.5 to 7.3% DOC improvement.
- The next step should be to plan for an engine demonstration that would include:
  - ◆ Optimization of chosen injection system concept.
  - ◆ Rig testing of injection system hardware.
  - ◆ Manufacture of engine components for rematching.
  - ◆ Engine build and testing.



## 8.0 Recommendations

The next phase of the SHCT program should be technology development and validation addressing the following key elements:

- Optimization of chosen injection system concept
- Rig testing of injection system hardware
- Manufacture and modification of special engine hardware
- Engine build and testing

This section describes a proposed approach to this engine demonstration and also describes other component-based programs aimed at developing an affordable SHCT powerplant for a 2005 entry into service (EIS).

### 8.1 Engine Demonstration Program

There are two potential uses for water/methanol injection on large tiltrotor aircraft. The most immediate use would be to provide a power boost during takeoff to the U.S. Navy AE 1107C powered V-22 fleet. The second use would be to provide a contingency power capability for a new SHCT aircraft. It is recommended an engine test program be conducted addressing both of these potential requirements.

If such a program is conducted, it needs to be recognized that the U.S. Navy's propulsion system objectives are somewhat different from NASA's. However, there is sufficient commonality to warrant consideration of a joint program. The U.S. Navy could be interested in the water/methanol injection system as a retrofit to the current V-22 fleet powered by the Rolls-Royce Allison AE 1107C. Water/methanol would only be taken onboard when a heavy vertical takeoff (VTO) was required. All of the fluid would be used during the VTO to minimize the weight penalty during cruise. The U.S. Navy, Bell-Boeing, and Rolls-Royce Allison have expended considerable effort to optimize the performance of the aircraft for its current mission. As such, the U.S. Navy is unlikely to be interested in rematching the engine.

NASA and the SHCT community are interested in demonstrating how much of the 35% power boost can be achieved using an existing AE 1107C as a baseline engine. This would require the application of the new prediction techniques to the AE 1107C and the validation of the results with an engine demonstration of the rematched engine.

The common element in these two engine tests is the development and optimization of the new water/methanol injection system. This will require further rig testing and several full-scale inlet suction tests prior to running in front of the AE1107C engine. The engine tests should incorporate every subsystem from the tank to the atomizing nozzles at the engine inlet.

A more complete description of the proposed engine testing is included in subsection 5.6.5.

### 8.2 Component Programs

This section describes selected component programs contributing significantly to the development of an affordable SHCT powerplant designed for 2005 EIS.

#### 8.2.1 Low Part Count Compressor Program

Beyond the validation of the OEI power boost potential of the new water/methanol injection system, the most significant and challenging aspect of the engine is the compressor development. Rolls-Royce Allison, therefore, recommends the SHCT community embarks upon the development and testing of a low parts count, low factory cost, high-stage loading HP compressor.

### 8.2.2 Affordable Low Emissions Combustor Program

To address the emissions requirements for the SHCT powerplant, Rolls-Royce Allison recommends the LDI based circumferentially staged low emissions combustor technology be demonstrated in full annular combustion rig testing. Additional work also needs to be directed toward the implementation and demonstration of low cost fuel staging control strategies. Finally, since water/methanol injection increases the tendency toward autoignition in the LDI module, these margins should be demonstrated in rig tests.

### 8.2.3 Reduced Part Count HP and LP Turbine Program

Another significant cost driver for the SHCT powerplant will be the development of low parts count, low factory cost, HP and LP turbines. Rolls-Royce Allison therefore recommends the development and testing a single-stage high work turbine, coupled with a counter-rotating LP turbine.

### 8.2.4 Mechanical Design Programs

Opportunities exist to simplify the engine lubrication system by adopting a flow-through design for selected bearing locations. This design eliminates scavenge lines and their associated pump elements. New face seal technologies that require no cooling lubrication are emerging. In addition, higher fidelity debris monitoring systems could predict problems before they occur. These are exciting new technologies in their early stages of development. Rolls-Royce Allison recommends conducting rig testing to validate the use of these technologies in the next-generation SHCT propulsion system.

## 9.0 References

1. Pike, L. T., "Effects of Water-Alcohol Injection of Turboprop Engine," Internal Rolls-Royce Allison Report.



**Appendix A**  
**NASA SHCT Reprogrammed Statement of Work**



# **NASA Short Haul Civil Tiltrotor (SHCT) Program**

**NAS3-97029**

## **Reprogrammed Statement of Work**

Issue 3

**Rolls-Royce Allison**

P.O. Box 420

Indianapolis, IN 46206-0420

Prepared by David J.H. Eames

Tel: (317) 230-2525

Fax: (317) 230-3691

Email: [David.Eames@Allison.com](mailto:David.Eames@Allison.com)



## 1. TASK 1 - Define Propulsion System Requirements

### 1.1. Define revised Statement of Work (SOW) and schedule

The SOW and schedule will be redefined for all reprogrammed tasks consistent with the remaining funding from NASA.

### 1.2. Agree reprogrammed effort with NASA LeRC

The revised SOW and schedule will be agreed and approved by NASA.

### 1.3. Define Resource Managers and Control Account Managers

Resource managers will be assigned by the program manager and control account managers will be appointed by the respective resource manager. For this program, the resource managers will be the department heads responsible for conducting the task.

### 1.4. Secure Rolls-Royce Allison Engineering resource commitments.

Resource managers will commit the required Engineering resources to the NASA SHCT reprogrammed effort prior to the kick-off meeting.

### 1.5. Publish work packages

The program manager will publish work packages in the form of MCS Cost Account Authorization sheets which will reference this revised SOW. These work packages will be approved by the resource managers prior to the kick-off meeting.

### 1.6. Hold kick-off meeting

The program manager will call a kick-off meeting to initiate the reprogrammed effort under the subject NASA contract. The objective of the kick-off meeting will be to brief the resource managers, control account managers and team members on the following: The team charter; project scope; deliverables and earned value program management practices to be applied.

### 1.7. Publish engine cycles

The engine technology will represent year 2005 Entry Into Service (EIS). Rolls-Royce Allison will use the definition of the tiltrotor aircraft OEI operation approved by the Short Haul Civil Tiltrotor (SHCT) Government/Industry Propulsion Working Group as presented in Section J, paragraph 4.1.1 of the RFP. The contingency power system will be designed to satisfy these requirements.

Rolls-Royce Allison will use the baseline aircraft and mission approved by the SHCT Government/Industry Propulsion Working Group as presented in Appendix B of the RFP.

For the purposes of this study, two cycles are identified: (1) Rolls-Royce Allison will define a baseline engine scaled to allow OEI operation without augmentation and will be referred to as the **Baseline Engine**. (2) the Rolls-Royce Allison Baseline Engine

will be airflow scaled and modified to achieve OEI operation by adding a water/methanol injection system and will be referred to as the *Injected Engine*.

1.7.1. Conduct Mission Analysis

Rolls-Royce Allison will conduct mission analyses to establish the SHCT engine OEI sizing points.

1.7.2. Publish Baseline Engine cycle

The Baseline Engine cycle, that meets the OEI power requirements, will be defined.

1.7.3. Publish Injected Engine cycle

The Baseline Engine cycle will be modified to include water/methanol injection in order to achieve the published OEI requirements. These modifications will include an accounting of the water/methanol in the engine cycle and any component rematching required in order to maximize the effectiveness of the water/methanol injection.

1.8. Publish aerodynamic flowpath

The Rolls-Royce Allison Baseline Engine aerodynamic flowpath will be published. This will form the basis of all component preliminary design studies conducted under the subject NASA contract.

1.9. Document Task 1 results for final report

Document the results of all sub-task activities in a form that can be inserted directly into the final report.

**2. TASK 2 - Identify Propulsion System Concepts**

2.1. Document down-selected and alternate concepts

Summarize the concepts identified in Phase 1 of the NASA SHCT contract, describe any additional concepts identified in the current effort. A rationale for rejecting the boost compressor concept and down-selecting the water/methanol injection system will be provided. This text should be in a form that can be inserted directly into the final report.

2.2. Define water/methanol system requirements

Using the engine thermodynamic cycle and the particle trajectory analysis results, define the design requirements for the water/methanol injection system.

2.2.1. Water/methanol injection system analysis

Expediently conclude the analysis.

#### 2.2.2. Water/methanol injection system design requirements

Define the design requirements in terms of the number and size of spray nozzles required, flow rates and pressures, pump location and sizing, and tank location and volume.

#### 2.2.3. Document analysis and requirements

Document both the analysis and the design requirements in a form that can be inserted directly into the final report.

#### 2.3. Define turbine bypass system requirements

Define the thermodynamic requirements of a turbine bypass system in order to maximize the potential OEI power available from water/methanol injection. Document these requirements in a form that can be inserted directly into the final report.

#### 2.4. Document Task 2 results for final report

Document the results of all sub-task activities in a form that can be inserted directly into the final report.

### **3. TASK 3 - Preliminary Design**

#### 3.1. Compressor PD

The starting point for the compressor preliminary design will be a defined engine cycle and aerodynamic flowpath. The program deliverable will be a 2D CADDSS5 layout drawing of the compressor module. The layout will be supported by analysis appropriate for the allocated budget. The preliminary design results will be documented in a form that can be inserted directly into the final report.

##### 3.1.1. Aerodynamic Design

The baseline flowpath will be finalized and preliminary blading will be designed. The number of stages requiring variable guide vanes will be determined. Performance maps and interstage data will be generated as appropriate.

##### 3.1.2. Heat Transfer

Preliminary heat transfer analysis will be performed to allow material selections to be made for both rotating and static components. A flow systems model will be developed in conjunction with the turbine preliminary design group.

##### 3.1.3. Stress and Weight Analysis

Appropriate materials will be selected to minimize weight, whilst meeting structural and life requirements. The use of cantilevered stators and/or rotor

blisks will be examined for weight reduction purposes in the latter compressor stages.

#### 3.1.4. Dynamic analysis

A dynamics analysis will be performed to ensure damaging resonances are not encountered in the engine operating range for the proposed compressor.

#### 3.1.5. Mechanical Design

Trade studies will be performed, in conjunction with the stress analysis above, to examine the use of cantilevered stators and/or rotor blisks for the latter compressor stages. In addition, a welded drum design of compressor rotor will be compared with a current technology stacked disk design to optimize weight and cost.

#### 3.1.6. Drafting

A layout will be prepared to define the compressor configuration and pass on to whole engine design group.

#### 3.1.7. Document PD for final report

Document the results of all sub-task activities in a form that can be inserted directly into the final report.

### 3.2. Combustor PD

The starting point for the combustor preliminary design will be a defined engine cycle and aerodynamic flowpath. The program deliverable will be a 2D CADDSS5 layout drawing of the combustor module. The layout will be supported by analysis appropriate for the allocated budget. The preliminary design results will be documented in a form that can be inserted directly into the final report.

#### 3.2.1. PD airflow analysis

The air flow distribution to various combustor zones will be defined using PD design tools including air management programs. The defined air distribution will satisfy the required fuel / air stoichiometry in the primary combustion zone for high efficiency and low emissions, combustor liner wall cooling, and combustor exit pattern factor and radial profile.

### 3.2.2. PD heat transfer analysis

Based on the air flow distribution defined in Task 3.2.1, 1D heat transfer calculations will be performed to determine optimum combustor liner wall cooling scheme needs to be adopted in the design. The preliminary design will address cooling air distribution to different combustor and transition regions, liner wall structure, and main features of cooling air admission through the liner walls.

### 3.2.3. PD emissions analysis

PD emissions design system will be applied to obtain estimates of pollutants of interest including CO, unburned hydrocarbons, NO<sub>x</sub>, and smoke over the entire engine cycle. The calculations will utilize the combustor airflow distribution defined under Task 3.2.1. The results of the analysis will be used to adjust the air distribution for optimum combustor performance and emissions characteristics.

### 3.2.4. Define PD layout

A PD layout of the combustor will be prepared based on the preliminary design effort performed under Tasks 3.2.1 through 3.2.3. Layout drawings of the combustion system will be prepared to illustrate the details of the combustor front end, fuel injector, liner walls, transition section, and mounting components.

### 3.2.5. Document PD for final report

Document the results of all sub-task activities in a form that can be inserted directly into the final report.

## 3.3. Turbine PD

The starting point for the turbine preliminary design will be a defined engine cycle and aerodynamic flowpath. The program deliverable will be a 2D CADD5 layout drawing of the turbine gas generator and power turbine modules. The layout will be supported by analysis appropriate for the allocated budget. The preliminary design results will be documented in a form that can be inserted directly into the final report.

### 3.3.1. Aerodynamic Design

A trade study will be conducted to determine whether the power turbine will require two or three stages. The baseline flowpath will be finalized, and vane and blade counts will be determined. Performance maps will be generated for the baseline configuration and with water/methanol injection. Interstage data will be generated for the baseline configuration and with water/methanol injection. Preliminary blading will be designed, and vane and blade weights will be determined.

### 3.3.2. Heat Transfer

Turbine cooling schemes will be defined. Airfoil cooling coefficients and allowable metal temperatures will be determined so that preliminary airfoils can be designed. Vane and blade cross-sections will be defined for the cooled airfoils. A flow systems model will be developed to determine preswirl requirements, leakage flow estimates, and thrust balancing. Cooling flow requirements will be determined for vanes, blades, and endwalls.

### 3.3.3. Stress Analysis

Appropriate materials will be selected for the vanes, blades, turbine wheels, and static structure to meet structural and life requirements. Turbine blade weights will be incorporated to determine the size of the wheels and attachments. The weights of the turbine components and the design life of each component will be defined.

### 3.3.4. Component Cost Estimates

The cost of the turbine vanes and blades, turbine wheels and rotating structure, shafting, and turbine static structure will be estimated.

### 3.3.5. Mechanical Design

Trade studies will be conducted to determine the configuration most appropriate for this application in terms of performance, weight, and life cycle costs. The preliminary design of each component will be incorporated into the component drawings and engine general layout drawings.

### 3.3.6. Cost Accounting Activity

Program manpower costs throughout the turbine preliminary design activity will be recorded and reported.

### 3.3.7. Document PD for final report

Document the results of all sub-task activities in a form that can be inserted directly into the final report.

## 3.4. Mechanical Systems PD

The starting point for this mechanical systems preliminary design will be a defined engine cycle and aerodynamic flowpath. The program deliverables will be 2D CADD5 layout drawings of: the main engine shafts and bearings; and engine accessory gearbox (scaled AE 1107C). The layouts will be supported by analysis appropriate for the allocated budget. The preliminary design results will be documented in a form that can be inserted directly into the final report.

#### 3.4.1. Define engine shaft & bearing PD

Preliminary definition of shafting, bearings, dampers, seals, sumps and sump lubrication and venting will be accomplished with appropriate static, dynamic and sump analysis to define sizing and life/reliability. The definitions will be applied to the layout which is a deliverable and the specifications of these components will be documented.

#### 3.4.2. Define scaled AE 1107C gearbox PD layout

Preliminary design will be accomplished by scaling of gearbox and its components. Appropriate static, dynamic and lubrication analysis will be used to ensure that mechanical performance is achieved. The definitions will be applied to the layout which is a deliverable and the specification of the individual components will be documented.

#### 3.4.3. Document results for final report

Document the results of all sub-task activities in a form that can be inserted directly into the final report.

### 3.5. Water Injection System PD

The water injection system will be integrated into the engine inlet. The starting point for the engine inlet and water injection system preliminary design will be a defined engine cycle and aerodynamic flowpath. The program deliverable will be a CADDSS5 layout drawing of the engine inlet and water injection system. The layout will be supported by analysis appropriate for the allocated budget. The preliminary design results will be documented in a form that can be inserted directly into the final report.

#### 3.5.1. Define water injection locations

The water/methanol injection system aero/thermal design requirements will be defined in Task 2.2.2. These requirements will be integrated into the design of the engine inlet.

#### 3.5.2. Define engine inlet and front frame flowpath

The engine inlet and front frame flowpath will be defined in consultation with the Compressor CofE. This will include both the passage shape and the number of struts/spokes required for bearing support and provision of oil, air system, and water/methanol injection services.

#### 3.5.3. Define front frame interfaces

All front frame interfaces will be defined to a preliminary design level. These interfaces will include engine mounts, air intake, compressor face, air system, oil system and water injection system. Since no definitive airframe design exists, the engine inlet will be scaled from the AE 1107C/V-22 application.

#### 3.5.4. Define PD scheme

A scheme of the engine inlet and front frame, with and without water/methanol injection will be defined.

#### 3.5.5. Define modifications to baseline engine

The differences between the baseline engine and the water/methanol injection engine will be defined. These differences will include a description of all hardware required together with cost and weight estimates.

#### 3.5.6. Document results for final report

Document the results of all sub-task activities in a form that can be inserted directly into the final report.

### 3.6. Whole Engine PD

The starting point for the whole engine preliminary design will be a defined engine cycle and aerodynamic flowpath. The program deliverable will be 2D CADD5 layout drawings of the two engines: the Baseline; and Injected Engine. As the component designs progress, the whole engine CADD5 models will be updated to reflect the most current configuration. The whole engine preliminary design group will be responsible for overall engine configuration control and will manage the module interfaces. Once all component preliminary designs are complete, cost and weight estimates will be obtained, for both engines, in order to conduct the required economic analysis. The preliminary design results will be documented in a form that can be inserted directly into the final report.

#### 3.6.1. Define a PD scheme for the Baseline Engine

This engine will allow OEI operation without augmentation. The OEI requirements will be those given in Section J, paragraph 4.1.1 of the RFP. The engine data will be fully scaleable. This engine data will be presented to the Government in sufficient detail to allow an analytical replication of the engine. The engine data will include but will not be limited to the following: three view drawings; weight; size; fuel use over the flight envelope; maintenance requirements; acquisition cost; expected reliability. Rolls-Royce Allison will provide sufficient information to the NASA to allow the Government to model the engine and to make DOC calculations.

#### 3.6.2. Define a PD scheme for the Injected Engine

The Baseline Engine will be modified to include a water/methanol injection system. The OEI requirements will be those given in Section J, paragraph 4.1.1 of the RFP. The engine data will be fully scaleable. This engine data will be presented to the Government in sufficient detail to allow an analytical replication of the engine. The engine data will include but will not be limited to the following: weight; size; fuel use over the flight envelope; maintenance requirements; acquisition cost; expected reliability. Rolls-Royce Allison will provide sufficient information to the NASA to allow the Government to model the engine and to make DOC calculations.

3.6.3. Define Baseline Engine cost & weight estimate

Cost and weight estimates will be prepared for use in the DOC analysis. A description of the techniques used to generate these estimates will also be provided for inclusion in the final report.

3.6.4. Define Injected Engine cost & weight estimate

Cost and weight estimates will be prepared for use in the DOC analysis. A description of the techniques used to generate these estimates will also be provided for inclusion in the final report.

3.6.5. Define tank volumes, line runs, and pump/valve locations

Rolls-Royce Allison will, in conjunction with BHT, define the water/methanol tank volumes and pipeline runs required to provide OEI power.

3.6.6. Update performance cycle

At a point approximately midway through the whole engine preliminary design, the latest component efficiency and cooling flow estimates will be used to update the performance cycle. The updated cycle will be released to all component groups. The component groups will then either update their preliminary design work or note that the changes cannot be accommodated within the scope of the contract. In the latter case, the impact of the cycle changes will need to be documented for the final report.

3.6.7. Engine Life Requirements

The requirements for engine life will be defined in a Product Requirements Document (PRD). This document will be included in the final report to NASA.

3.6.8. Define engine cycle input to VASCOMP II

At the conclusion of the whole engine preliminary design, the final engine cycle component updates will be performed. The deck will be re-run to generate the input files to VASCOMP II in order to perform the economic analysis.

3.6.9. Conduct economic analysis

Rolls-Royce Allison will use DOC as the economic evaluation criteria and will present key engine related costs including engine acquisition cost. The specific items in the DOC shall be those used by NASA-Ames Research Center (ARC) for SHCT computations as presented in Appendix C of the RFP.

Rolls-Royce Allison will use the mission and payload specified in Section J, paragraph 4.1.2 of the RFP for the preliminary OEI DOC evaluation. Rolls-Royce Allison will use the fixed baseline aircraft, also specified in 4.1.2, for this evaluation. Using the sensitivity factors furnished by ARC, included in

Appendix B of the RFP, the improvements resulting from using a rubberized aircraft will be estimated. Rolls-Royce Allison will also use the VASCOMP II computer program to calculate DOC independent of the sensitivity analysis.

Rolls-Royce Allison will provide to the NASA COTR the data necessary for ARC to make the final DOC calculations. Engine scaling information will be included to enable rubberized aircraft computations. Rolls-Royce Allison will document the following information for the final report:

- aircraft-related data as specified in Sect. J, paragraph 4.1.3 of the RFP
- engine data as specified in Section J, paragraph 4.1.4 of the RFP
- key aircraft DOC inputs
- DOC results

#### 3.6.10. Document results for final report

Document the results of all sub-task activities in a form that can be inserted directly into the final report.

### **4. TASK 4 - Meetings and Reporting**

#### 4.1. Weekly Progress Meetings

The program manager will hold weekly progress meetings during which the control account managers will present progress in their area of responsibility. The objective of these meetings will be to identify and implement any corrective action necessary in order to ensure customer satisfaction. The program manager will chair the meeting and ensure that minutes and action items are recorded. The minutes and action items will be published on the following day to all team members.

#### 4.2. Monthly written reports

In view of the short remaining duration of this reprogrammed effort, Rolls-Royce Allison will submit the following monthly reports: Technical Progress Reports; Contractor Financial Management Reports (NASA Form 533M); and Contractor Financial Management Performance Analysis Reports (NASA Form 533P).

#### 4.3. Prepare final report outline

At an early stage in the program, the program manager will define a final report outline. All reporting sub-tasks will use this format to facilitate the final report preparation process.

#### 4.4. Document completed work

All work performed under the NASA SHCT contract, prior to this reprogrammed effort, will be documented ready for inclusion in the final report.

#### 4.5. Prepare final report

A final report will be prepared that delivers to NASA all elements required under this reprogrammed effort. The final report will also describe all activities performed prior to the reprogramming.

**REPORT DOCUMENTATION PAGE**Form Approved  
OMB No. 0704-0188

Public reporting burden for this collection of information is estimated to average 1 hour per response, including the time for reviewing instructions, searching existing data sources, gathering and maintaining the data needed, and completing and reviewing the collection of information. Send comments regarding this burden estimate or any other aspect of this collection of information, including suggestions for reducing this burden, to Washington Headquarters Services, Directorate for Information Operations and Reports, 1215 Jefferson Davis Highway, Suite 1204, Arlington, VA 22202-4302, and to the Office of Management and Budget, Paperwork Reduction Project (0704-0188), Washington, DC 20503.

<b>1. AGENCY USE ONLY (Leave blank)</b>		<b>2. REPORT DATE</b> January 2006	<b>3. REPORT TYPE AND DATES COVERED</b> Final Contractor Report	
<b>4. TITLE AND SUBTITLE</b>  Short Haul Civil Tiltrotor Contingency Power System Preliminary Design			<b>5. FUNDING NUMBERS</b>  Cost Center 2250000013 NAS3-97029	
<b>6. AUTHOR(S)</b>  David J.H. Eames				
<b>7. PERFORMING ORGANIZATION NAME(S) AND ADDRESS(ES)</b>  Rolls-Royce Corporation P.O. Box 420 Indianapolis, Indiana 46206-0420			<b>8. PERFORMING ORGANIZATION REPORT NUMBER</b>  E-15416	
<b>9. SPONSORING/MONITORING AGENCY NAME(S) AND ADDRESS(ES)</b>  National Aeronautics and Space Administration Washington, DC 20546-0001			<b>10. SPONSORING/MONITORING AGENCY REPORT NUMBER</b>  NASA CR-2006-214059 EDR 18694	
<b>11. SUPPLEMENTARY NOTES</b>  Project Manager, Joseph Eisenberg (Retired). Responsible person, Robert C. Hendricks, organization code R, 216-977-7507.				
<b>12a. DISTRIBUTION/AVAILABILITY STATEMENT</b>  Unclassified - Unlimited Subject Categories: 07, 26, 27, 37, and 45 Available electronically at <a href="http://gltrs.grc.nasa.gov">http://gltrs.grc.nasa.gov</a> This publication is available from the NASA Center for AeroSpace Information, 301-621-0390.			<b>12b. DISTRIBUTION CODE</b>	
<b>13. ABSTRACT (Maximum 200 words)</b>  This NASA "Short Haul Civil Tiltrotor (SHCT) Contingency Power System Preliminary Design" contract represents the second phase of an ongoing effort to study low cost and safe one engine inoperative (OEI) contingency power propulsion system concepts. Phase I of this study developed several candidate contingency power system concepts that held the potential for significantly increasing the OEI power available from the powerplant. The objective of the current Phase II study was to select two different high ranking concepts from the Phase I study and develop these to a point where more refined vehicle direct operating cost (DOC) computations could be performed. The concepts selected were: advanced water-methanol injection; and a variable geometry boost compressor. The advanced water-methanol injection system showed the highest potential DOC improvement and was the subject of a preliminary design study. Bell Helicopter Textron, Inc. provided information to Rolls-Royce Allison on tank location, sizing, and mounting for a conceptual SHCT aircraft. The work was concluded by performing a direct operating cost analysis for an aircraft powered by a baseline unaugmented engine compared with a resized SHCT aircraft powered by a smaller water-methanol injection engine.				
<b>14. SUBJECT TERMS</b> Rotorcraft; Tiltrotor; Turboshaft; Contingency power; Turbomachines; Seals; Water injection; Compressor; Turbine; Design			<b>15. NUMBER OF PAGES</b> 122	
			<b>16. PRICE CODE</b>	
<b>17. SECURITY CLASSIFICATION OF REPORT</b> Unclassified	<b>18. SECURITY CLASSIFICATION OF THIS PAGE</b> Unclassified	<b>19. SECURITY CLASSIFICATION OF ABSTRACT</b> Unclassified	<b>20. LIMITATION OF ABSTRACT</b>	



